

Nonlinearities in Carbon Allocation and Vegetation Functioning

Dissertation

zur Erlangung des akademischen Grades doctor rerum
naturalium
(Dr. rer. nat)

vorgelegt dem Rat der Chemisch-Geowissenschaftlichen Fakultät der
Friedrich-Schiller-Universität Jena

von ***Verónica Ceballos-Núñez***

MSc Molecular Biosciences, Ruprecht-Karls-Universität Heidelberg

geboren am 10.12.1987 in Cali, Kolumbien

Gutachter:

1. Prof Dr. Anke Kleidon-Hildebrandt
2. Prof Dr. Susan Trumbore

Tag der Verteidigung: Donnerstag, den 20.12.2018

Summary

Vegetation, one of the major C sinks with respect to the atmosphere, has an indispensable role in the global carbon cycle; it assimilates atmospheric CO₂ via photosynthesis and distributes the assimilated C among plant parts with different cycling rates. These processes can be generalized into one main concept: *carbon allocation (CA)*. Since vegetation has different CA strategies to survive changing climate and disturbance regimes, the efforts towards a better understanding of CA in vegetation have increased, particularly through the development of Dynamic Vegetation Models (DVMs). However, there is no consensus in the model representation of CA, i.e., there are discrepancies among predicted trajectories, as well as between model predictions and empirical observations. This lack of consensus goes in hand with the quest to find a balance between precise predictions and a good level of abstraction; detailed models require high computer power, whereas simpler models may fail to capture complex dynamics such as nonlinearities. Additionally, not all processes that are relevant for ecosystem dynamics take place at the same space/time resolution, and they are not understood with the same level of detail. Thus, upscaling and simplification are another source of uncertainty. These issues have motivated several model intercomparisons and conceptual reviews, yet none of them have focused on their mathematical formulation.

In this PhD thesis, three fundamental aspects of the CA component in ecosystem models are assessed. First, common mathematical representations of CA are evaluated and synthesized into a new framework that benefits from concepts of dynamical systems theory; second, this framework is used to select pertinent diagnostics of model performance, such as the distributions of carbon ages and transit times, based on model properties (e.g. autonomy and linearity); and third, the long standing puzzle of source and sink limitation on CA is approached from the dynamical systems perspective of the proposed framework, using a simple nonlinear model. The implications that these nonlinearities have for the model behaviour are also discussed.

- *Towards better representations of carbon allocation in vegetation: A conceptual framework and mathematical tool*

Given that current ecosystem models are written in different programming languages, and their descriptions are often incomplete, the comparison between components of carbon allocation in vegetation is not a simple task. This means that the structural problems that may exist remain hidden despite all previous model intercomparison studies that have been performed so far. Here, a new conceptual framework and mathematical tool is proposed in order to study carbon allocation in vegetation. This tool includes a model database and a Python 3 package that is now publicly available. Within this framework models can be classified according to their linearity and autonomy, with important consequences for the predicted biogeochemical dynamics, model stability, and the applicability of certain performance diagnostics.

- *Ages and transit times as important diagnostics of model performance for predicting carbon dynamics in terrestrial vegetation models*

The alternative representations of carbon allocation in ecosystem models has lead to differences in their performance, and this has prompted the development of diagnostic methods, some of which include calculations that have as a requisite the steady state of the system. However, not all models can fulfill this requirement because some models do not converge to a single fixed point, particularly those that are driven by variables that depend on time (i.e. non-autonomous models). The framework proposed in this thesis can help in that matter, since it offers a model classification according to their autonomy. Therefore, in this thesis, three autonomous models with a different number of storage compartments are compared using various performance diagnostics. It is shown that the diagnostics with the highest sensitivity to model structure is the distribution of C ages and transit times. The use of *distributions* instead of *mean values* is not only valuable as a performance diagnostic, but it also has biological relevance, which is discussed in the context of the mixing of old and newly fixed carbon.

- *Sink and source limits on carbon allocation in vegetation: A dynamical system perspective*

Another long standing puzzle approached with this new framework was the interplay between source and sink limits of carbon allocation in vegetation, and the central role that non-structural carbon (NSC) plays in this subject. A simple analytical model is used to predict the response of vegetation to different limitation scenarios. The implications that this limitation has for the stability of the system is also discussed; it is shown that strong sink limitations can lead to oscillations in the neighborhood of fixed points, as well as changes in the ratios of carbon stocks and predicted C mean ages. The latter changes were enhanced by the nonlinearities of the model.

In conclusion, the field of theoretical ecosystem ecology could benefit immensely from a common modeling language. This could ease the comparison of models and the identification of potential problem sources. Furthermore, the matrix representation and the overall framework presented here could be of great use as a building block towards this goal, since with it complex models can be represented in a compact form where key structural characteristics are discernible. This has indeed proven to be invaluable in the prediction of model properties and the selection of modeling approaches and diagnostics suitable for particular research questions. The knowledge gained with the comparison of models in terms of their mathematical representation can also help in the development of improved models. Moreover, it was also found that the nonlinear interactions from some models have important repercussions in the system stability, among other properties. Thus, given that models applied to large space/time scales are often linear, whereas the nonlinear models are mostly used in shorter scales, it would be interesting to find different types of behaviors that can be derived from the nonlinearities. These types of behaviour include oscillations and bifurcations, and could ultimately reflect scaling effects in the predictions of the sustainability of vegetation as a terrestrial carbon sink under changing climate regimes.

Zusammenfassung

Die Vegetation, eine der wichtigsten Kohlenstoffsinken bezüglich der Atmosphäre, spielt eine unersetzliche Rolle im globalen Kohlenstoffkreislauf: Sie assimiliert CO_2 durch Photosynthese und verteilt den aufgenommenen Kohlenstoff auf verschiedene Pflanzenteile mit verschiedenen Umsetzungsraten. Diese Prozesse lassen sich zum Konzept der *Kohlenstoffallozierung (KA)* verallgemeinern. Da sich die Strategien der Pflanzen mit Klimawandel und Störungsszenarien umzugehen unterscheiden, bemüht man sich zunehmend um ein besseres Verständnis der KA, insbesondere durch die Entwicklung dynamischer Vegetationsmodelle (DVM). Allerdings gibt es über die Darstellung der KA in den Modellen keinen Konsens, was sich unter anderem an den Differenzen zwischen den Lösungen verschiedener Modelle zeigt, die sich sowohl voneinander als auch von den beobachteten Daten unterscheiden. Dieser fehlende Konsens ist eng mit der Aufgabe verbunden eine Balance zwischen Vorhersagegenauigkeit und Abstraktionsgrad zu finden: Detaillierte Modelle erfordern mehr Rechenleistung, während einfachere Modelle komplexe Dynamik, wie Nichtlinearitäten, nur unzureichend beschreiben. Außerdem unterscheiden sich die für die Ökosystemdynamik relevanten Prozesse hinsichtlich ihrer zeitlichen und räumlichen Auflösung und auch darin wie detailliert sie bereits verstanden sind. Demzufolge tragen auch Maßstabsvergrößerung und konzeptionelle Vereinfachungen zur Unsicherheit in der Modellierung bei. Obwohl diese Probleme bereits einige Studien zum Vergleich verschiedener Modelle, sowohl bezüglich der Ergebnisse als auch hinsichtlich ihrer konzeptionellen Grundlagen, motiviert haben, fehlt es bisher an Untersuchungen die sich auf die Unterschiede in ihrer mathematischen Formulierung konzentrieren.

In dieser Dissertation werden drei fundamentale Aspekte der KA Komponenten verschiedener Ökosystemmodelle untersucht. Erstens werden verschiedene, gebräuchliche mathematische Darstellungen der KA untersucht und zu einem neuen System zusammengefasst, das Konzepte der Theorie dynamischer Systeme nutzt.

Zweitens wird dieses neue System verwendet um für die Beurteilung der Modellqualität relevante diagnostische Variablen auszuwählen, wie z.B. die Verteilung des Kohlenstoffalters oder der Transitzeiten in Abhängigkeit von Modelleigenschaften wie Linearität und Autonomie.

Drittens wird das seit Langem bestehende Rätsel der Quell und Senken-Limitierung der KA aus der, dem neuen System inhärenten, Perspektive der Theorie dynamischer Systeme behandelt, wobei ein einfaches nichtlineares Modell zum Einsatz kommt. Die Auswirkungen dieser Nichtlinearitäten auf das Modellverhalten werden ebenfalls diskutiert.

- *Auf dem Weg zu besseren Repräsentationen der Kohlenstoffallozierung in der Vegetation: Ein konzeptionelles System und mathematisches Werkzeug.*

Dadurch, dass gegenwärtige Ökosystemmodelle in verschiedenen Programmiersprachen geschrieben sind und ihre Beschreibung zu dem häufig nur unvollständig vorliegt, ist es schwierig verschiedene Modelle hinsichtlich ihrer Komponenten für die Kohlenstoffallozierung der Vegetation zu vergleichen. Konkret heißt das, dass potentiell existierende strukturelle Probleme trotz vorangegangener Modellvergleichsstudien unerkannt bleiben. Das hier vorgestellte Werkzeug enthält eine Modelldatenbank und ein frei verfügbares Python 3 Paket. Innerhalb des konzeptionellen Systems können Modelle hinsichtlich Linearität und Autonomie klassifiziert werden. Beide Faktoren haben große Auswirkungen auf die vorhergesagte biochemische Dynamik, Stabilität der Modelle und die Anwendbarkeit verschiedener diagnostischer Variablen zur Evaluierung ihrer Leistungsfähigkeit.

- *Alter und Transitzeiten als wichtige Diagnosevariablen für die Vorhersagequalität der Kohlenstoffdynamik in terrestrischen Vegetationsmodellen.*

Es ist klar, dass Ökosystemmodelle sich hinsichtlich ihrer Leistungsfähigkeit unterscheiden, und man hat deshalb versucht ihre Vorhersagequalität zu ermitteln. Einige der Diagnoseverfahren benutzen Vergleichsrechnungen die voraussetzen, dass sich das System in einem Gleichgewichtszustand befindet. Bevor ein solches Diagnoseverfahren gewählt wird, ist es deshalb wichtig zu wissen, ob das Modell überhaupt jemals zu einem Fixpunkt konvergiert, was z.B. für nichtautonome Systeme keineswegs zu erwarten ist. Hier kann das konzeptionelle System helfen.

In dieser Dissertation werden drei Modelle unterschiedlicher Anzahl von Speicherreservoirien hinsichtlich verschiedener Qualitätskriterien verglichen. Es wird gezeigt, dass das Kriterium mit der größten Sensitivität gegenüber der Modellstruktur die Verteilung der Kohlenstoffalter und Transitzeiten ist. Die Verwendung der kompletten Verteilungsdichten anstatt der Mittelwerte ist nicht nur nützlich als Qualitätskriterium, sondern hat auch biologische Relevanz, die im Kontext der Mischung von neuem und altem fixierten Kohlenstoff diskutiert wird.

- *Der Einfluss von Beschränkungen von Kohlenstoff-Quellen und Senken aus Sicht der Theorie dynamischer Systeme*

Ein weiteres seit Langem bestehendes Rätsel, das mit dem neuen konzeptionellen System untersucht wird, besteht im Wechselspiel zwischen den Beschränkungen der Kohlenstoff-Quellen und Senken bei der Kohlenstoffallozierung der Vegetation und der zentralen Rolle, die die nichtstrukturierten Kohlenwasserstoffe (NSKW) dabei spielen. Um die Reaktion der Vegetation auf verschiedene Beschränkungsszenarien zu untersuchen wird ein einfaches analytisches Modell verwendet. Die Implikationen, die die Beschränkungen für die Stabilität des Modells haben, werden ebenfalls diskutiert. Es wird gezeigt, dass starke Beschränkungen der Kohlenstoffquellen sowohl zu Schwingungen in der Umgebung von Fixpunkten als auch zu Änderungen im Verhältnis der Inhalte der einzelnen Kohlenstoffreservoirie und deren mittleren Altern führen können. Diese Änderungen verstärkten sich durch Nichtlinearitäten im Modell.

Schlussfolgernd kann man sagen, dass die theoretische Ökosystemökologie von einer gemeinsamen Modellierungssprache extrem profitieren könnte. Sie könnte den Vergleich verschiedener Modelle und die Identifikation potentieller Probleme erleichtern.

Darüber hinaus könnten die Matrixdarstellung und das konzeptionelle System, die hier vorgestellt werden, ein sehr nützlicher Baustein zum Erreichen dieses Zieles sein, da komplexe Modelle in kompakter Form dargestellt werden können und damit entscheidende strukturelle Charakteristika erkennbar bleiben.

Tatsächlich haben sich diese als unschätzbar wertvoll erwiesen, sowohl in der Vorhersage von Modelleigenschaften als auch der Auswahl von Modellierungsansätzen und diagnostischer Variablen anhand einer bestimmten Forschungsfrage.

Die im Vergleich der mathematischen Darstellung verschiedener Modelle neu gewonnenen Erkenntnisse können auch zur Entwicklung verbesserter Modelle genutzt werden.

Zudem wurde deutlich, dass sich die nichtlinearen Interaktionen mancher Modelle unter anderem auf deren Stabilität auswirken.

Angesichts der Tatsache, dass Modelle denen grobe räumliche und zeitliche Maßstäbe zugrunde liegen oft linear sind, während nichtlineare Modelle hauptsächlich kleinskalig sind, wäre es interessant verschiedene Typen im Verhalten der Modelle in Abhängigkeit der Nichtlinearitäten zu finden.

Diese Verhaltenstypen schließen Schwingungen und Bifurkationen ein und könnten Ausdruck von Skalierungseffekten in der Vorhersage der Zukunftsfähigkeit der Vegetation als globaler Kohlenstoffsene unter veränderlichen klimatischen Bedingungen sein.

Acknowledgements

This PhD thesis is the result of almost four years of research insightfully guided by Carlos A. Sierra, to whom I am wholeheartedly grateful. His teachings surpass this thesis, and include valuable lessons on scientific communication and how to consolidate a participative group where inspiring scientific discussions and team work are a constant. I appreciate the opportunity of being part of the Theoretical Ecosystem Ecology group, whose members further enriched this experience. Particularly Markus Müller translated the summary of this thesis to German, and coached me with great kindness and patience through the acquisition of new programming skills, to a level beyond my imagination. I really enjoyed our conversations while trying to make sense out of cryptic pieces of code. In addition, Holger Metzler always had an answer to my questions and gave me valuable constructive criticism. It has been encouraging to share this experience with all of you, as well as with the ones who have visited our group and the new members David, Alison, Ingrid and Mina.

Moreover, I also acknowledge the critical view and pertinent advice that I received from Susan Trumbore, Henrik Hartmann, Gerd Gleixner and the members of my PhD Advisory Committee: Anke Hildebrandt, Sönke Zaehle, and Andrew Richardson. Their feedback and interest in my work were an additional motivation to pursue this thesis. Special thanks to Andrew for welcoming me into his group during my research stay abroad, which were three months of intellectually stimulating experiences. My gratefulness is of course extensive to the rest of the Richardson Lab at the Department of Organismic & Evolutionary Biology, Harvard University.

Furthermore, I would like to express my gratitude to Kerstin Lohse for diligently organizing my trips, and to Steffi Rothhard for her advice and for carefully planing the curriculum and scientific events that enriched the research environment at the Max Planck Institute for Biogeochemistry. A warm thanks to my friends and colleagues for interesting discussions and friendly chats. I am foremost grateful to Gan and David for their friendship and for embarking with me, Ben, Melanie, and all the others on the tough journey of learning to dance Rueda de Casino; Thursdays would have never been as fun without you.

This work would have not been possible without the financial support of the German Research Foundation, project *Nonlinearities and Alternative States of Biogeochemical Cycling in Terrestrial Ecosystems* (SI 1953/2-1).

Efectivamente no podría haber alcanzado esta meta de no haber sido por mis padres, Luis Alberto y María Stella, mi hermana Carolina y el resto de mi familia en Colombia: gracias por creer en mí y manifestarme su amor y constante apoyo. Gracias a Dios y a ustedes he perseverado y sobrellevado los momentos más difíciles.

Ein großes Dankeschön für Ralf, Sabine und die ganze Familie. Ihr seid eine großartige Unterstützung hier in Deutschland.

Finally I would like to thank my husband Jan for his love and support, and for encouraging me with his example to keep the hard work while living a balanced life. I am looking forward to sharing with you all the next challenges and wonderful experiences.

Contents

Summary	i
Zusammenfassung	iii
Acknowledgements	v
1 State of the art and research questions	1
Vegetation in the context of the global carbon cycle	1
Carbon allocation in vegetation: from cells to ecosystems	2
Uncertainties in scaling-up	3
The quest to find the source of uncertainties	4
Importance of assessing model structure	5
Caveats of assessment of model structure	7
Research questions	10
Thesis overview and related publications	11
2 Towards better representations of carbon allocation in vegetation: A conceptual framework and mathematical tool	13
Introduction	13
Methods	16
Working definition of <i>carbon allocation</i>	16
Selection of published model descriptions (PMDs)	17
Protocol for analyzing the PMDs using the Python package bgc-md	18
Results	19
The new mathematical framework	24
Implications of nonlinearities using an example of a vegetation system with four compartments	24
Discussion	25
Implications and future studies	27
Conclusions	27
3 Ages and transit times as important diagnostics of model performance for predicting carbon dynamics in terrestrial vegetation models	31
Introduction	32
Definitions: ages and transit times	33
Methods	36
Model Implementation	36

Optimization procedures	37
Uncertainty analysis	38
Results	39
Simulations of carbon stocks	39
Influence of carbon allocation strategies on ecosystem level C cycling	39
Discussion	44
Diagnosing model performance with C release fluxes, and age and transit time distributions	45
Model equifinality (identifiability)	49
Conclusions	51
4 Source and sink limits on carbon allocation in vegetation: A dynamical system perspective	53
Introduction	53
Methods	57
Working definitions	57
Model description	57
Stability analysis	61
Results	61
Stability analysis	61
Simulation of carbon allocation limits in steady state	63
Discussion	64
Representing the central role of non-structural C in vegetation functioning with an analytical model	64
Source and/or sink limitation can lead to changes in equilibria and alter the ratio between C stocks	65
Implications for C cycle modelling	67
Conclusions	67
5 Concluding remarks and outlook	75
Bibliography	85
Selbständigkeitserklärung	103
Curriculum Vitae	105
Appendix chapter 2	107
Appendix chapter 3	111
Appendix chapter 4	117

List of Figures

1.1	Conceptual depiction of carbon allocation in vegetation across space/time scales.	3
1.2	Matrix approach to carbon cycle modeling (Luo <i>et al.</i> , 2003).	9
2.1	<i>Carbon allocation</i> is a general term that overarches patterns (biomass) and processes (flux and partitioning) according to Litton <i>et al.</i> (2007).	14
2.2	General mathematical representation of carbon allocation (CA) in a 2-compartment vegetation model.	17
2.3	Workflow.	18
2.4	Comparison between published model descriptions where it was claimed that the model intended to have a partitioning scheme that favoured a limiting compartment, versus which of those had indeed a dynamic partitioning scheme.	21
2.5	Comparison between number of state variables in models, and whether their cycling matrices are diagonal or not.	22
2.6	Model classification according to their mathematical formulation.	24
2.7	Examples of two models of carbon allocation in vegetation.	29
3.1	Graphical representation of the concepts of age and transit time distributions in a vegetation model.	34
3.2	Three carbon allocation strategies in vegetation models.	37
3.3	Carbon stocks estimated for each model, comparing the observed data and the model predictions of C stocks in Wood (A) and Foliage (B).	39
3.4	Carbon stocks estimated for each compartment and their uncertainties.	40
3.5	C release fluxes from the compartments at steady state, with uncertainty ranges obtained from the set of posterior parameters obtained by Bayesian optimization.	42
3.6	Radiocarbon simulations for the three model structures.	43
3.7	System ages and transit times.	44
3.8	Age densities simulated for the compartments	45
3.9	Age densities simulated for the models with storage compartments.	46
4.1	Carbon allocation scheme based on (Hartmann <i>et al.</i> , 2018).	55
4.2	Schematic representation of limits of C allocation based on (Hartmann <i>et al.</i> , 2018)	56
4.3	Schematic representation of the model.	58
4.4	Damping coefficients under the different limitation scenarios.	69
4.5	Complex planes for the model under different limitation scenarios.	70
4.6	Complex plane for a selection of eigenvalues and limitation scenarios.	71
4.7	Carbon stocks with respect to time.	71

4.8	Phase planes of different combinations of vegetation compartments.	72
4.9	Carbon stocks of each compartment under different limitation scenarios	73
5.1	Mathematical tool and conceptual framework to study carbon cycle modeling. .	83

Figures in appendices 107

2	Pairwise plots of sensitivity functions for the model <i>Storage: 0</i>	111
3	Pairwise plots of sensitivity functions for the model <i>Storage: 1</i>	112
4	Pairwise plots of sensitivity functions for the model <i>Storage: 2</i>	113
5	Carbon stocks estimated for each model	113
6	Radiocarbon simulations for the three models. The three models were run using the same parameter set. The black curve corresponds to the $\delta^{14}C$ accumulation in the atmosphere, and the other colors depict the vegetation compartments. .	114
7	System ages and transit times. (A) Age and transit time (B) distributions calculated for each of the three models using the same parameter set; the dashed and dotted lines mark the mean and median ages, respectively. Some of the lines may be overlapping others.	114
8	Age densities simulated for the compartments: (A) Photoassimilates, (B) Str. Foliage, (C) Wood and (D) Roots. The three models were run using the same parameter set. Each model is depicted in a different color. The dashed lines correspond to the mean ages of each model for each compartment.	115
9	Age densities simulated for the models with storage compartments; the models were run using the same parameter set. (A) Fast cycling compartment of models <i>Storage: 0</i> and <i>Storage: 2</i> . (B) Slow cycling storage of the only model with 2 storage compartments.	116
10	Scatter plot of mean age Vs. mean transit times in log scale. The three models have distributions below the 1:1 line.	116
11	Carbon stocks of each compartment under different limitation scenarios	119
12	Carbon stocks with respect to time for a model with constant photosynthetic input.	120
13	Phase planes of different combinations of vegetation compartments for a model with constant photosynthetic input.	121
14	Mean ages predicted for the initial model proposed in this work, in steady state under different limitation conditions	122
15	Mean ages predicted for the model with constant photosynthetic input, in steady state under different limitation conditions; (a) source limitation only $-\zeta$, (b) aboveground sinks limitation $-\alpha$, (c) belowground sinks limitation $-\rho$, (d) above and belowground limitation $-\alpha, \rho$, and (e) Source and sink limitation $-\zeta, \alpha, \rho$. The highest source or sink strength is achieved when the respective scalar is equal to 1.	123
16	Mean ages predicted for the linear model with constant photosynthetic input, in steady state under different limitation conditions	124

List of Tables

2.1	Classification of the different models analyzed according to their mathematical structure.	20
2.2	Classification of the carbon allocation (CA) module of different models according to the main conceptual and mathematical approach used.	21
2.3	Sets of equations of the models from the example	25
3.1	Parameter values obtained from the optimization procedures [$year^{-1}$].	41
4.1	Variables and parameters of the model.	59
4.2	Matrix representation of the model	60
Tables in appendices		107
1	Variables and parameters of the linear model.	107
2	Matrix representation of the Autonomous Linear Model, see variables and parameters in table 1	108
3	Variables and parameters of the nonlinear model.	108
4	Matrix representation of the Autonomous Nonlinear Model, see variables and parameters in table 3	109
5	Number of positive and negative correlations between parameters. Only R^1 values < -0.1 and > 0.1 were assumed to account for correlations.	111
6	Matrix representation of the model with fixed photosynthetic input (u no longer depends on foliage)	117
7	Matrix representation of the linear model with constant photosynthetic input and constant maintenance respiration ($R_m = rm$)	118

State of the art and research questions

Vegetation in the context of the global carbon cycle

In the Anthropocene, the currently proposed geological epoch, the effects of humans on the environment have provoked the rise of temperature and other noticeable changes in climate (Crutzen and Stoermer, 2000). This is the reason why some ecosystems have undergone very drastic and abrupt transformations, mainly when the strength of the external perturbations surpassed their resilience. *Resilience* is a measure of the ability of a system to persist by absorbing changes and bouncing back into its original state after a perturbation (Holling, 1973). Hence, the maintenance and enhancement of the ecosystem's resilience is critical for the conservation of the ecosystems as we know them (Scheffer *et al.*, 2001). In the interest of preserving the current state of the Earth ecosystems, it was proposed to manage our planet within the framework of a *safe operating space* that defines the boundaries among which we should keep acceptable levels of global stressors in order to reduce their risk to collapse (Rockström *et al.*, 2009; Scheffer *et al.*, 2015). Interestingly, the ability of a system to persist despite critical global perturbations can also increase if some conditions (e.g. ecosystem properties) are managed locally (Scheffer *et al.*, 2015).

In order to design effective local strategies that aim at the conservation of ecosystems threatened by climate change, it is necessary to understand the local processes that are affected. One of these processes is the CO₂ exchange between the atmosphere and the biosphere. Carbon dioxide is a greenhouse gas increasingly emitted to the atmosphere by fossil fuel combustion, but a significant portion of it is removed from the atmosphere by terrestrial ecosystems (Schimel *et al.*, 2001; Canadell *et al.*, 2007). However, not all ecosystems absorb and store the same amount of carbon at all times; in fact the C-storage capacity, which is directly proportional to the amount of time that carbon remains in a reservoir -the ecosystem residence time (τ)- (Luo *et al.*, 2003), is not a concept of static pool sizes but a dynamic measure of the photosynthetic carbon influx and the time that C atoms take to transit the ecosystem from their entrance to their exit. This process can be sensible to external and internal cues, which means that plants acclimate to new circumstances by adjusting their carbon intake (Luo *et al.*, 2003). The plants sensitivity and acclimation to changes in the environment can indicate whether the photosynthetic C influx will be sustainable or not; the sensitivity is independent of growth environments and interspecific variation (varies only with [CO₂] and temperature), and the acclimation (i.e., adjustment in photosynthetic capacity) is frequently related to many factors

such as nitrogen supply (Luo *et al.*, 2003). The sustainability of terrestrial carbon sequestration has been the subject of several modeling studies (De Kauwe *et al.*, 2014; Luo *et al.*, 2003).

In the same way as the photosynthetic carbon influx can vary, the sequestered carbon is stored into terrestrial reservoirs of different residence times (Trumbore, 2006). Therefore, understanding the mechanisms by which carbon is preferentially partitioned to compartments where it would remain for longer versus shorter periods is imperative. However, despite all the empirical and theoretical studies that have pursued a better understanding of the mechanisms behind carbon partitioning within vegetation, the uncertainties with respect to the representation of carbon allocation in vegetation persist and have lead to divergent predictions. For example, Keenan *et al.* (2013b) found that 13 different models could not accurately predict the experimentally assessed water use efficiency of the forests they sampled. Furthermore, Zaehle *et al.* (2014) found a case in which 11 ecosystem models could predict early responses to elevated atmospheric CO₂ concentration, but the simulations failed to fit the experimental results in a larger time scale (10 years).

Evidently, there is a need to achieve a better understanding on the dynamics of carbon allocation in vegetation, particularly in terms of the mathematical structure needed to represent this process at different scales; this was the main motivation of this thesis. Here, I developed a synthesis of a representative sample of carbon allocation models and explore their main mathematical properties, focusing mainly on the relation between nonlinear interactions and predicted vegetation functioning.

Carbon allocation in vegetation: from cells to ecosystems

Terrestrial plants have different strategies to survive in environments with changing conditions such as variations in water or nutrient availability, or increasing temperatures and CO₂ concentration. One of these strategies is the adjustment of their carbon allocation scheme to prioritize limiting organs (Lacointe, 2000; Franklin *et al.*, 2012). According to this carbon allocation theory, plants maximize their growth rate by optimizing the capture of limiting resources, and this is done by partitioning carbon to key organs (Franklin *et al.*, 2012). For example, when competing for scarce nutrients in the soil, vegetation would rather use its carbon resources for the growth of roots than to become taller.

Here, *carbon allocation* is referred to as all carbon-cycle-related processes that take place within vegetation, from the fixation of carbon particles during photosynthesis, until they leave the system via autotrophic respiration or litterfall. Although these processes take place in different space/time scales, as summarized in figure 1.1, they are interconnected. Photosynthesis, for example, is the result of metabolic reactions in the chloroplast (i.e., organelle -cell organ-) and require CO₂, water and light.

The rate of gas exchange of CO₂ entering and water vapor leaving the plants is often called *stomatal conductance*. Stomata are pairs of cells -guard cells- in the epidermis of leaves, whose movement controls the opening and closing of pores in relation to the absolute concentration gradient of water vapor from the leaf to the atmosphere (Waring and Running, 1998). Water is generally absorbed by the plant through its roots, from where it is transported to the rest of the plant by the vascular tissue: xylem. The other type of vascular tissue, the phloem, transports the products of photosynthesis. The efficiency with which the available light is

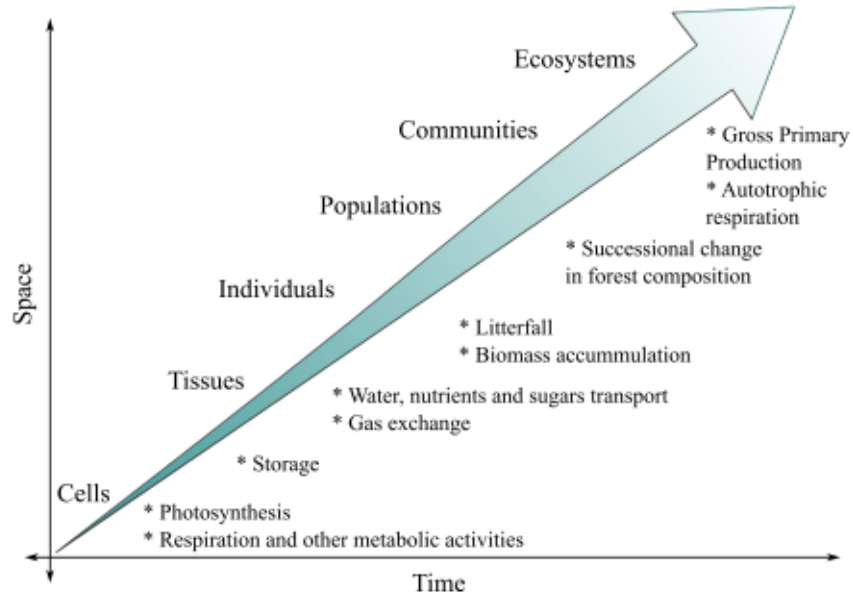


Figure 1.1: Conceptual depiction of carbon allocation in vegetation across space/time scales.

captured by the photosynthetic tissue depends on the photosynthetic pigments located in the chloroplasts. Deciduous plants, for example, have green leaves at the beginning of the growing season because they are rich in chlorophyll, which is a pigment that can absorb blue and red lights. Thus, when chlorophyll is no longer produced and is broken down (in autumn), the leaves take the colors of the remaining pigments, which are not as efficient absorbing light. This means that the amount of captured light available for photosynthesis depends on molecules whose abundance is determined by the phenological state of the plant. Ontogeny also plays an important role, because older plants have slower metabolism than younger ones (Hartmann *et al.*, 2018). Nevertheless, not all leaves in a plant are exposed simultaneously to light, some may be shaded by other leaves of the same plant or competing plants. This means that the light availability, on a larger scale, also depends on the leaf area index (LAI), i.e., the sum of all leaf layers in a canopy (Waring and Running, 1998).

Uncertainties in scaling-up

It is then evident that the metabolic activities that occur at short space/time scales, depend on precursors whose availability is determined by processes taking place at larger scales, such as competition for light, water and other resources. This has to be taken into account when leaf level processes are scaled to upper levels such as populations, communities and ecosystems. For example, in some individual-based models the leaf level processes are scaled to the whole plant level, and other characteristics are estimated using allometric equations that relate biomass in plant compartments to height, basal area, canopy area, leaf area index and rooting depth (Scheiter and Higgins, 2009). The rooting depth, together with the soil water content, determines the water available for the plant; and this and the light availability are used to scale the leaf level photosynthetic rate to the canopy level photosynthetic rate (Scheiter and Higgins, 2009).

In process based models, photosynthesis is generally calculated using the set of basic equations proposed by Farquhar *et al.* (1980). These equations take into account limitations by enzymes, electron transport, and stomatal conductance. Therefore, at the ecosystem level, the Gross Primary Productivity (GPP) is calculated as the difference between the photosynthesis

rate and the leaf maintenance respiration during daytime (Govingjee, 2009). If the autotrophic respiration is subtracted from GPP, one can calculate the Net Primary Productivity (NPP) (Govingjee, 2009). By association, NPP is limited by resources (e.g. water, nutrients), and climate and soil conditions, all of which vary in different space/time scales; in a narrow time scale (hours-weeks) the patterns of NPP are mostly determined by short term controls over photosynthesis, whereas annual patterns of NPP are governed by soil resources (Chapin *et al.*, 2002). Space-scale wise, there is a 14-fold range in average NPP between biomes (think of how different the Tundra and the Rain forest are in terms of ecosystem productivity) (Chapin *et al.*, 2002). This has been the subject of many in depth reviews, for more information on plant–environment interactions across scales please refer to (Waring and Running, 1998; Reichstein *et al.*, 2014; Hartmann and Trumbore, 2016; Hartmann *et al.*, 2018).

It is then clear that robust models can be built on the available experimental evidence, but some observations are not attainable at the same level of detail and, or spatio-temporal resolution as modelled processes. Therefore, some upscaling has to be done, which leaves room for multiple interpretations and uncertainties. For instance, it is very common that the meteorological drivers that are used to run models have a time step faster than that of the model, e.g., some drivers are measured with a time resolution of minutes or hours, while models are resolved in years. Thus, to adapt the time steps, the values of the fast dynamic variables (smaller time steps) are averaged over the time step that is implemented in the model (Govingjee, 2009). However, this is not an error free adaptation, particularly when there are nonlinear dynamics in play, because the average output value of nonlinear functions (e.g. photosynthesis rate) may not match the output value achieved by using average values of variables (e.g. for radiation or temperature) in nonlinear equations. For this reason, the calculated value for a daily time step may be lower or higher versus the average output value of the nonlinear function (Govingjee, 2009).

Averaging is not only used to solve problems with temporal scales, but also with spatial heterogeneity. While the ecosystems are highly heterogeneous entities, the observation towers and measuring instruments used in the field can only cover a limited area. This makes it difficult to track changes in the dynamics of ecosystems as a whole, but this can be approached using process-based models. In such models the mentioned measurements are averaged over larger areas, also known as grid cells. It should be noted that even though these models can be used to address the spatial heterogeneity and the interaction between ecosystem patches, it is very important to select relevant processes and to combine measurements taken at different resolutions to estimate fluxes and parameters (Chapin *et al.*, 2002); all of these steps are of course susceptible to multiple interpretations and errors. The Box “Spatial scaling through ecological modeling” in Chapin *et al.* (chapter 14 2002) has a thorough explanation of how the spatial heterogeneity and scaling is accounted for in ecosystem models, and a couple of models is used to give examples.

The upscaling process can also be impaired by the fact that not all the processes that are relevant to the ecosystem dynamics are well represented in current models (Urbanski *et al.*, 2007). The underrepresentation of key factors in models is problematic because if processes are addressed with a different level of detail, there is an unbalanced representation of reality (Waring and Running, 1998); this biased representation can lead to inconsistent predictions where a single modeled process may dominate the system (Govingjee, 2009). For example,

photosynthesis -as opposed to litter decomposition- may seem to dominate the ecosystem response to changes in environmental drivers, only because it is represented in greater detail in the models. In order to achieve a balanced representation of reality, it would also be necessary to improve our understanding of other factors such as the long-term increases in tree biomass that drive the interannual and decadal changes of ecosystem productivity, or the successional change in forest composition, and disturbance events.

The quest to find the source of uncertainties

Seemingly, vegetation is a dynamical system and as such its response to changing environmental cues has been represented using Dynamic Vegetation Models (DVMs). One of the most common representations of vegetation in DVMs consists on dividing it into three carbon compartments, i.e. foliage, wood and roots. The C balance of these compartments depends on their input, i.e. photosynthetically fixed C, and output (e.g. carbon transferred to other compartments, respiration, litterfall, among others), and the speed at which these fluxes take place depends on transfer rates. These rates are mostly represented by parameters whose values are often unknown because they are not measurable (Trumbore, 2006). Some parameters may also vary in such a wide range among forests that the variation can be even greater than the one associated to C partitioning (Litton *et al.*, 2007). Thus, despite all of the advances in the field, there is still uncertainty and consequently disagreement among different model predictions.

The quest to find the source of uncertainties has motivated several model intercomparison studies. Although some of these studies are multimodel experiment frameworks that focus on punctual aspects such as the drought-induced vegetation mortality (McDowell *et al.*, 2013) where model runs are compared, other studies have reviewed the modeling approaches and derived model classifications from them. One of these classifications was proposed by (Litton *et al.*, 2007), who claimed that ecosystem models can be classified according to whether their carbon allocation scheme is static or dynamic. Another classification proposed by Franklin *et al.* (2012) has more specific categories based on the conceptual design of the models: 1) Fixed allocation -bottom up approach used for large time scales in steady state forests- 2) Allometric -used at the population level, e.g. pipe model- 3) Functional balance or optimal partitioning theory -coordination theory, growth rate maximization- 4) Eco-evolutionarily-based -top down approach, whose commonly used proxy for fitness is the instantaneous growth rate-, and 5) Thermodynamic approach -Maximum Entropy Production-.

The above mentioned classifications can inform about the potential predictive uses of the model (until a certain extent), which could aid the researchers in the selection of appropriate models to answer their particular research questions. Unfortunately, these classifications are only based on the “descriptive rather than analytic” assessment of models (Xia *et al.*, 2013). This means that they ignore the implications that the mathematical representations of ecosystem processes may have for the predicted dynamics. Some of these implications have been assessed in analytic reviews of models on soil organic matter dynamics (Manzoni and Porporato, 2009; Sierra and Müller, 2015), studies that have given us deep insight into some model properties such as mass balance, stability, among others, and have discussed the effects that these properties may have on the predicted dynamics of carbon in soils.

Importance of assessing model structure

“Since all models are wrong the scientist must be alert to what is importantly wrong” (Box, 1976). While the parameter non-identifiability and a wrong choice of modeling approach are undeniable causes of poor model performance, an important cause of error in models involves problems with model structure. It is indeed known that simple but evocative models are preferred over overelaborated and overparameterized models (Box, 1976), but there is more to the model structure than meets the eye.

Some characteristics of model structures can help to identify a priori certain model behaviours, e.g. the stability of the system modelled. The stability analysis of dynamical systems is a research field on its own and, as such, it has been the subject of in depth studies (Jost, 2005; Strogatz, 2014). One of the outcomes of a stability analysis is the notion of whether a system can potentially converge to one or multiple fixed points, also referred to as steady states. The state of a system is assessed by the way in which its state variables (model attribute that changes according to model parameters and external variables) vary. The steady state or equilibrium is a point in the state-space where the state variables remain constant, i.e., their rate of change is zero. Further analysis can confirm the stability of the fixed points, where stable fixed points are those to which the system returns after small perturbations, and unstable fixed points are those from which any trajectory will eventually move away. The stability of a fixed point can be analyzed through its slope; given that the reciprocal of the slope of a fixed point determines the time required for the function to vary significantly in the neighborhood of the fixed point, if this slope is negative, the fixed point is stable (Strogatz, 2014). It is also possible to obtain the rate of decay to a stable fixed point by linearizing about a fixed point, which is further explained by Strogatz (2014).

The analysis of the models stability can have a tremendous impact in the perception of its resilience and the safe operating space of the ecosystems under study (Holling, 1973). Due to the fact that the ecosystems resilience is a measure of the maximum perturbation that they can take without causing a shift to an alternative stable state, the larger the size of the basin of attraction, the stronger the resilience of the system.

Another important aspect of model structure is the way in which the interactions between the parts of the modelled system are portrayed. For example, interactions such as interference, cooperation, and competition can be symbolized mathematically with nonlinear terms such as products and powers (Strogatz, 2014). These nonlinear interactions increase the intricacy of the model dynamics with interesting consequences for the stability and resilience of the ecosystem, since they can lead to hysteresis loops, oscillations, and multiple steady states. For more details on this topic, Strogatz (2014) gave an interesting outlook of nonlinear dynamics and chaos.

In addition to the above mentioned significance of the stability analysis for the understanding of predicted dynamics, the identification of fixed points is a prerequisite to select adequate diagnostics, because some of their calculations are applicable to systems in steady state only. For example, one of the diagnostics used to assess model performance is the carbon residence time. This diagnostic not only is defined by an ambiguous concept, but there has also been a lack of understanding of its applicability, since it is only applicable to systems in steady state, but has also been used for non-autonomous models, which are constantly changing by the forcing of external drivers, i.e. they do not converge to a *steady state* (Sierra *et al.*, 2016).

The residence time of carbon in ecosystem compartments (e.g. storage pools in vegetation)

has been estimated from the dilution rate of labels such as radiocarbon (^{14}C) (Trumbore *et al.*, 2002). This radioactive isotope of carbon has an atomic nucleus with six protons and eight neutrons, and is produced at a relatively constant rate in the upper atmosphere through the interaction of cosmic rays with nitrogen. It is oxidized to CO_2 and enters the terrestrial carbon cycle via photosynthesis. Radiocarbon also decays at a constant rate (half-life = 5 730 years), which means that the atmospheric ^{14}C has a relatively constant value. Certainly, given the fact that the cosmic radiation and radioactive decay kept a relatively balanced ^{14}C atmospheric concentration around the 1800s, and that it can be absorbed by the biosphere, Willard F. Libby developed a dating method (the ^{14}C dating method) whose importance and applicability has transcended barriers across research fields, which is the reason why he was awarded the Nobel Prize in 1960 (Trumbore *et al.*, 2016).

The ^{14}C data has been used to a) estimate ages of C in closed systems (which are those that no longer exchange C with their surroundings, e.g. fossils); b) estimate mean ages and transit times of C in different reservoirs of the Earth system (open systems such as living tissues or organisms); and identify relative contributions of sources in a mixture (Trumbore *et al.*, 2016). For conversions of ^{14}C age to calendar age (for closed systems), it is necessary to use calibration curves, which account for isotopic ratios and radioactive decay and have been assembled from thousands of samples whose ages are known (Trumbore *et al.*, 2016). Thus, the amount of radiocarbon that remains in a reservoir relative to the atmospheric value has been used to estimate the time (century to millennial timescales) that the carbon has remained in the reservoir since the moment it stopped receiving carbon (Trumbore *et al.*, 2002). For systems that still exchange C with their environment (open systems), it is only possible to estimate mean ages and transit times, and models need to be used to account for other factors, such as the ones that will be explained in the next paragraphs.

Although the generation and decay of atmospheric ^{14}C was thought to keep a balanced concentration of radiocarbon, it has been reported to decline and increase as a result of human activity. Between 1800s and 1945 it declined because the input of C from land-use change and fossil fuel combustion diluted the atmospheric radiocarbon (Trumbore *et al.*, 2016). Furthermore, the aboveground testing of thermonuclear weapons in the decades of 1950 and 1960 duplicated the amount of ^{14}C in the Northern Hemisphere, so, by comparing how much of that carbon has been incorporated to a given reservoir (with respect to the atmospheric ‘bomb’ ^{14}C) it is possible to model the exchange rate between the atmosphere and the carbon reservoir (decadal timescale). This calculation is performed with the use of models that account for C exchange between model compartments, the radioactive decay, and the difference in the absorption of C isotopes by the vegetation (heavier atoms tend to be absorbed by the vegetation at a slower rate than the lighter ones, which is a characteristic known as fractionation) (Trumbore *et al.*, 2016). In this order of ideas, slow cycling reservoirs incorporate less radiocarbon than the fast cycling ones, which exhibit a dynamic closer to the atmospheric incorporation curve. This method has been called the *bomb spike*.

However, the atmospheric $^{14}\text{CO}_2$ concentration has been diluting with the incorporation of un-labeled CO_2 released from the ocean and terrestrial reservoirs. For this reason, in order to be able to use the incorporation of radiocarbon as a measure of carbon exchange in shorter timescales (< 1 year), researchers have deliberately added tracer ^{14}C . As an example, this *pulse-chase labelling* technique has been used to assess the allocation and residence time of

photosynthetic products in a boreal forest (Carbone *et al.*, 2007). Other carbon isotopes such as ^{13}C , which is stable, have also been used as tracers. For example, Blessing *et al.* (2015) used a $^{13}\text{CO}_2$ pulse-labelling approach to study the allocation dynamics of recently fixed carbon in response to increased temperatures and drought. For more information on the subject, Epron *et al.* (2012) reviewed some of the methods used to apply this technique on trees as means to study carbon allocation dynamics.

Caveats of assessment of model structure

Overall, a better understanding of model structure can contribute to develop concrete criteria for selecting relevant modeling approaches and performance diagnostics. However, the comparison of the mathematical formulation of multiple dynamic vegetation models is impaired by the fact that they are encoded in different (often cryptic) programming languages, and the published model descriptions do not follow a standard such as the ODD (Overview, Design concepts, and Details) protocol (Grimm *et al.*, 2006, 2010), which means that sometimes the sets of equations are incomplete or the parameter values are missing. But perhaps the main caveat is that when equations are presented as lists, independent from each other, the interactions between variables are not conspicuous. Thus, it is not always clear if there are dependencies between variables that can lead to structural non-identifiabilities (Raue *et al.*, 2009) or nonlinearities.

The above mentioned caveat is one of the reasons why the general matrix model of the terrestrial carbon cycle (see equation 1.1 in Fig. 1.2) was a leap forward in the field (Luo *et al.*, 2003, 2012). Luo *et al.* (2003) proposed this framework as means to ease the analytical assessment of models; it was the result of an important effort in regards to the theoretical analysis of the carbon dynamics represented in ecosystem models, which focused on the mathematical representation of biogeochemical processes, and used mathematical tools to generalize the equations in a compact matrix form (Xia *et al.*, 2013). Thus, within this framework, the modelled terrestrial C storage capacity can be decomposed into a few traceable components that are built upon biogeochemical principles of the terrestrial C cycle.

Notice, however, that in this system of first order differential equations, the carbon processes are expressed as the sum of the C transferred between compartments (state variables) and the C fixed in the compartments -terms 1 and 2 of the first row in equation 1.1 (Fig. 1.2), respectively-. In addition, the partitioning of photosynthetically fixed C is depicted as a vector of fixed coefficients (B), with no interactions among the state variables. This indicates that this framework ignores possible nonlinear interactions among vegetation processes, which is a disadvantage because complex systems such as terrestrial ecosystems are not precisely equal to the sum of their parts (as it is assumed in linear systems). It is known that since “the carbon, nitrogen, water and energy cycles interact with each other, none of them can be calculated as a single, linear, casual relationship. These interactions are organized as feedback loops.” (Govingjee, 2009). In fact, nonlinearities have been revealed when there is competition for light in individual-based models that can accurately predict productivity and species composition (Purves and Pacala, 2008), revealing the intricate interactions vegetation-environment that are responsible for the potential capacity of vegetation to adapt to variable climatic conditions. Thus, it is necessary to find a new framework that can accommodate the nonlinear interactions that shape the ecosystem processes.

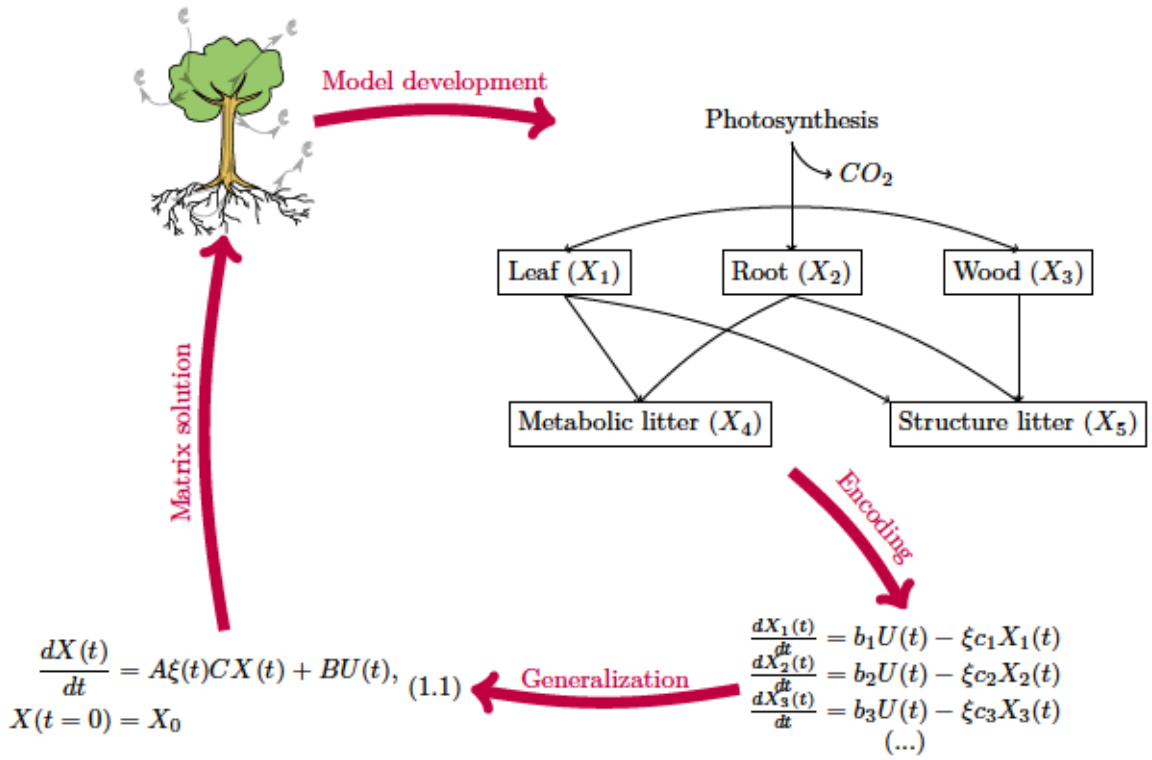


Figure 1.2: Matrix approach to carbon cycle modeling (Luo *et al.*, 2003). Empirical observations inspire model development, and the models can be encoded using ordinary differential equations. These equations can be generalized into a matrix representation, which in turn can be used to evaluate how the C sinks vary with environmental forcing over time. $X(t)$ is a vector of ecosystem carbon pools, ξ is a scalar representing effects of temperature and moisture on the carbon transfer among pools, A and C are carbon transfer coefficients between plant, litter, and soil pools, B is a vector of partitioning coefficients of the photosynthetically fixed carbon to plant pools, $U(t)$ is the photosynthetically fixed carbon, and X_0 is a vector of initial values of the carbon pools. Adapted from <http://www.cesm.ucar.edu/events/wg-meetings/2017/presentations/bgcwg+lmwg/luo.pdf>.

Research questions

The process of carbon allocation in vegetation has not yet been holistically understood, and the remaining knowledge gaps have contributed to the persistence of uncertainties in model predictions. This is a great caveat in the prediction of the response of ecosystems to abrupt changes in the environmental stressors, and the sustainability of the terrestrial carbon sequestration in the face of climate change. The working hypothesis of this thesis is that one of the main sources of the uncertainties in model predictions can be found by assessing the representation of carbon allocation in vegetation, particularly by analyzing key characteristics of model structure. Thus, the present theoretical study was designed to tackle issues such as the need of a common programming language to describe the mathematical representation of carbon allocation in vegetation. A synthesis of mathematical representations is also proposed as a framework that can be used to support the selection of relevant performance diagnostics, as well as to explore the implication of certain structures (particularly nonlinearities) in predicted dynamics. In this thesis I address the following three main questions:

1. Is there a robust framework in the realm of dynamical systems that can be used to identify key aspects of carbon allocation linked to model uncertainties?

One of the main objectives of this work was to construct a repository with a representative sample of models of carbon allocation in vegetation, and propose a mathematical generalization derived from the common model characteristics such as driving variables and their type of interactions. More specifically, I asked whether the reviewed models followed the general linear model structure proposed by Luo *et al.* (2012), or whether another structure that could accommodate nonlinearities was necessary. This general representation was intended to boost the prediction of model properties based on associated mathematical structures, and in this way be used as a standardized tool to identify modeling approaches that could better suit given questions or data assimilation projects.

2. What diagnostics can be used to assess model performance?

Certain model uncertainties can be evidenced by the fact that some model predictions are far off from expected behaviours, i.e. not all models perform well. Given that the former methods to diagnose model performance were ambiguous and not sensible enough to changes in model structure, the second objective of this work was to explore alternative diagnostics. For this purpose, three simple models were developed with structures that differed only in the number of storage compartments. Their parameters were estimated using published empirical data, and their performance was compared in terms of predictions of C age and transit time distributions. The applicability of these diagnostics was also discussed with regard to the linearity and autonomy of the models.

3. How can nonlinear interactions lead to the emergence of different patterns over time?

There are particular dynamics that can only be simulated with nonlinear models. In fact, some nonlinearities can lead to oscillations and alternative steady states, which have implications for predicted ecosystem resilience and stability. For this reason, the third objective of this work was to develop a simple nonlinear model and assess the impact of decreasing C source and sink strengths on its steady state.

Thesis overview and related publications

The three major questions that guided this research are answered in the following three chapters. Each chapter encapsulates a complete story, with an introduction, methods, results, discussion and conclusions.

Chapter 2, *Towards better representations of carbon allocation in vegetation: A conceptual framework and mathematical tool*, consists of an in depth review of a representative sample of published model descriptions. Some of these models had been previously reviewed (Malhi *et al.*, 2011; Franklin *et al.*, 2012), but not with the mathematical rigor that could enable the inference of common properties and generalizations, as the ones proposed here. These generalizations lead to the formulation of a new conceptual framework to study carbon allocation in vegetation, and a mathematical tool that can accommodate nonlinearities. This tool includes a model database and a Python 3 package that is now publicly available.

Chapter 3, *Ages and transit times as important diagnostics of model performance for predicting carbon dynamics in terrestrial vegetation models*, focuses on the effects of model structures, mainly the addition of one or two storage compartments, on the predicted distributions of ages and transit times. Given that these distributions were highly sensitive to model structures and have important consequences on predicted vegetation functioning, they are proposed as important diagnostics of model performance.

Finally chapter 4, *Sink and source limits on carbon allocation in vegetation: A dynamical system perspective*, makes use of the above mentioned Python package, and the Python library for symbolic mathematics SymPy, to study the impact of source and sink limitation on carbon allocation, in the context of dynamical systems.

The model formulated in this chapter is nonlinear, and exhibits oscillations under strong sink limitation conditions. This chapter also challenges common representations of non-structural carbon in ecosystem models and highlights its double role as a carbon source and a sink.

Chapter 2 was submitted to the journal Theoretical Ecology, and is currently under review¹, chapter 3 was published in Biogeosciences², and chapter 4 will soon be submitted for publication³.

¹Ceballos-Núñez, V., M. Müller, and C. A. Sierra. Towards better representations of carbon allocation in vegetation: A conceptual framework and mathematical tool. (in review)

²Ceballos-Núñez, V., A. D. Richardson, and C. A. Sierra. 2018. Ages and transit times as important diagnostics of model performance for predicting carbon dynamics in terrestrial vegetation models. *Biogeosciences*, 15:1607–1625.

³Ceballos-Núñez, V., J. Huang, H. Hartmann, and C. A. Sierra. Sink and source limits on carbon allocation in vegetation: A dynamical system perspective. (in prep)

Towards better representations of carbon allocation in vegetation: A conceptual framework and mathematical tool

The representation of carbon allocation (CA) in ecosystem models differs tremendously, resulting in diverse responses to climate change as evidenced by their divergent trajectories in results from model inter-comparisons. Several studies have also highlighted discrepancies between empirical observations and model predictions, attributing these differences to problems of model structure. We analyzed the mathematical structure of CA in models using concepts from dynamical systems theory; we reviewed a representative sample of models of CA in vegetation, and developed a model database within the Python package `bgc-md`. We ask whether these representations can be generalized as a linear system, or whether a more general framework is needed to accommodate nonlinearities. We found that some of the vegetation systems portrayed in the reviewed models have a fixed partitioning of photosynthetic products, independent of environmental forcing. Vegetation is often represented as a linear system without storage compartments. Yet, other structures with non-linearities have also been proposed, with important consequences on the temporal trajectories of ecosystem carbon compartments. The proposed mathematical framework unifies the representation of alternative CA schemes, facilitating their classification according to mathematical properties, as well as their potential temporal behavior. It can represent complex processes in a compact form, which can potentially facilitate dialog among empiricists, theoreticians, and modelers.

Introduction

Coupled climate-carbon cycle models predict divergent trajectories of future fluxes among Earth's major carbon reservoirs, with no consensus on whether terrestrial ecosystems will act as a net source or sink of carbon with the atmosphere (Friedlingstein *et al.*, 2006, 2014). This

net flux is the result of the overall rate at which CO_2 is assimilated by the vegetation via photosynthesis, the partitioning of the photosynthetic assimilates to vegetation parts, from here on *compartments*, and the time carbon atoms remain in these compartments before being released back to the atmosphere (Lacointe, 2000; Schimel *et al.*, 2001; Trumbore, 2006; Canadell *et al.*, 2007; Franklin *et al.*, 2012; Körner, 2017). All these processes, which are associated with the concept of carbon allocation (CA), have been implemented in different ways in ecosystem models (Sitch *et al.*, 2003; Purves and Pacala, 2008; Schiestl-Aalto *et al.*, 2015), and this may be one of the reasons behind the lack of consensus between their predictions (Xia *et al.*, 2017).

Although there is increasing attention towards improving the representation of CA in models, there are still ambiguities in concepts and definitions. Despite previous attempts to clarify terminology, the concept of *carbon allocation* is still being used to describe both, **patterns** and **processes**, which leads to an ambiguity that has persisted over a decade after first being exposed by Litton *et al.* (2007) (see Fig. 2.1). Furthermore, models have been classified according to their conceptual design of the CA scheme, as models with constant coefficients, or dynamic¹ allocation, among others (Franklin *et al.*, 2012); but, yet another ambiguity arises here with the term *dynamic carbon allocation*, because it is unclear whether this implies dynamic functions for fluxes or for partitioning of photosynthetic input.

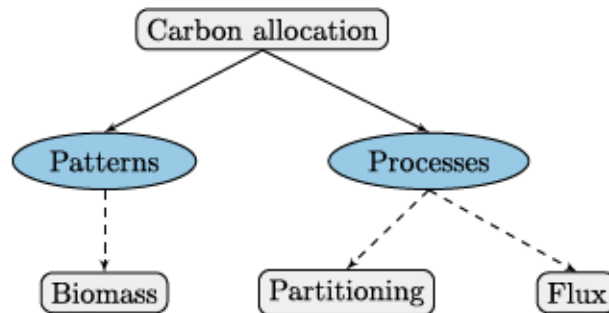


Figure 2.1: *Carbon allocation* is a general term that overarches patterns (biomass) and processes (flux and partitioning) according to Litton *et al.* (2007). As an example, the sentence *the carbon allocated to the vegetation compartment X*, may have three different meanings depending on the context: a) the amount of carbon present in *X* at a certain time (**biomass**), b) the portion of photosynthetic input that goes to *X* (**partitioning**), and c) the **flux** of carbon into and out of *X*.

Some CA schemes have been partly inspired by experimental results or by theoretical analyses, but it is still uncertain how the different mathematical expressions of the models affect the overall dynamics of the vegetation system. Several factors have hindered the reduction of this uncertainty. On the one hand, previous synthesis studies have only focused either on very general ideas about modeling CA, or on the numerical output of the models *per se* (Franklin *et al.*, 2012; De Kauwe *et al.*, 2014; Walker *et al.*, 2014). On the other hand, the effort to reconcile diverse empirical findings and attain realistic predictions has prompted the use of a

¹*Dynamic* is a term used for time-evolutionary phenomena or the part of mathematical science that is used for the representation and analysis of such phenomena (Luenberger and Hill, 1979).

large number of functions and parameters in models (Quaiser *et al.*, 2011), and this increase in model complexity has obscured the identification of the main represented processes and the understanding of overall system behavior. Indeed, cryptic programming styles make it much more difficult to understand what is going on and what specific functions are implemented in a particular model. For this reason, new approaches have been proposed to express these models in tractable mathematical expressions that can be easily related to ecological ideas or principles, with known mathematical properties (Luo *et al.*, 2003; Xia *et al.*, 2013; Luo *et al.*, 2017).

To the best of our knowledge, a comprehensive analysis of the common mathematical expressions used to model CA in vegetation has not been performed yet. This was the main goal of this study: to synthesize different mathematical expressions used to represent CA in models. For this purpose, we took advantage of the mathematical concept of *dynamical system*, which is a general abstraction to describe a rule that determines the future behavior of a set of variables based on their current state (Luenberger and Hill, 1979). In other words, the patterns from the present are a result from the patterns in the past. These time linkages among variables can be represented using difference or differential equations depending on whether the dynamic behavior occurs in discrete or continuous time, respectively. A *difference equation* relates the value $y(k)$, at point k , to values at other points (e.g., $y(k+1) = ay(k)$, $k = 0, 1, 2, \dots$). And a *differential equation* connects a function $y(t)$ defined on an interval of continuous time and some of its derivatives. For further details on these concepts please refer to (Luenberger and Hill, 1979, p.27).

The equations used to model CA in vegetation can then be studied within a comprehensive framework. A valuable contribution to this was the general matrix model of the terrestrial carbon cycle proposed by Luo *et al.* (2003). This matrix decomposes terrestrial carbon storage into a few traceable components (Xia *et al.*, 2013). Interestingly, these components were built upon biogeochemical principles of the terrestrial carbon cycle, as it is observed in the following linear dynamical system:

$$\begin{aligned}\frac{dX(t)}{dt} &= \xi ACX(t) + BU(t), \\ X(t=0) &= X_0,\end{aligned}\tag{2.1}$$

where $X(t)$ is a vector whose elements represent the size of individual carbon compartments, A is a square matrix of transfer coefficients among compartments, C a square matrix of processing rates within each compartment, ξ scales the effects of temperature and moisture on C processing and transfer rates, B is a vector of partitioning coefficients of C to growth of tissues, $U(t)$ is the ecosystem C influx, and X_0 is a vector of initial values of the carbon compartments (Luo *et al.*, 2012).

Although this matrix equation has an important role mapping the mathematical formulations

to the modeled biogeochemical processes, it has a few limitations: the partitioning coefficients (B) are fixed; and it does not allow for nonlinear interactions such as the case when photosynthetic rates depend on the storage of carbon in other compartments. This is problematic because complex systems such as terrestrial ecosystems are not necessarily linear (Luenberger and Hill, 1979; Zobeley *et al.*, 2005). In fact, certain nonlinearities have been revealed when there is competition for light in models that can accurately predict productivity and species composition (Purves and Pacala, 2008). Thus, it is necessary to define a new framework that: a) has more flexibility to accommodate different type of inputs (e.g. C assimilation rate, Gross Primary Productivity -GPP, Net Primary Productivity -NPP), b) allow for a dynamic partitioning of inputs or storage reserves, and c) can accommodate nonlinearities among system components.

In this contribution, we studied the process of CA in vegetation from a dynamical systems perspective. We addressed the following questions: 1. How can we express the carbon allocation concept within the context of dynamical systems? 2. Is there a mathematical framework that can accommodate nonlinearities? 3. Can we systematically identify common model properties and categorize the models accordingly? We reviewed published model descriptions and constructed a database with a selection of them. This database aided us during the analysis of the sets of equations that represent CA in vegetation. Based on this model synthesis, we were able to identify key characteristics from which we inferred the proposed conceptual framework and mathematical tool.

Methods

In order to avoid the ambiguities mentioned in the introduction, we contextualized the CA concept within the more general theory of dynamical systems. Thus, by modifying the matrix representation from equation 2.1, we propose the following definition:

Working definition of *carbon allocation*

Carbon allocation is the balance (net flux) of the C flows into, between, and out of the vegetation compartments, because the amount of carbon in a single compartment at a given time (t) is the balance between the C that has flown into and out of this compartment. This is illustrated with an example of a two-compartment system (Fig. 2.2).

This definition makes it possible to distinguish between the different cases constantly grouped as *carbon allocation* (see example in Fig. 2.1), by assigning each case to its corresponding term in the equation 2.2 (Fig. 2.2) as follows: a) “the C in X ” refers to the *biomass* = x , b) “the C partitioned to X ” is the fraction of the input that goes to that compartment, i.e. *partitioning* = $\vec{\beta}$, and c) “the carbon allocated to X ” is the result of the whole process, i.e. the net *flux* =

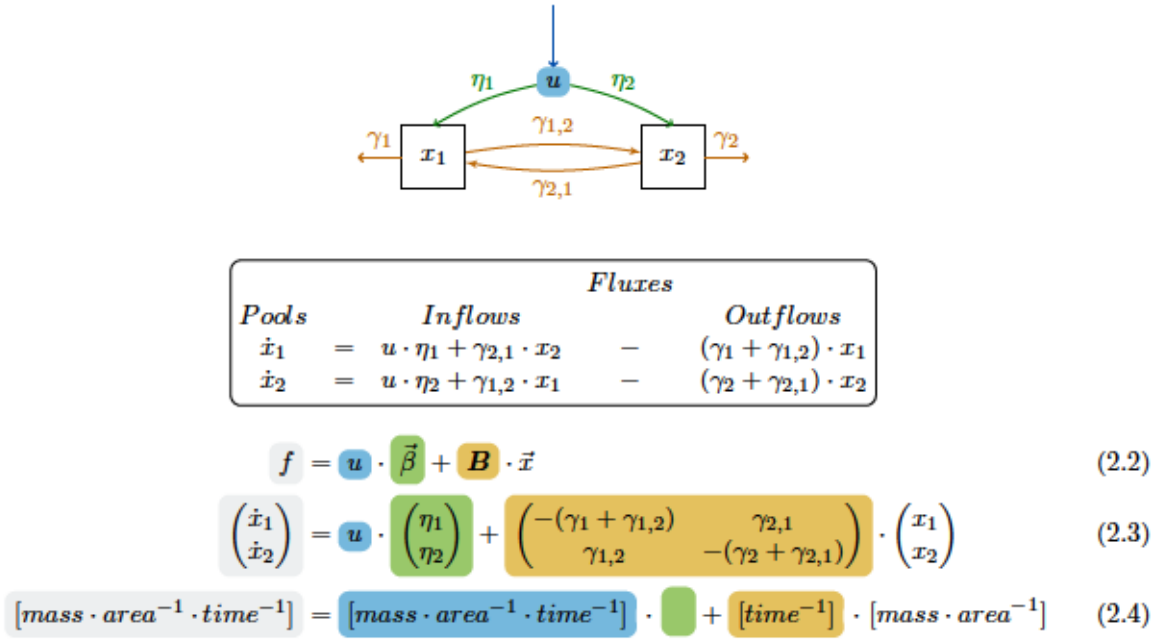


Figure 2.2: General mathematical representation of carbon allocation (CA) in a 2-compartment vegetation model. The colors facilitate the identification of the different modules; grey: entire CA process, blue: photosynthetic input, green: partitioning of the input, and orange: C transfers between and out of the compartments. The arrows point towards the direction of the movement of the compartment content. The letters above them symbolize the parameters that regulate this flux. Other symbols are \vec{x} : vector of states for vegetation (state variables); $\dot{\vec{x}} = d\vec{x}/dt$: Changing quantity of vegetation compartment x with respect to time (state variables x_1 and x_2); f : Function valued vector that relates the changing quantities that take place between the vegetation compartments; u : Scalar function that represents the primary productivity -system input- and may be an assimilation rate, GPP, or NPP; $\vec{\beta}$: Vector containing the partitioning coefficients of photosynthetic input; B : Carbon transfer coefficients between plant, litter, and soil compartments. Equation 2.3 was derived as described in (Anderson, 1983) and (Sierra *et al.*, 2012). Equation 2.4 shows the units that the different components may have, highlighting their participation as fluxes (f , u), coefficients -fractions- ($\vec{\beta}$), and rates (B) in the model.

right hand side of the Ordinary Differential Equation -ODE (equations 2.2 and 2.3).

This definition was the result of the review of several published model descriptions, and is the basis of the mathematical framework that we propose and use to further analyse the main characteristics of the model descriptions (e.g. driving variables and parameters², nonlinearities). The organization of the equations within this framework also facilitates the identification of rates ($[mass \cdot time^{-1}]$), fractions ($[\]$, unitless), and fluxes ($[mass \cdot area^{-1} \cdot time^{-1}]$), just by observing their units. As means to automate the PMDs analysis and promote the use of this framework to understand the CA representation in models, we developed a model database and an accompanying Python 3 package called bgc-md (Fig. 2.3).

Selection of published model descriptions (PMDs)

We reviewed PMDs of ecosystem models, and extracted the equations and descriptions contained in the CA module. Our literature search was not exhaustive, but we obtained a representative

² Variable is a model attribute that changes during the model simulation. A parameter is a model attribute that (e.g. rates) does not change during the model simulation. Note that some factors that have been called parameters (e.g. soil moisture...) but actually are dynamic (are functions of time or other variables) are indeed variables (<http://web.hwr.arizona.edu/hwr642/Generic/Content/Definitions/DefinitionsText.html> and <http://www.math.tamu.edu/~phoward/m647/modode.pdf>).

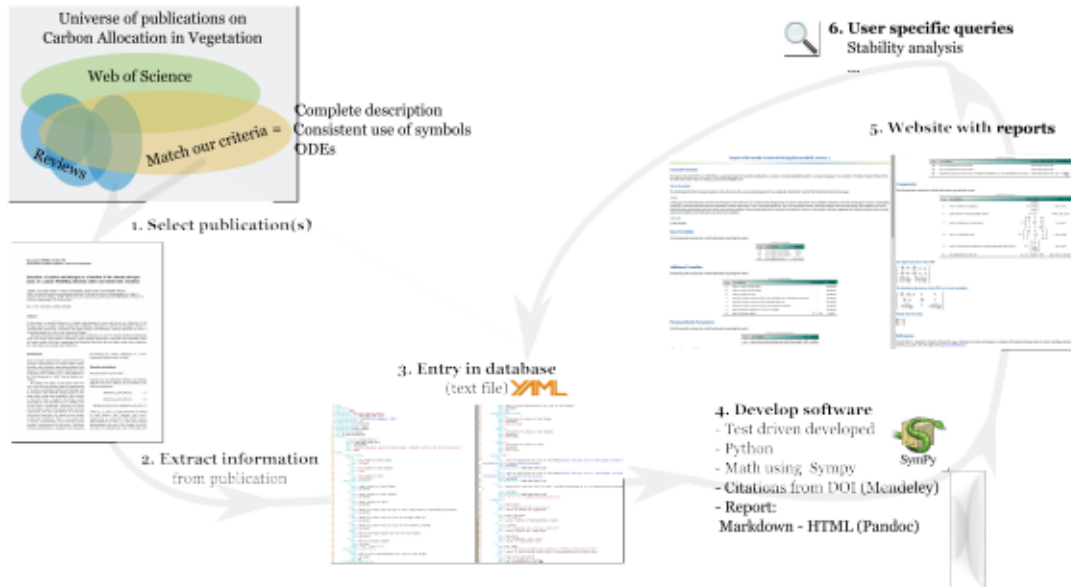


Figure 2.3: This figure summarizes our methods, and highlights the software that we have used and the one that we are developing. As it may be seen, the development of the entries and of the software is shaped by the user queries. This database is dynamic, and will be enriched with future contributions of model entries and implementation of new functionalities.

sample of PMDs by focusing our selection to published reviews (Franklin *et al.*, 2012; De Kauwe *et al.*, 2014; Walker *et al.*, 2014), and Web of Science. In the latter case, we found 135 published articles about models of CA by searching for the following keywords: Major concepts: Models “and” simulations AND Major concepts: Environmental Sciences; ts=(carbon near/4 allocat*). From these, we selected complete PMDs in which the models were described using ordinary differential equations (ODEs) with a consistent use of symbols.

Protocol for analyzing the PMDs using the Python package bgc-md

The Python 3 package, bgc-md (<https://github.com/MPIBGC-TEE/bgc-md>) consists of a model database, and additional code that (a) extracts the information from each database entry, (b) generates reports, and (c) performs computations such as model runs, calculation of jacobian and eigenvalues, and generates various plots for comparison. The entries in the database consist of text files written in YAML format (www.yaml.org). Each entry corresponds to a selected publication -PMD, and is created as follows:

1. The first lines of an entry are used for the metadata -information needed in order to identify the model, the author of the entry, the publication where it came from, and some model characteristics:

```
name: [model's short name]
longName:
version:
entryAuthor:
entryAuthorOrcid:
modApproach: [e.g. process based]
```

```
partitioningScheme: [fixed or dynamic]
claimedDynamicPart: ["yes" if they claimed to prioritize a compartment during partitioning, else "no"]
doi:
model:
```

The doi of the original publication is used with the API from Mendeley (www.mendeley.com) to automatically generate citations.

2. ‘model:’ is a section that is divided into subsections (e.g. state variables, photosynthetic parameters, among others), which consist of a list of symbols that represent variables or parameters; for example:

```
- state_variables:
  C_f:
    desc: Carbon in foliage
    unit: "kgC*m^{-2}"
    type: [parameter or variable]
```

If the function to calculate a variable is provided (e.g. $\text{NPP} = \text{GPP} - \text{R}$), the equation is written using symbolic mathematics according to the syntax of the python package SymPy (Meurer *et al.*, 2017).

The final component of the ‘model’ section is the subsection ‘components’. Here the sets of ODEs are factorized into the matrix form $\dot{f} = u \cdot \vec{\beta} + \mathbf{B} \cdot \vec{x}$.

```
- components:
  - x:
    key: state_vector
    exprs: "x=Matrix(3,1,[C_leaf, C_stem, C_roots])"
    desc: vector of states for vegetation
  - u:
    desc: scalar function of photosynthetic inputs
    exprs: "u = NPP"
    key: scalar_func_phot
  - beta:
    key: part_coeff
    exprs: "beta=Matrix(4,1,[eta_L,eta_S,eta_R])"
    desc: vector of partitioning coefficients of photosynthetically fixed carbon
  - B:
    key: cyc_matrix
    exprs: "B = Matrix([[ -gamma_L,0,0],
                        [0, -gamma_S 0],
                        [0, 0, -gamma_R]])"
    desc: matrix of cycling rates
  - f_v:
    desc: the righthandside of the ode
    exprs: "f_v = u*beta + B*x"
    key: state_vector_derivative
```

3. The bgc-md package computes the equations in the matrix form and produces reports in html format. These reports summarize the PMDs and display the set of equations in a readable way. In order to allow a quick comparison of a list of models, the package can also generate a website with reports and graphs that can be navigated. Two of such graphs are Fig. 2.4 and 2.5.

Code availability

All of the simulations and figures for this work can be reproduced using the code and data provided in the supplementary material.

Results

From a total of 150 reviewed publications, only a few of them (17) met the requirements of having a CA scheme described with a complete set of difference or differential equations (Table 2.1). Evidently, we did not include PMDs without equations (e.g. Chen and Reynolds, 1997). Other types of publications excluded from our review were those concerned with aquatic vegetation (e.g. Soetaert *et al.*, 2004), tree ring simulations (e.g. Eglin *et al.*, 2010; Lazzarotto *et al.*, 2009; Li *et al.*, 2014), pipe models (Valentine, 1999), annual plants (Fox, 1992), and vegetation systems with two compartments or less (e.g. Huntingford *et al.*, 2000).

Table 2.1: Classification of the different models analyzed according to their mathematical structure.

Structure	Models with corresponding structure				
Linear ODEs	Name	Number of Compartments	Partitioning of photosynthetic input	Diagonal matrix?	Source
$f = u(t) \cdot \vec{\beta} + \mathbf{B} \cdot \vec{x}$	FOREST-BGC	4	fixed	yes	(Running and Coughlan, 1988)
	CASA	4	fixed	yes	(Potter <i>et al.</i> , 1993)
	G'DAY	3	fixed	yes	(Comins and McMurtrie, 1993)
	-	3	fixed	yes	(Murty and McMurtrie, 2000)
	CABLE	3	fixed	yes	(Wang <i>et al.</i> , 2010)
	-	3	fixed	yes	(Luo <i>et al.</i> , 2012)
Nonlinear ODEs	-	5	fixed	yes	(DeAngelis <i>et al.</i> , 2012)
	$f = u(x, t) \cdot \vec{\beta} + \mathbf{B} \cdot \vec{x}$	-	3	fixed	(King, 1993)
	IBIS	3	fixed	yes	(Foley <i>et al.</i> , 1996)
	CTEM	4	dynamic	yes	(Arora and Boer, 2005)
	IBIS	3	dynamic	yes	(Castanho <i>et al.</i> , 2013)
	$f = u(x, t) \cdot \vec{\beta}(x, t) + \mathbf{B} \cdot \vec{x}$	CEVSA2	3	dynamic	(Gu <i>et al.</i> , 2010)
	$f = u(t) \cdot \vec{\beta} + \mathbf{B}(x, t) \cdot \vec{x}$	ACONITE	6	fixed	(Thomas and Williams, 2014)
	$f = u(x, t) \cdot \vec{\beta} + \mathbf{B}(x, t) \cdot \vec{x}$	-	5	dynamic	(Hilbert and Reynolds, 1991)
	JeDi-DGVM	6	dynamic	no	(Pavlick <i>et al.</i> , 2013)
	$f = \vec{u}(x, t) + \mathbf{B} \cdot \vec{x}$	DALEC	4	dynamic	(Williams <i>et al.</i> , 2005)
	ISAM	4	dynamic	yes	(El-Masri <i>et al.</i> , 2013)

The vegetation systems described in the PMDs correspond to different hierarchies, ranging from individual plants (1 model), to forests (4 models), regions (2 models), up to the whole globe (10 models). In terms of time resolution, the processes described in the PMDs often take place at different scales; there can be daily simulations of photosynthesis, evapotranspiration, and soil water dynamics, and annual updates of vegetation structure and plant functional type population densities (Sitch *et al.*, 2003). Another example of such a wide time scale range was observed in the model Tethys-Chloris by (Fatichi and Leuzinger, 2013), in which the photosynthesis, energy and water fluxes are resolved hourly, and the ‘carbon allocation’ and turnover take place at a daily time step. This means that the input (u) of these models is often portrayed as a faster process as the partitioning ($\vec{\beta}$) and cycling (\mathbf{B}).

Moreover, different modeling approaches (conceptual and mathematical) have been used to simulate CA as a whole, and the partitioning in particular. Table 2.2 summarizes the main groups in which the models can be classified according to these different approaches. Our contribution to this classification, which builds on the previous work of De Kauwe *et al.* (2014)

and Walker *et al.* (2014), is a classification based on the mathematical formulation of CA ($f(\vec{x}, t)$), derived from the fact that several models have been described using linear ODEs, nonlinear ODEs, or difference equations.

Table 2.2: Classification of the carbon allocation (CA) module of different models according to the main conceptual and mathematical approach used.

Modeling approach	Mathematical formulation	Conceptual design of C partitioning
Process based	Difference equations	Fixed coefficients
Individuals based	Linear ODEs	Dynamic
	Nonlinear ODEs	

ODEs: Ordinary differential equations.

Our literature search revealed that in nine of the 17 PMDs selected, it was claimed that they had a ‘dynamic carbon allocation’ because their objective was to simulate the vegetation response to environmental cues (e.g. lack of water or light) via selective partitioning of newly photosynthesized carbon to a limiting compartment. However, three of these nine PMDs had a fixed partitioning scheme (fixed coefficients) and the environmental scalars were only found in the photosynthesis or turnover modules (see Fig. 2.4). Within such a scheme, the changes in environmental conditions only affect the amount of C entering or leaving the system as a whole, i.e. the limiting compartment would not be favored in the partitioning of C. This is an example of how alternative interpretations of the term ‘dynamic carbon allocation’ can lead to misleading model descriptions. Other examples of this were also observed in publications that were not selected for further review because they did not abide to our criteria -e.g. model ForCent by Parton *et al.* (2010).

This supports the need to use the working definition of CA proposed in the methods to continue with our analysis, leaning on the biogeochemical relevance of the terms in equation 2.2 (i.e., photosynthetic input- u , partitioning- $\vec{\beta}$, cycling- \mathbf{B} , and stocks (state variables)- \vec{x}). For this reason we analyzed the components of each term instead of searching for connections between numerous equations spread across modules (e.g. stomata, physiology, canopy, carbon balance), which is a very common way to organize the equations in ecosystem models. Identifying these connections, and especially the type of interactions between variables and parameters is important because some dependencies between state variables can lead to nonlinearities.

In light of this working definition, we could find the characteristics that the 17 PMDs had in common, such as their driving variables and their interactions. We found that in 13 of the 17 PMDs, there is a lack of carbon exchange between the vegetation compartments. This characteristic was diagnosed by the bgc-md package, which automatically identified that their cycling matrix \mathbf{B} is diagonal -the elements of the off diagonal are zeros (see Fig. 2.5). Moreover, the only cases in which the compartments exchange C is when there is a labile C

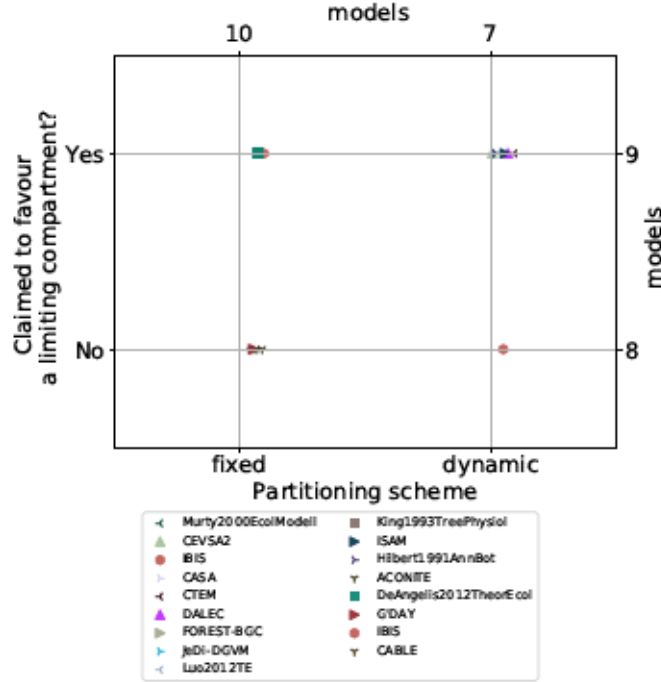


Figure 2.4: Comparison between published model descriptions where it was claimed that the model intended to have a partitioning scheme that favoured a limiting compartment, versus which of those had indeed a dynamic partitioning scheme.

compartment, e.g. the model DALEC (Williams *et al.*, 2005), but such compartments (labile or nonstructural carbohydrates -NSC) were ignored in eight of the 17 PMDs, which only have three state variables: foliage, wood, and roots.

Furthermore, we found two distinct ways to represent respiration in vegetation: (a) growth respiration is often portrayed as a percentage of the C influx, which is a calculation performed within u independently from the amount of C stored in the compartments -state variables; in contrast, (b) maintenance respiration is a flux that depends on the amount of C stored, because it is the product of the multiplication of state variables and cycling rates ($\mathbf{B} \cdot \vec{x}$). These two representations have different implications. In case (a), respiration represents the cost of growing organs, which is the amount of photosynthetically fixed C that cannot be used to build new tissues. In case (b), respiration is the metabolic cost of maintaining the existent tissue, which depends on how much tissue there is.

In most PMDs, the environmental variables driving the models (e.g. temperature, water and nutrients content, light availability) were found in the equations that compute the photosynthetic input (u), but sometimes air temperature and atmospheric CO_2 concentration were implicitly included in environmental scalars. In addition, the photosynthetic input generally does not

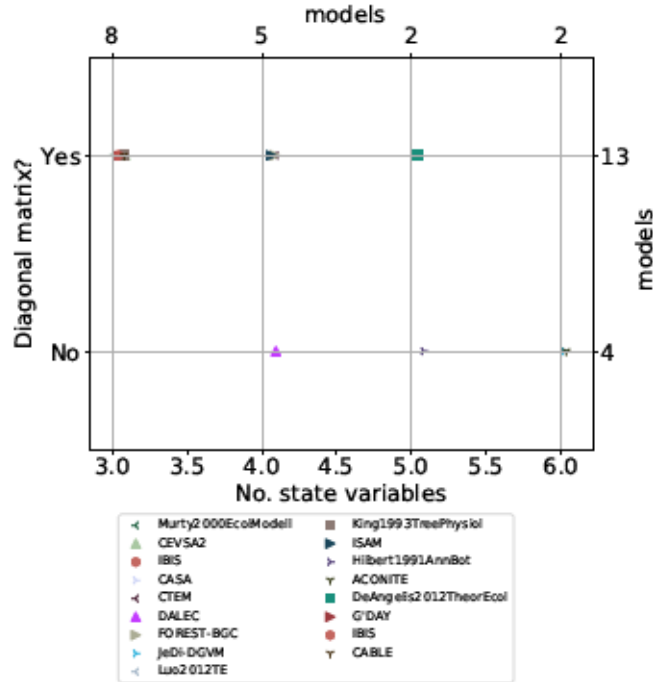


Figure 2.5: Comparison between number of state variables in models, and whether their cycling matrices are diagonal or not. In models with diagonal cycling matrices (off diagonal = 0), there is no C exchange between the compartments.

depend directly on the C content of the leaves (one of the state variables), rather on the leaf area index (LAI), which is not always expressed in terms of leaf C.

In contrast to the input dependency on environmental cues, the C transfers that shape the compartments via partitioning ($\vec{\beta}$) of photosynthetic input and C cycling (\mathbf{B}) are seldom driven by climate. In some cases the partitioning is constrained by the ratio between some compartments (e.g. C foliage : C roots), but the most common constraint is the use of fixed coefficients that should sum up to 1 (see Fig. 2.4). One example is the model by King (1993), which was designed to analyze the influence of partitioning to root and foliage on forest production. This model has a structure in which the partitioning ($\vec{\beta}$) and the cycling (\mathbf{B}) contain parameters, instead of state variables or time dependent variables. Thus, its partitioning scheme is independent of changes in the environment. In other schemes the partitioning can switch between fixed and dynamic, depending on the sensitivity to changes in resource availability (e.g. the model CEVSA2 by (Gu *et al.*, 2010)).

Some PMDs have an intricate C cycling dynamic; for example, the model proposed by Hilbert and Reynolds (1991) has a structure inspired in the hypothesis of balanced root and shoot activity (Davidson, 1969) and the response of specific shoot activity to resource availability. This model has five state variables: mass of leaf proteins, leaf structural components, roots,

substrate carbon, and substrate nitrogen. The photosynthetic carbon is produced in the substrate compartments, and from there it is cycled to the other compartments. In cases like this, where all the photosynthetically fixed C is first stored in a compartment, there is either no partitioning or $\vec{\beta} = [1, 0, 0, 0]$. Conversely, the \mathbf{B} matrix is highly nonlinear because the C cycling depends on the state variables. This is why we broadened the mathematical framework and propose a new one that can accommodate nonlinearities.

The new mathematical framework

Based on the three categories in Table 2.2 and the fact that equation 2.2 can have particular cases based on the dependencies of its terms, we propose a new mathematical framework to study the CA representation in models (Fig. 2.6).

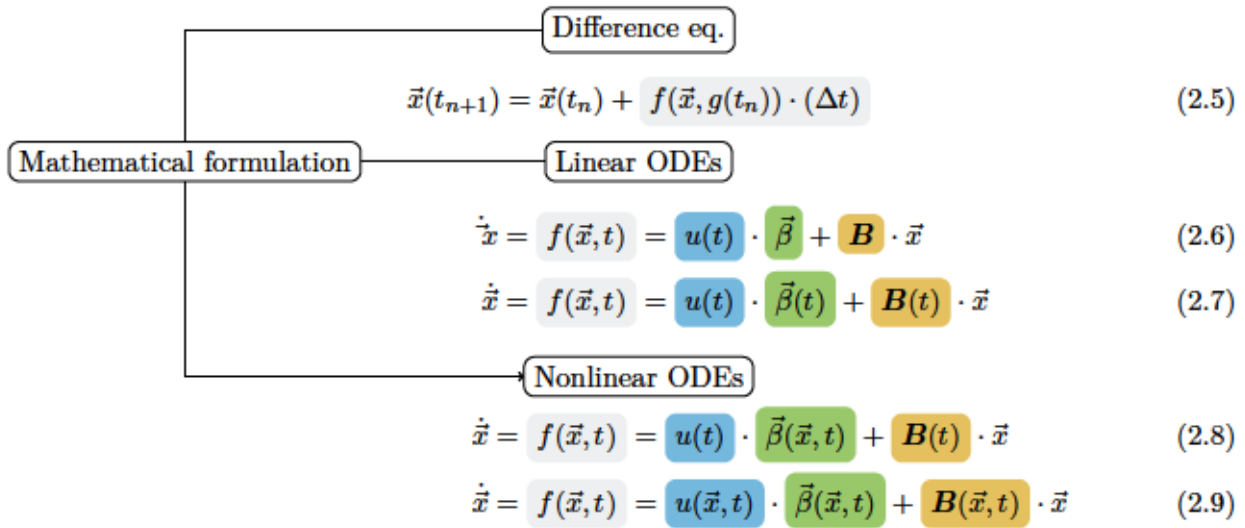


Figure 2.6: Model classification according to their mathematical formulation, where $\vec{x}(t_{n+1})$ is a vector of states for vegetation at time t_{n+1} . $f(\vec{x}, g(t_n))$ represents the dependency of the function valued vector f on state variables (\vec{x}) and time-dependent functions ($g(t_n)$); it can also depend on state variables and time: $f(\vec{x}, t)$. The time step size is $\Delta t = t_{n+1} - t_n$. The dependency of u in time and state variables is represented by $u(\vec{x}, t)$. $\vec{\beta}(t)$: partitioning function valued vector that represents the time dependency of $\vec{\beta}$, which may also depend on vegetation compartments (allowing for nonlinearities): $(\vec{\beta}(\vec{x}, t))$. $\mathbf{B}(t)$ represents the time dependency of the cycling matrix \mathbf{B} .

We classified the 17 PMDs according to their mathematical formulation -structure (see Table 2.1). The analysis behind this classification can be found on the reports generated for each of the PMDs using the bgc-md package (see supplementary material).

Notice that not all models have separated photosynthetic input u and partitioning $\vec{\beta}$. Particularly, the models with a partitioning scheme that depend on phenology often formulate this dependency as a set of *if* statements or piecewise functions. Thus, the u and $\vec{\beta}$ fuse together into the vector of photosynthetic inputs to each compartment \vec{u} , e.g. DALEC (Williams *et al.*, 2005) and ISAM (El-Masri *et al.*, 2013) (see Table 2.1). Another model with a partitioning scheme that depends on phenology according to its description is CASTANEA (Dufrene *et al.*, 2005), but this publication could not be included in the database because of the lack of equations.

Implications of nonlinearities using an example of a vegetation system with four compartments

This new framework takes into account that the mathematical abstraction from Fig. 2.2 may vary among models, depending on how their variables and parameters interact with each other, i.e. whether they depend on each other or not. These dependencies have informative ecological implications such as positive feedback loops in the scalar function of system input u , or sink-dependent fluxes of the cycling matrix \mathbf{B} (see Fig. 2.2 and 2.6), which will be further explained later in this section. These dependencies ultimately determine whether a model is linear or nonlinear. Nonlinearities are the result of multiplicative interactions between the state variables on which the fluxes depend. They can have a major impact on the model dynamics, when compared to a linear model with the same compartments. We can illustrate this using a couple of simple models; a linear model, and a nonlinear model (see Table 2.3). Both of them are autonomous systems (with no external drivers) with four compartments: foliage, nonstructural C (NSC), wood, and roots (see Fig. 2.7). For practical purposes, we show the results of only two compartments.

Table 2.3: Sets of equations of the models from the example

Type of model	Linear	Nonlinear
Matrix representation	$\dot{\mathbf{f}} = \mathbf{u} \cdot \vec{\beta} + \mathbf{B} \times \vec{x}_t$	$\dot{\mathbf{f}} = \mathbf{u}_x \cdot \vec{\beta} + \mathbf{B}_x \times \vec{x}_t$
ODEs	$\dot{C}_f = u \cdot \eta_f + \gamma_{f,NSC} \cdot C_{NSC} - (\eta_{NSC} + \gamma_f) \cdot C_f$ $\dot{C}_{NSC} = \eta_{NSC} \cdot C_f - (\eta_r + \eta_w + \gamma_{f,NSC}) \cdot C_{NSC}$ $\dot{C}_w = \eta_w \cdot C_{NSC} - \gamma_w \cdot C_w$ $\dot{C}_r = \eta_r \cdot C_{NSC} - \gamma_r \cdot C_r$	$u = k_1 \cdot C_f \cdot C_{NSC}^{-1}$ $\eta_{NSC} = v_1 \cdot (k_1 + C_{NSC})^{-1}$ $\gamma_{f,NSC} = v_2 \cdot (k_2 + C_f)^{-1}$

Both models have the same sets of ordinary differential equations (ODEs), but the nonlinear has replaced some parameters for functions (right column). \dot{C} : changing amount of carbon in foliage (f), nonstructural carbohydrates (NSC), wood (w) and roots (r), with respect to time; u : photosynthetic input; k_1 : absorption rate; k_1 , k_2 , v_1 and v_2 : Michaelis-Menten parameters; η_f : flux rate of photosynthetically fixed C to foliage; η_{NSC} : flux rate of C from foliage to NSC; η_w : flux rate of C from NSC to wood; η_r : flux rate of C from NSC to roots; $\gamma_{f,NSC}$: flux rate of C from NSC to foliage; $\gamma_{f,w,r}$: rate at which C leaves each compartment (e.g. respiration, litter).

In the model comparison from Fig. 2.7 it is evident that the differences in the schemes of C cycling between the foliage and NSC impacted the model outcome. Given the intricate nonlinear interactions between these compartments, the C stocks oscillated, reducing the chance to predict the C stocks at a given time; i.e. while one can predict that increasing amounts of C in the foliage will result in increased NSC in the linear case, the C accumulation of NSC with respect to foliage is constantly changing in the nonlinear case (see the phase planes in Fig. 2.7). Another particular characteristic of the nonlinear model was the positive feedback loop in the input, which resulted in a rapid C gain in the foliage at the beginning of the simulation.

Discussion

A detailed analysis of the mathematical representation of the CA component of the ecosystem models has allowed us to identify common structures and do generalizations. We were able to obtain a deep insight into the properties of a system, by identifying the factors on which photosynthesis, and C partitioning and cycling depend. This assessment motivated the formulation of this new mathematical framework, which emerges as a powerful tool to study carbon allocation in models.

Seemingly, the published model descriptions that we reviewed overlook key properties, and thus they might be a too simplistic representation of the processes involved in carbon allocation in vegetation. One of the oversimplifications that we observed was the fixed partitioning scheme from most of the PMDs. Evidently, models with fixed coefficients for C partitioning and cycling would fail to simulate a vegetation that responds to environmental cues by changing its partitioning scheme.

Another oversimplification was the lack of carbon exchange between the vegetation compartments, as well as the absence of storage (or labile) compartments. In fact, the role of non-structural or labile carbon has proven to be more important than just an overflow compartment (Richardson *et al.*, 2013; Dietze *et al.*, 2014; Doughty *et al.*, 2015; Hartmann *et al.*, 2015; Martínez-Vilalta *et al.*, 2016; Muhr *et al.*, 2016). We speculate that the source-sink relationship between the vegetation C compartments may have important implications in phenology (seasonal variability) in deciduous forests, because the stored C can be cycled to the other compartments when the growing season starts, thus explaining the rapid loss and replenishment of carbon in foliage (Trumbore *et al.*, 2015). Unfortunately, this model structure was rarely observed in large-scale models.

The model structures are also too simplistic because they are mostly linear; the carbon processes are expressed as the sum of the C fixed in the compartments and the one leaving the compartments -terms 1 and 2 of the first row in equation 2.1, respectively-. This linear structure ignores possible nonlinear interactions among vegetation processes that can arise when partitioning depends on state variables ($\vec{\beta}(\vec{x}, t)$), as an example. Even though these simplifications increase the speed of model runs without jeopardizing the trends at global scales, they could result in prediction errors while trying to simulate finer spatio-temporal scales. Most importantly, these oversimplifications could be the reason why some models fail to capture the response of vegetation to extreme climatic changes.

Categorizing models of interest in this framework has several advantages (as described above and in the following section), but a categorization performed solely based on the published model descriptions (PMDs) might not be advisable because they leave out important details. The

PMDs of complex models such as the Dynamic Vegetation Models (DGVMS) often lack complete sets of equations, parameter values, and, when difference equations are used, they do not describe the way in which the time steps are performed (e.g. LPJ by Sitch *et al.* (2003) and O-CN by Zaehle and Friend (2010)). Given that these details not only guarantee the reproducibility of the results, but the reliability of the model categorization within this framework, the source code of these models also needs to be assessed. As challenging as that process may be, the development of such models within this framework can be an efficient way to improve their performance and the one of the Earth system models to which they are coupled. Thus, we highly encourage other researchers to contribute with their own models to this database. It is also important to mention that the current functionalities of the database limit the inclusion of individual-based models (e.g. aDGVM by Scheiter and Higgins (2009)), but this issue will hopefully be solved in the future.

Implications and future studies

We have identified some of the impacts that certain model structures have on the simulations, in agreement with other systematic studies (Holling, 1973; Jacquez and Simon, 1993; Strogatz, 1994). This leads us to another of the main contributions of this framework, which is the ease to identify models that fall into the Compartmental Systems category. Compartmental systems are those whose compartments exchange material, and according to the qualitative theory proposed by Jacquez and Simon (1993), their structure may have important implications in the stability of the system. As an example, systems with time-dependent variables such as $f(\vec{x}, t) = u(\vec{x}, t) \cdot \vec{\beta}(\vec{x}, t) + \mathbf{B}(\vec{x}, t) \cdot \vec{x}$, are classified by this theory as non-autonomous systems and one of their characteristics is that they do not have a steady state (see stability of non-autonomous systems in Jacquez and Simon (1993)). This is an important property to consider, especially when choosing methods to make other calculations (e.g. mean age of carbon) under the steady state assumption (Sierra *et al.*, 2016).

Given that the structure of the models determines the dynamics that can be simulated (Holling, 1973; Strogatz, 1994), the simulated response of vegetation to changing climatic conditions depends on the variables and parameters used, as well as on their interactions, i.e. whether the systems are linear or not. Evidently, finding the right combinations remains the most challenging part, because several aspects of the potential capability of vegetation to exploit climatic conditions remains unclear. Empirical findings suggest that climate change alone has contrasting effects on vegetation, and the effects of multiple driving factors on vegetation is not always additive (Leuzinger *et al.*, 2011; Dieleman *et al.*, 2012). Nonetheless, these and other interesting dynamics could be explored using models, and the software implemented in the database can help to test different hypothesis and parameter values. Finally, this could lead to

a close dialog between empirical and theoretical research fields that could result in interesting findings.

Conclusions

Carbon allocation in vegetation is a complex process that involves C flowing into, between and out of plant compartments, at different rates. This concept can be generalized and formalized using the mathematical concept of dynamical systems. Here, we found that many vegetation models can be represented in matrix form as a non-autonomous compartmental system of nonlinear ODEs. However, many models, particularly those used for large-scale simulations, use a linear representation with no interactions among ecosystem compartments.

We also identified some general properties of models according to the linearity and autonomy of the systems. We found that, although the linear structure is common, other structures with nonlinearities have been also proposed. These nonlinearities can be accommodated in the new mathematical framework proposed here. This framework has allowed us to assess models in a simple way, and can be a powerful aid in the interaction between theoretical and empirical research in ecosystem ecology and other related fields. It is an interface that summarizes the models' perspective of carbon allocation, and highlights relations (dependencies) between factors that are normally studied separately and in detail in the field and the lab; so, hopefully both could find a common language to share their knowledge. This conceptual/mathematical framework may allow us to find new insights into the study of the global carbon cycle under changing climate and disturbance regimes, and identify gaps where more experiments and theoretical work are needed.

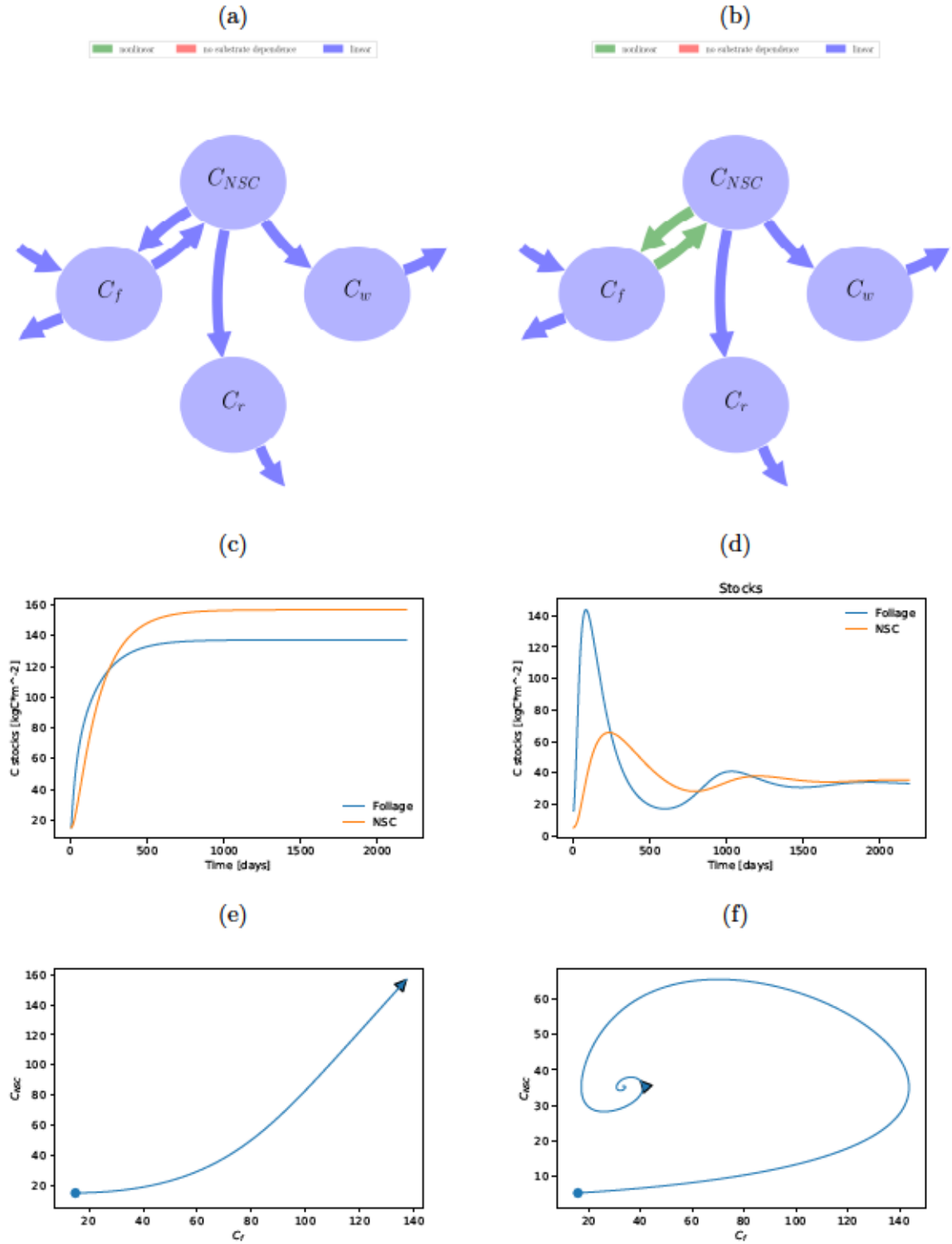


Figure 2.7: Examples of two models of carbon allocation in vegetation. Each representing a linear (a), and nonlinear (b) system. In both systems the photosynthetically fixed C enters through the foliage (C_f), and part of it is transferred to the non-structural C (C_{NSC}). From there, part of this C goes to the wood (C_w), and another to the roots (C_r). The difference between both models is the nonlinear fluxes represented by the three green arrows in (b). Their model runs illustrate the impact of these differences on the model predictions, such as the time course of the C stocks in foliage and NSC from the linear (c) and nonlinear (d) models. Notice that both compartments in the linear model have a transient increase in their stock, until they reach a stationary state, while in the nonlinear model they have damped oscillations. This is supported by the phase planes of these two compartments. In the linear model (e), the C in the NSC increases as the foliage increases. This is not always the case for the nonlinear model (f), since the relation between these two compartments varies with time, resulting in a spiral.

Ages and transit times as important diagnostics of model performance for predicting carbon dynamics in terrestrial vegetation models

The global carbon cycle is strongly controlled by the source/sink strength of vegetation as well as the capacity of terrestrial ecosystems to retain this carbon. These dynamics, as well as processes such as the mixing of old and newly fixed carbon, have been studied using ecosystem models, but different assumptions regarding the carbon allocation strategies and other model structures may result in highly divergent model predictions. We assessed the influence of three different carbon allocation schemes on the C cycling in vegetation. First, we described each model with a set of ordinary differential equations. Second, we used published measurements of ecosystem C compartments from the Harvard Forest Environmental Measurement Site to find suitable parameters for the different model structures. And third, we calculated C stocks, release fluxes, radiocarbon values based on the bomb spike, ages, and transit times. We obtained model simulations in accordance to the available data, but the time series of C in foliage and wood need to be complemented with other ecosystem compartments in order to reduce the high parameter collinearity that we observed, and reduce model equifinality. Although the simulated C stocks in ecosystem compartments were similar, the different model structures resulted in very different predictions of age and transit time distributions. In particular, the inclusion of two storage compartments resulted in the prediction of a system mean age that was 12-20 years older than in the models with one or no storage compartments. The age of carbon in the wood compartment of this model was also distributed towards older ages, whereas fast cycling compartments had an age distribution that did not exceed 5 years. As expected, models with C distributed towards older ages also had longer transit times. These results

suggest that ages and transit times, which can be indirectly measured using isotope tracers, serve as important diagnostics of model structure and could largely help to reduce uncertainties in model predictions. Furthermore, by considering age and transit times of C in vegetation compartments as distributions, not only their mean values, we obtain additional insights on the temporal dynamics of carbon use, storage, and allocation to plant parts, which not only depends on the rate at which this C is transferred in and out of the compartments, but also on the stochastic nature of the process itself.

Introduction

The global carbon cycle is strongly controlled by the source/sink strength of terrestrial ecosystems. Vegetation in particular, is one of the major controls of global C sources and sinks with respect to the atmosphere (Canadell *et al.*, 2007); it has the capacity to be either a strong C sink or a source, depending on the amount of C fixed by the canopy and the time that C takes to transit through its components back to the atmosphere (Luo *et al.*, 2003). Strong sinks therefore, not only fix carbon at a fast rate, but have also the capacity to store this carbon for long periods of time (Körner, 2017).

The C storage capacity of an ecosystem is determined by the collective behavior of vegetation compartments such as foliage, wood, and roots, which may also act as C sources and sinks among each other (Xia *et al.*, 2013; Luo *et al.*, 2017). The capacity of a vegetation compartment to oscillate between C source and sink has important implications for ecosystems in their response to perturbations and environmental change, i.e. their resilience. Carbon fixed during photosynthesis is transported from the leaves (sources) to other parts of the plant (sinks). One of these sinks is the labile or non-structural carbon (NSC) (Hartmann and Trumbore, 2016; Trumbore *et al.*, 2015; Martínez-Vilalta *et al.*, 2016), which may turn into a C source during critical events, such as the start of the growing season (after periods of limited photosynthesis) (Richardson *et al.*, 2013), and the recovery from disturbances such as drought (Hartmann *et al.*, 2013), cold temperatures (Hoch and Körner, 2003), pollution (Grulke *et al.*, 2001), or nutrient stress (Ericsson *et al.*, 1996). Despite the importance of the source-sink capacity of NSC reserves, many questions remain unsolved. For example, are NSCs completely depleted when needed, and replenished afterwards? Is the C that has remained stored for many years still available for the plant? (Richardson *et al.*, 2013).

It is indeed possible that the carbon stored in vegetation compartments, including NSCs, have been fixed at different times, resulting in a mix of ages (Muhr *et al.*, 2016). Studies across wood rings in temperate forest trees revealed that the mean age of NSCs in stemwood can be up to several decades old (Richardson *et al.*, 2013; Trumbore *et al.*, 2015). Trumbore *et al.* (2015)

explained these old ages with a simple model consisting of one NSC compartment with inward mixing of younger and older C. Alternatively, Richardson *et al.* (2013) proposed a model with two separate storage compartments (NSC)-with old and young C, respectively- that exchange material among each other. It is therefore uncertain how this mixing of NSCs of different ages occurs: In the form of one single compartment in which all ages are mixed, or in different compartments with separate ages?

Previous studies have focused mostly on determining ages of NSCs using radiocarbon-derived mean residence times, but this approach has limitations. One limitation is the ambiguity in the term “mean residence time”, which has been defined in different ways across studies; in some cases it implies the mean age of C in an ecosystem or ecosystem compartment and in other cases it implies the time it takes C molecules to leave the system of compartments (Sierra *et al.*, 2016). Another limitation is the use of mean values instead of complete frequency or density distributions to assess the spread of C ages in vegetation compartments.

The study of C age distribution in vegetation requires challenging empirical methods, but can also be approached using ecosystem C cycle models. However, not all of the models perform equally well because the assumptions behind their structures may result in highly divergent predictions (Lacointe, 2000; Friedlingstein *et al.*, 2006; Friend *et al.*, 2014; Schiestl-Aalto *et al.*, 2015). The performance of such models has been diagnosed by comparing their predicted C storage capacity and residence times (Friend *et al.*, 2014; Yizhao *et al.*, 2015), but if the above mentioned ambiguities are resolved, ages of carbon in vegetation and in respiration fluxes can serve as excellent additional diagnostics of ecosystem models, and can give important insights about carbon metabolism in vegetation under stress conditions, such as in the case of drought stress.

Definitions: ages and transit times

CO₂ molecules are fixed continuously by photosynthesis during the growing season; so, C particles enter the vegetation (from here on called “system”) at different times during the year. After fixation, the photosynthetic products transit through the vegetation compartments until they eventually leave the system, either as CO₂ back to the atmosphere or as litter and exudates to the soil. This means, that at a given time (t) each particle in the system has a different *age*, which is the time that it has remained within the system since its fixation from the atmosphere. The time that each particle spends transiting through the system, from arrival until exit, is called *transit time* (Bolin and Rodhe, 1973).

At each time step, a particle may stay where it is, given certain probability, or flow to the next compartment with a rate or probability given by the transfer coefficients (also know

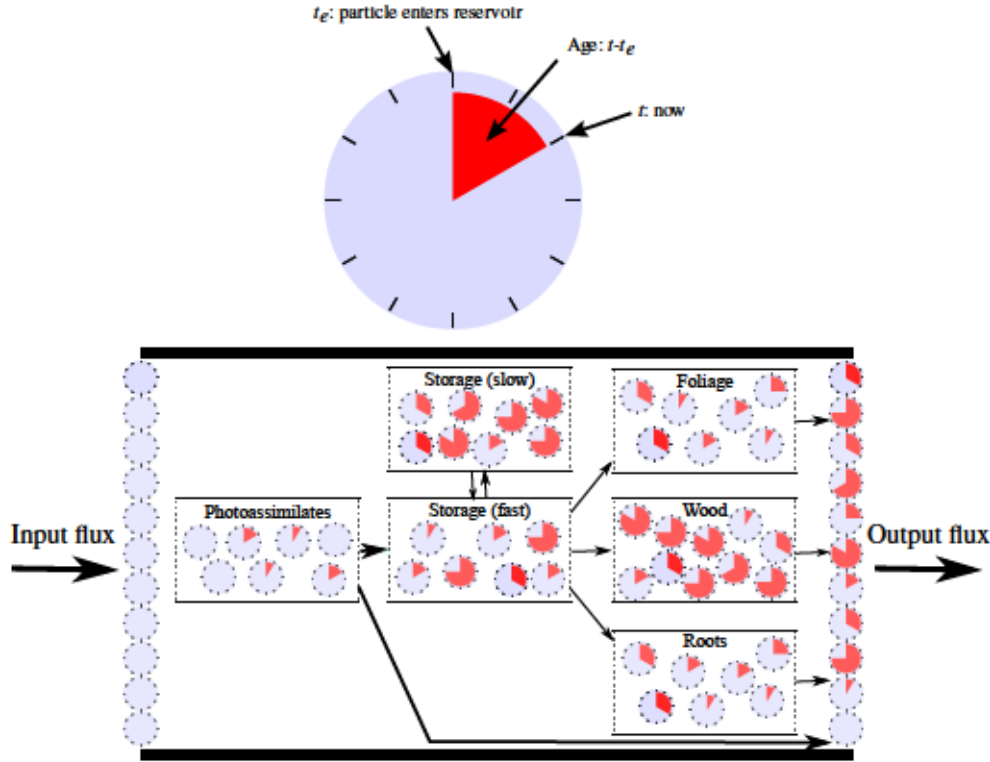


Figure 3.1: Graphical representation of the concepts of age and transit time distributions in a vegetation model. Carbon particles are represented here as clocks that measure the time they have been in the system. **System age** can be defined as the age of all particles in the system at a given time, while **transit time** as the age of particles in the output flux. Adapted from Sierra *et al.* (2016)

as cycling rates). This means that the age of carbon in a system results from stochastic and deterministic processes, which can be illustrated in Figure 3.1; given two organic molecules in a compartment, one that has remained in the system for longer time than the other, they both have the same chance to either leave the system, or move on to another compartment. Thus, if by chance older molecules remain for longer times, then the system's age gets older. But the pace at which these molecules are transiting is moderated by the cycling rates. This is why slow cycling compartments have older C.

Lets describe a system of well-mixed C (distributed in multiple compartments) with the system of ordinary differential equations

$$\begin{aligned}\dot{\vec{x}}(t) &= \mathbf{B} \times \vec{x}(t) + \vec{\beta} \cdot u, \\ \vec{x}(0) &= \vec{x}_0,\end{aligned}\tag{3.1}$$

where $\dot{\vec{x}}(t)$ is how much the quantity of carbon in vegetation compartment x changes with respect to time, \mathbf{B} is a matrix of carbon transfer coefficients between the plant compartments, $\vec{x}(t)$ is a vector of states for vegetation (state variables), $\vec{\beta}$ is a vector containing the partitioning coefficients of photosynthetic input, and u is a scalar that represents that input. This linear system does not include environmental variables, or any other variables that depend on time,

thus, it is an *autonomous linear system* with multiple interconnected compartments.

Given that each particle in the system has its own age and transit time, the age and transit time of the whole system can be considered as random variables. Additionally, the age and transit time of particles in a system's compartment is exponentially distributed. Then, the age and transit time distributions of the entire system would be the sum of those exponential distributions, i.e. a phase-type distribution (PT) (Metzler and Sierra, 2018).

The calculation of how many C particles have a certain age, or *the age density distribution of a system* ($f_A(y)$), is determined by the probability of entering the system through a given compartment and the rates at which C is transferred from one compartment to another until it leaves the system. Consistent with the symbols from the previous equation

$$f_A(y) = \vec{z}^T \cdot e^{y \cdot \mathbf{B}} \cdot \frac{\vec{x}^*}{\|\vec{x}^*\|}. \quad (3.2)$$

$f_A(y)$ is a function of (i) how fast the carbon is leaving the system: the row vector of release rates, which is the column-wise sum of the elements of the \mathbf{B} matrix ($\vec{z}^T = -\vec{1}^T \mathbf{B}$), (ii) the transition probability matrix ($e^{y \mathbf{B}}$), and (iii) the relative amount of C stock at steady state with respect to the total ($\frac{\vec{x}^*}{\|\vec{x}^*\|}$). Notice that we use here the symbol $\|\cdot\|$ to represent the vector norm, which is the sum of all entries of the vector.

The mean age is given by the expected value ($\mathbb{E}[A]$)

$$\mathbb{E}[A] = \frac{\|\mathbf{B}^{-1} \times \vec{x}^*\|}{\|\vec{x}^*\|}. \quad (3.3)$$

Likewise, the transit time density distribution ($f_{FTT}(t)$) is also a function of \vec{z}^T and the transition probability matrix ($e^{t \mathbf{B}}$), as well as the vector of input distributions ($\vec{\beta}$).

$$f_{FTT}(t) = \vec{z}^T \cdot e^{t \cdot \mathbf{B}} \cdot \vec{\beta}. \quad (3.4)$$

The mean transit time is defined as ($\mathbb{E}[FTT]$):

$$\mathbb{E}[FTT] = \|\mathbf{B}^{-1} \times \vec{\beta}\| = \frac{\|\vec{x}^*\|}{\|\vec{u}\|} \quad (3.5)$$

In this case, the definition of mean transit time coincides with the commonly used *stock over flux* approach (turnover time), but note that the definitions presented here can only be applied to autonomous systems at steady state. For non-autonomous systems, i.e. models in which inputs and process rates change over time, formulas for the estimation of mean age and transit time can be found in Rasmussen *et al.* (2016).

From these equations it is evident that age and transit time calculations mainly depend on the schemes of C partitioning ($\vec{\beta}$) and cycling (\mathbf{B}) within a vegetation model. Therefore, if we want

to understand processes such as the mixing of old and newly fixed NSC using ecosystem models, it is critical to model proper carbon allocation (CA) strategies. Unfortunately, it is still uncertain what assumptions and simplifications should be done: How many carbon compartments are necessary to describe carbon cycling in vegetation? How are these compartments interconnected and how fast are they transferring C among each other? These are important questions that need to be addressed to improve our understanding of vegetation dynamics, and predict consequences of environmental change on vegetation.

In this contribution, we address the question: how different C allocation schemes affect the ages and transit times of carbon in vegetation models? In particular, we are interested in understanding whether different carbon allocation strategies would lead to different patterns of mixing of ages for the NSC compartment. For this work, we implemented 3 carbon allocation schemes based on Richardson *et al.* (2013); the models have either no storage, 1 storage compartment, or 2 storage compartments (fast and slow C cycling). Our approach is mostly theoretical, and we are mainly interested in introducing the concepts of age and transit time distributions as useful model diagnostics as well as as an approach to explain mixes of C age in NSC compartments. For this purpose, we used published measurements on ecosystem C compartments from the Harvard Forest Environmental Measurement Site to find suitable parameter values for the different model structures. We also diagnosed the performance of these models using as metrics 1) C release fluxes (respiration and other carbon losses such as litterfall), 2) the dynamics of radiocarbon (based on the bomb spike) for individual compartments, 3) the transit time distribution of the system, and 4) the age distribution of C in the system and in each compartment.

Methods

Model Implementation

Each model was written as a set of ordinary differential equations (based on Equation 3.1) within the environment of the R package *SoilR* (Sierra *et al.*, 2012). All models met the requirements of equation 3.1; they are autonomous (their dynamics do not depend on variables that change with time) linear systems with multiple interconnected compartments. The initial carbon stocks, and some of the parameter values needed to solve those equations were obtained from the literature, from a deciduous-evergreen model with similar carbon allocation schemes (Fox *et al.*, 2009). Other parameter values were obtained from an optimization procedure (see below).

As means to assess whether the carbon allocation strategies had an impact on the mixing of C age in vegetation compartments, we implemented three models whose carbon allocation

strategies varied depending on the number of storage compartments (0, 1, or 2) (Figure 3.2), following the hypotheses proposed by Richardson *et al.* (2013). Given that we aimed at a theoretical comparison of the above mentioned strategies, we eliminated other potential sources of variation that may act as confounding factors by assuming that all C transfers between the compartments depended on constant rates. We also assumed that there was a constant photosynthetic input -gross primary production (GPP): u -of $1400 \text{ gCm}^{-2}\text{year}^{-1}$ (Urbanski *et al.*, 2007). Environmental variability, which operate mostly on an hourly-daily time scales, was not considered here because we ran the models at an annual time scale; i.e., without diurnal cycles or phenology.

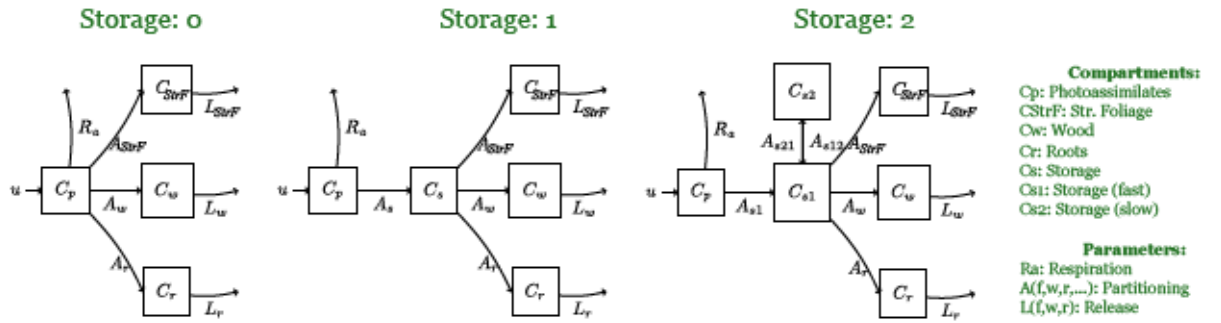


Figure 3.2: Three carbon allocation strategies in vegetation models. These strategies differ in the number of storage compartments, Storage: 0, Storage: 1, and Storage: 2. Adapted from (Richardson *et al.*, 2013). The parameters are the rates at which the carbon cycles into and out of the compartments; thus, the fluxes are proportional to the C stocks and the rates. Notice that the foliage is divided into two compartments: Photoassimilates and Structural Foliage.

Fixed photosynthetic input enters the system through the Photoassimilates compartment, and part of the carbon is released back to the atmosphere at each time step, in a flux proportional to the size of Photoassimilates and the constant rate R_a (Figure 3.2). In the model without storage compartment, the C stored in the Photoassimilates is partitioned into Structural foliage (from here on: Str. Foliage), Wood (including branches and coarse roots) and Fine roots (from here on: Roots), with the constant rates A_f , A_w , and A_r ; part of the C stored in these three compartments also leaves the system with constant rates L_f , L_w , and L_r , which comprise all the carbon released through respiration and other losses (e.g. litterfall). For the models with storage, the C is transferred from the Photoassimilates to the fast cycling storage, from which it is then partitioned to the rest of the compartments. In addition to the fast cycling storage, the model with 2 storage compartments also has a slow cycling compartment.

Optimization procedures

To obtain results that can be related to a particular ecosystem, we performed a parameter estimation procedure using published measurements of two ecosystem C compartments from

the Harvard Forest Environmental Measurement Site (see links ¹, ², and ³, and the raw LAI⁴). Harvard Forest is a regenerating temperate forest located in Petersham, Massachusetts (42.54°N, 72.18°W, 340 m asl). Among the tree species that are found in this 65- to 85-year-old mixed deciduous forest are: red oak, red maple, white and red pine, yellow and white birch, beech, ash, sugar maple and hemlock (Wofsy *et al.*, 1993).

We calculated C stocks in wood and foliage from the above mentioned aboveground biomass, LAI and LMA, using allometric equations. Although in previous studies performed at the same site the use of woody biomass increment and LAI reduced the uncertainties in the predictions of net C sequestration and foliage dynamics, respectively (Keenan *et al.*, 2013a), and the wood stock observations have been used to successfully constrain fine root mass simulations (Smallman *et al.*, 2017), we obtained unrealistic simulations of C stocks in storage and roots because these pools were not well constrained. Thus, we estimated C stocks of roots based on the assumption that shoot:root ratio = 1:5, and we also used published ratios to calculate NSC from Wood carbon (p. 5 Richardson *et al.*, 2010).

We were also interested in observing the uncertainty of the model simulations (see section below), so we performed a Bayesian optimization, which gave us alternative parameter sets after exploring the parameter space. This optimization procedure was started using the result of a classical optimization method using the *R* package *FME* (Soetaert and Petzoldt, 2010). Taking into account that data uncertainties have a direct influence on the fit of the outcome of the parameter estimation (Richardson *et al.*, 2010), we accounted for the uncertainty in the data using the standard deviation of the measurements in the cost functions.

As means to evaluate whether the parameters could be estimated from the given data sets, i.e. parameter identifiability, we performed a local sensitivity analysis and estimated the collinearity of the parameter sets with the package *FME*. The obtained collinearity index γ expresses the degree at which pairs of parameters are linearly related. Values of $\gamma > 20$ indicate high collinearity among parameters and poor identifiability of the model given the available data (Soetaert and Petzoldt, 2010).

Given the high correlation between some of the parameters, we decided to run all model simulations using the parameter set that was most frequently chosen by the Bayesian optimization method. We then calculated C stocks, release fluxes, radiocarbon values based on the bomb spike, ages, and transit times, using functions implemented in *SoilR*. The functions that calculate age and transit time distributions are based on the formulas proposed by Metzler and Sierra (2018).

¹<http://atmos.seas.harvard.edu/lab/hf/index.html>

²<http://ameriflux.lbl.gov/doi/AmeriFlux/US-Ha1>

³<http://ameriflux.lbl.gov/sites/siteinfo/US-Ha1>

⁴http://ftp.as.harvard.edu/pub/nigec/HU_Wofsy/hf_data/ecological_data/lai/lai.98.15.txt

Uncertainty analysis

In order to explore model predictions that could result from different parameter sets that were possible and likely, we extracted a random sample of 1000 posterior parameter sets from the Bayesian optimization that used Markov chain Monte Carlo. We ran the models with the unique sets, and calculated the weighted mean and standard deviation of the C stocks, the released C from each compartment, and the system's mean age and transit time. The weights corresponded to the number of times that each parameter set was repeated in the sample.

Code availability

All of the simulations and figures for this work can be reproduced using the code and data provided in the supplementary material.

Results

Simulations of carbon stocks

The C stocks simulations obtained from the three models were within the uncertainty range of the available data (Figures 3.3 and 3.4). The simulations of Wood and Foliage C (Photoassimilates + Structural) stocks were in accordance with the stocks estimated from the aboveground biomass inventory data and the LAI, respectively.

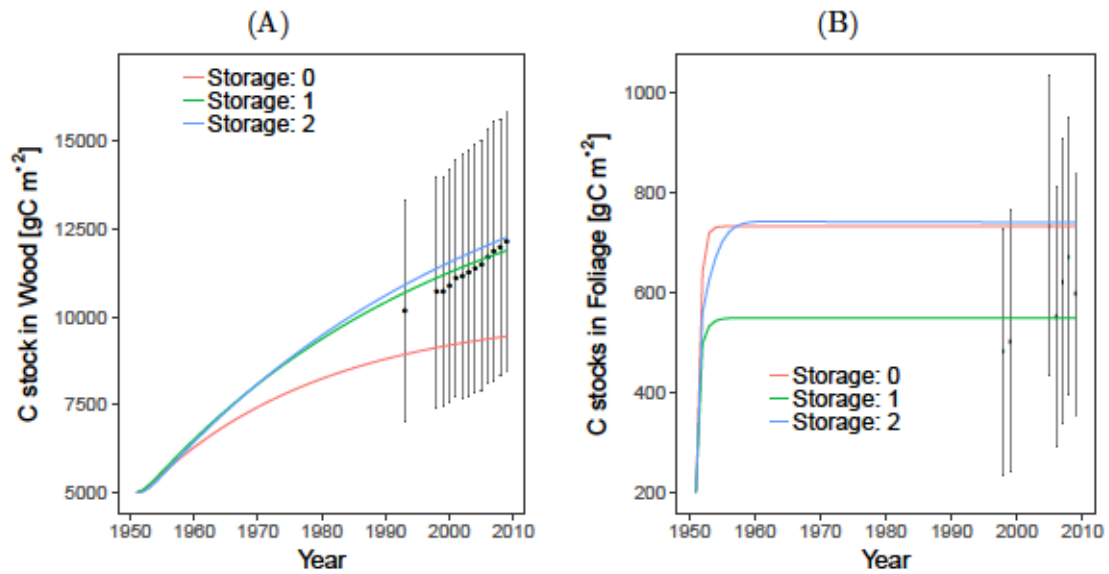


Figure 3.3: Carbon stocks estimated for each model, comparing the observed data and the model predictions of C stocks in Wood (A) and Foliage (B).

All of these predictions were obtained using the parameter set that was most frequently chosen by the Bayesian optimization method (Table 3.1). This table also shows two quantiles of the distribution of each parameter value after exploring the parameter space.

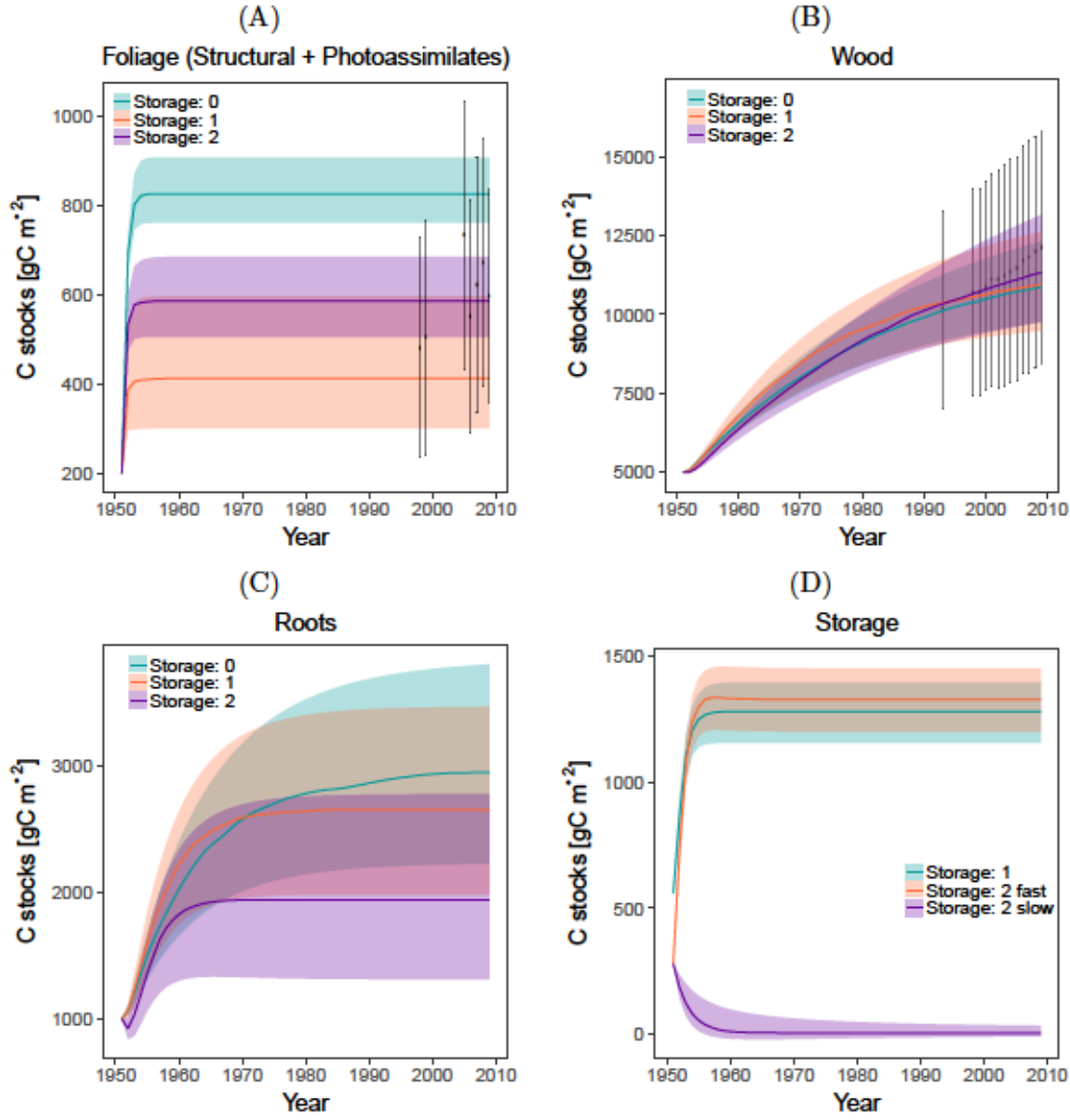


Figure 3.4: Carbon stocks estimated for each compartment and their uncertainties. Carbon in the (A) Foliage (Photoassimilates + Structural), (B) Wood, (C) Roots, and (D) Storage compartments.

Interestingly, some of the parameters were strongly correlated among each other. For the three model structures and the available empirical data, the number of parameters that can be simultaneously estimated with a collinearity index < 20 for the models *Storage: 0*, *1*, and *2* was 3, 4, and 5, respectively. The correlations can be seen in the pairwise plots of sensitivity functions (Figures 2-4). Table 5 summarizes the number of parameter correlations that we observed under the diagonal of the pairwise plots of sensitivity functions. For this reason, the results presented here need to be interpreted within the context of predicted uncertainties.

Influence of carbon allocation strategies on ecosystem level C cycling

To assess the impact of different carbon allocation strategies on the ecosystem C cycling, we used the following metrics: 1) C release fluxes, 2) dynamics of radiocarbon for individual compartments, 3) transit time distribution of C through the system, and 4) age distribution

Table 3.1: Parameter values obtained from the optimization procedures [$year^{-1}$].

Model	Parameter	Final	Best1	Best2	Median	q_{25}	q_{75}
Storage: 0	Ra	0.64	0.7	0.7	0.57	0.45	0.64
	Af	0.48	0.5	0.5	0.42	0.32	0.46
	Ar	0.32	0.5	0.5	0.33	0.26	0.4
	Aw	0.5	0.49	0.49	0.47	0.43	0.49
	Lf	35.09	17.84	17.84	32.12	28.47	34.92
	Lr	0.06	0.12	0.12	0.09	0.07	0.1
	Lw	0.04	0.02	0.02	0.03	0.03	0.04
Storage: 1	Ra	0.61	0.32	0.32	0.52	0.35	0.61
	Af	0.31	0.17	0.17	0.19	0.13	0.3
	Ar	0.47	0.5	0.5	0.36	0.3	0.43
	Aw	0.29	0.3	0.3	0.37	0.32	0.44
	Lf	3.04	7.9	7.9	10.82	6.49	14.18
	Lr	0.13	0.21	0.21	0.17	0.14	0.19
	Lw	0.02	0.03	0.03	0.04	0.03	0.05
	As	2.55	2.14	2.14	3.55	2.26	4.29
Storage: 2	Ra	0.65	0.7	0.7	0.58	0.5	0.65
	Af	0.15	0.1	0.1	0.16	0.14	0.18
	Ar	0.47	0.5	0.5	0.44	0.39	0.47
	Aw	0.23	0.19	0.19	0.23	0.21	0.28
	Lf	0.74	17.52	17.52	17.89	12.03	21.6
	Lr	0.23	0.21	0.21	0.27	0.23	0.35
	Lw	0.02	0.01	0.01	0.02	0.02	0.03
	As	2.27	1.69	1.69	1.96	1.67	2.26
	As12	2.77E-03	1.00E-03	1.00E-03	1.83E-03	1.43E-03	2.16E-03
	As21	0.09	0.82	0.82	0.41	0.22	0.6

Final: Parameter set that was most frequently chosen by the Bayesian optimization method and was used for all of the simulations, unless otherwise noted.

Best1: Parameter set obtained from the classical optimization procedure.

Best2 and the remaining columns were the result of the Bayesian optimization.

of C in the system and in each compartment. The calculations required for these metrics were performed using the parameter set that was most frequently chosen by the Bayesian optimization method for each model, unless otherwise noted.

Fluxes of C released from the compartments

The three models predicted different mean fluxes of C released from each compartment at steady state (Figure 3.5). Nonetheless, the Structural Foliage compartment had large uncertainties and overlaps among the flux distributions of the three models. This means that certain combinations of model structures with parameter sets result in similar predictions of Str. Foliage C release fluxes. However, for the other compartments these differences were larger. Thus, regardless of the parameter sets, the differences in model structure lead to the prediction of different C release fluxes at steady state.

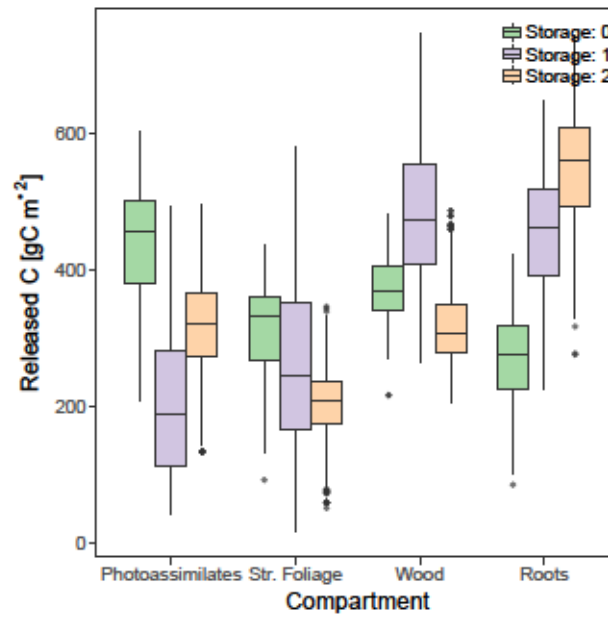


Figure 3.5: C release fluxes from the compartments at steady state, with uncertainty ranges obtained from the set of posterior parameters obtained by Bayesian optimization.

Radiocarbon content in each compartment

The simulated radiocarbon content of fast cycling compartments (e.g. Photoassimilates, Str. Foliage, and Storage (fast)) had a stronger resemblance to the atmospheric $\delta^{14}C$ values than the slower cycling compartments (Figure 3.6). However, for the Str. Foliage of the models with storage there was a time lag of about 3-5 years with respect to the peak that corresponds to the ‘bomb-spike’. Furthermore, the accumulation of radiocarbon in slow cycling compartments such as Wood and the Storage (slow), was characterized by a slow incorporation of radiocarbon that resulted in large $\delta^{14}C$ values of the last part of the curve. The radiocarbon accumulation in the Roots compartment was not as fast as in the Foliage compartments, but was faster than that of the Wood.

Differences in radiocarbon values for the different compartments hint to different levels of mixing of carbon fixed at different times. For the fast cycling compartments such as the Photoassimilates, the degree of mixing is relatively low because most of the radiocarbon reflects the values in the atmosphere. For other compartments that cycle at slower rates, the mix of recent and old radiocarbon results in important divergences from the atmosphere. Mixing of carbon of different ages can be further studied with ages and transit times distributions.

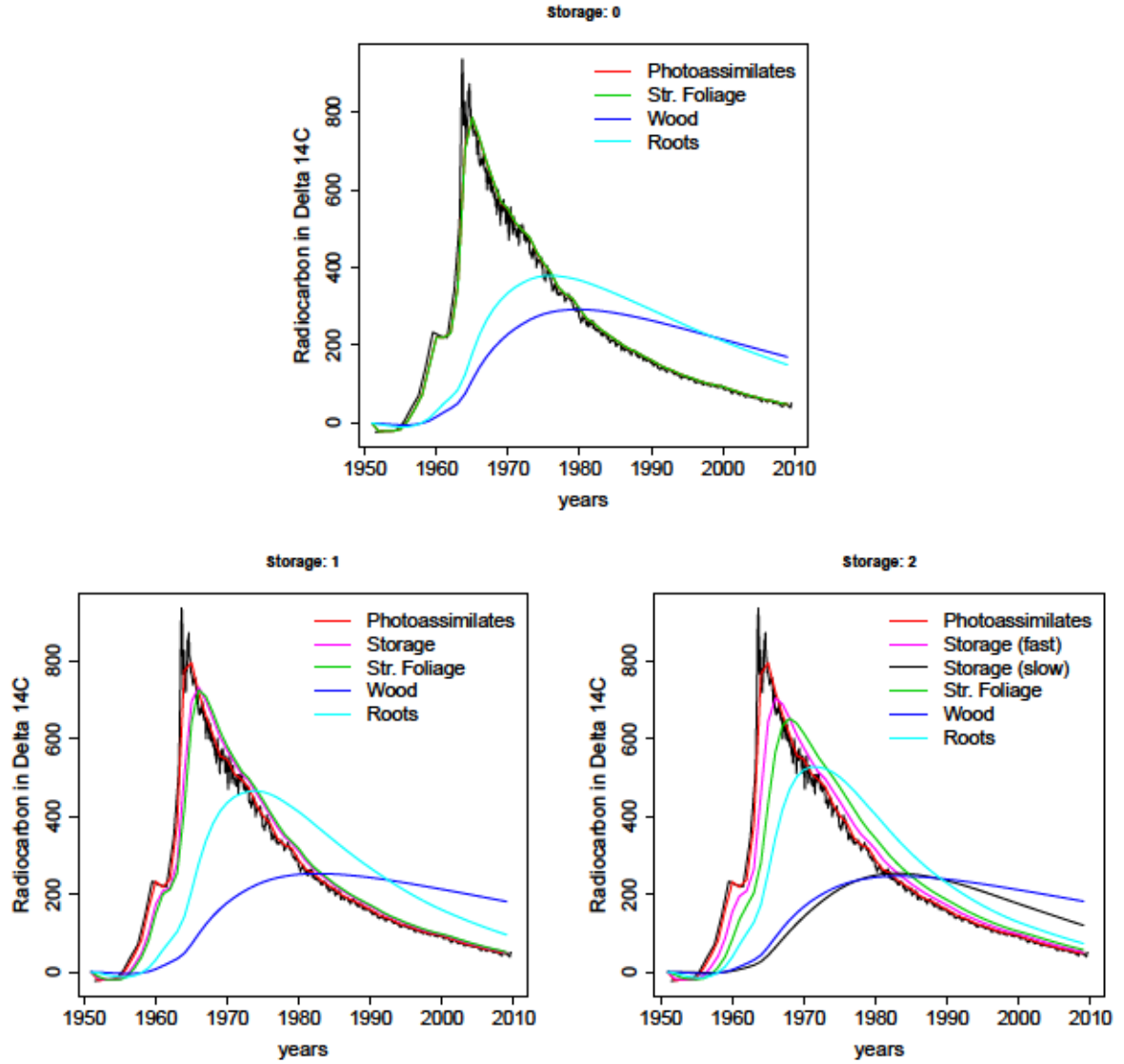


Figure 3.6: Radiocarbon simulations for the three model structures. The black curve corresponds to the $\delta^{14}\text{C}$ in the atmosphere, and the other colors depict the vegetation compartments.

Age and transit time distributions

The age and transit time distributions were calculated assuming that the system was in steady state. These distributions had a wide range, expanding from 0 to several decades old carbon, and their shape varied according to the model structure (Figure 3.7). The ascending order of the models according to their mean age, from young to old, was: *Storage: 0*, *Storage: 1*, *Storage: 2*. As expected, the model with the oldest ages (*Storage: 2*) had the longest transit time. These trends were partially observed when we analyzed the uncertainties in mean age and mean transit times (Figure 3.7 (C) and (D)), but the uncertainties were large. These large uncertainties may have resulted from the high correlation between the models parameters.

At the compartment level, the above mentioned age-dependent ranking of the models only holds true for Wood (Figure 3.8), which was the compartment with the closest resemblance to the overall system age densities because it comprised most of the mass in the system. The

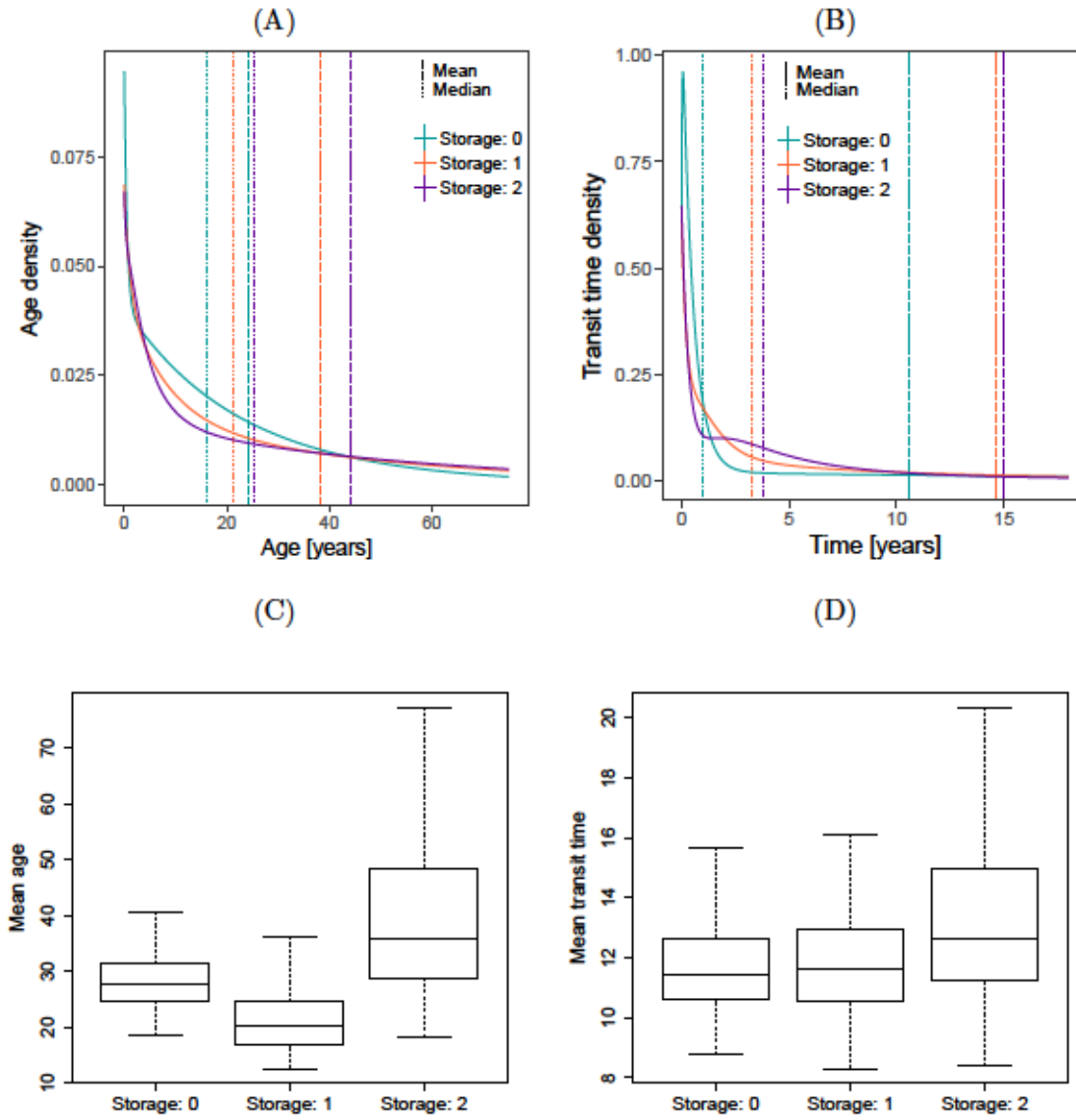


Figure 3.7: System ages and transit times. (A) Age and transit (B) time density distributions calculated for each of model structure using the best parameter set from the optimization; the dashed and dotted lines mark the mean and median ages, respectively. (C) Spread of mean ages (left) and mean transit times (D) obtained from all posterior parameter sets from the Bayesian optimization.

inclusion of two storage compartments in *Storage: 2* resulted in a relatively ‘flat’ distribution; with a long tail that leads to a mean age 12-20 years older than the other two models, but with a peak at very young ages. This contrasts with the other models, which peaked at around the same time, but had steeper declines with age.

The only compartment that had an age maximum at 0 years was the Photoassimilates. Hence, this compartment had a unique distribution curve reflecting the fact that all new carbon (age = 0 years) enters the models only through this compartment. Although the other fast cycling compartments (Str. Foliage and Roots) had peaks after 0 years, their C age was distributed towards young ages, with mean ages between 1 and 3 years. This spread in the C age of Str. Foliage for the models with storage may suggest either that the cycling rate of this

compartment was relatively slow or that it received C from compartments with older carbon.

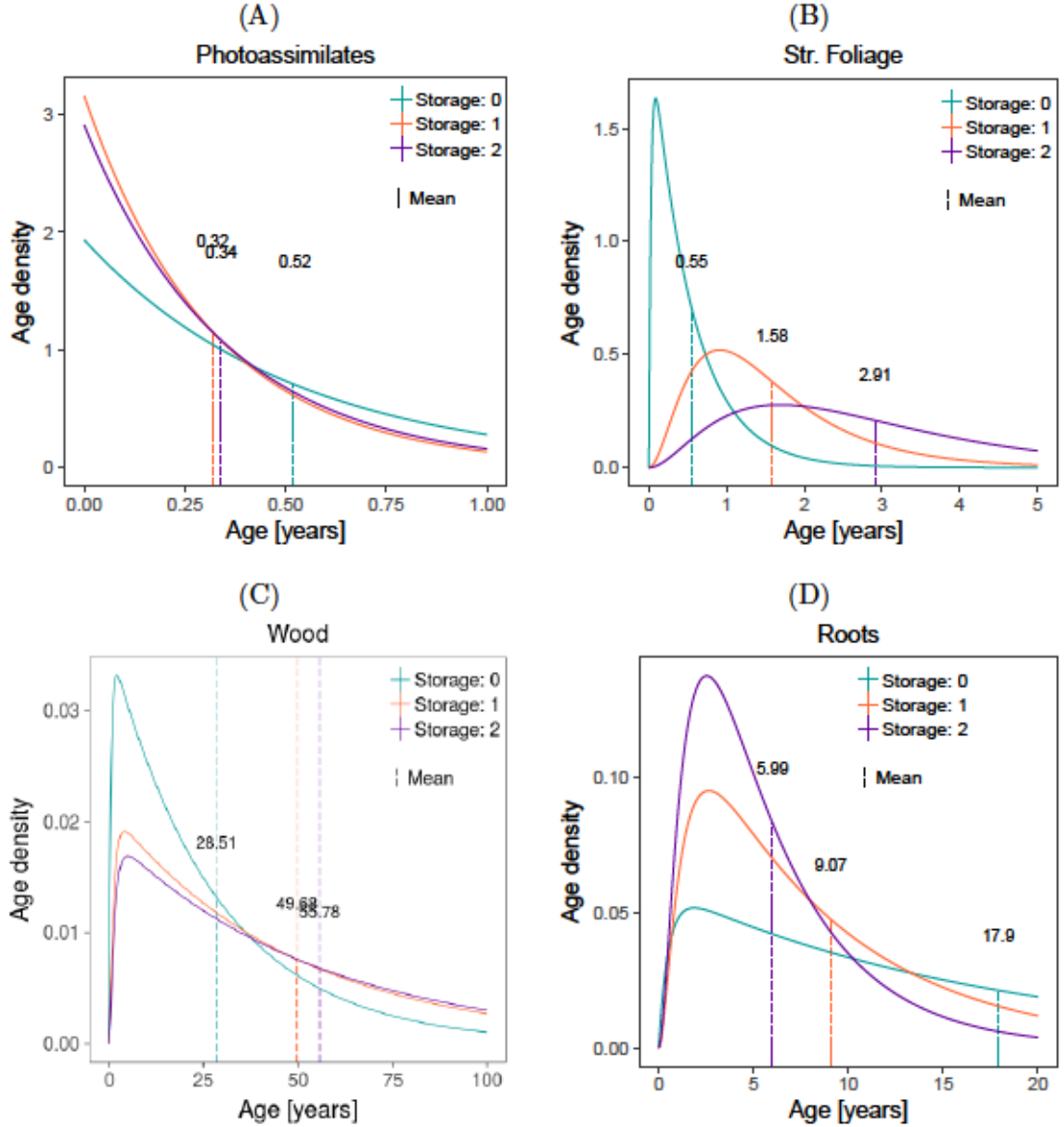


Figure 3.8: Age densities simulated for the compartments: (A) Photoassimilates, (B) Str. Foliage, (C) Wood and (D) Roots. Each model structure is depicted in a different color. Dashed lines correspond to mean ages.

The age densities of the storage compartments, just as the ones for Foliage, Wood, and Roots, consisted of curves with peaks at young ages and long tails (Figure 3.9). In the case of the fast cycling compartments, the mean age of the models *Storage: 1* and *Storage: 2* was 1.25 and 1.55 years, respectively, but the long tail indicates that it is also probable to find 5-year-old C in this compartment. The mean age of the slow cycling compartment was 13.25 years, but the mixing of ages is also observed in the density curve, in which the age of C ranged from 0 to more than 50 years.

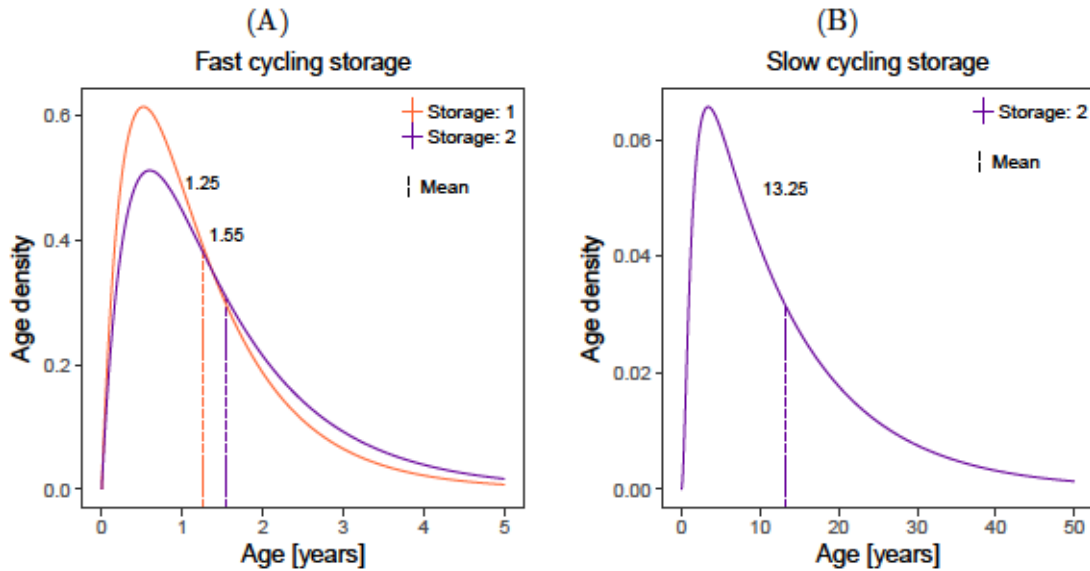


Figure 3.9: Age densities simulated for the models with storage compartments. (A) Fast cycling compartment of models *Storage: 1* and *Storage: 2*. (B) Slow cycling storage of the only model with 2 storage compartments.

Discussion

Our simulation results showed that C cycling in ecosystems can be largely influenced by different carbon allocation strategies, which may result in diverging carbon cycling predictions for specific simulations. However, not all of the different prediction metrics were impacted with the same strength by the assumed number of compartments and values of cycling rates, so results here need to be interpreted within the context of predicted uncertainties.

Diagnosing model performance with C release fluxes, and age and transit time distributions

The simulated ecosystem properties that were more strongly impacted by the assumptions behind model structure were: the fluxes of C released from each compartment, and the ages and transit time distributions of carbon in the system and in each compartment. This sensitivity to different carbon allocation strategies makes them good candidates for diagnosing model performance.

Given that the C release fluxes from Photoassimilates, Roots, and Wood were highly sensitive to the three model structures, empirical measurements of these compartments could be used as constraints during the parameter estimation procedure. The radiocarbon accumulation was less sensitive, but can be useful to diagnose the models' performance according to the cycling speed of their compartments. As an example, we could identify the short delay of the $\delta^{14}\text{C}$ signature of the Str. Foliage compartment with respect to the current year's atmosphere, in the models with storage (Figure 3.6). Although such a delay could indicate that this compartment had a slightly slower C cycling than what is expected for a deciduous forest (Trumbore *et al.*,

2002, 2015), it could also indicate the flux of old C from the slow cycling compartments into the foliage. This delay in radiocarbon accumulation was also observed as shifts to older ages in the age distributions (Figure 3.8), with a resolution of months. In general, radiocarbon measurements can also help to constrain model parameters with respect to how fast or slow different compartments cycle C (Trumbore *et al.*, 2016), but with less resolution than the age and transit time distributions.

Overall, the age and transit distributions were the best candidates to diagnose model performance and potentially constrain parameter estimations, because they were the most sensible to differences in model structure and parameter values. So, what had the highest impact on these distributions, the differences in cycling rates or the inclusion of storage compartments? It seems like these two characteristics had direct and indirect effects on the predictions of the above mentioned distributions, respectively.

On the one hand, as we initially inferred from the equations 3.2-3.5, the calculation of age and transit time distributions depends on the C partitioning schemes ($\vec{\beta}$) and the transfer-cycling-rates between plant compartments (\mathbf{B}). Therefore, different parameter values that compose the vector $\vec{\beta}$ and matrix \mathbf{B} directly result in the different calculations of ages and transit times. This was tested by running the three models using the same parameter set; although they still differed in the number of storage compartments, there was almost no difference between the age and transit time distributions in the whole system and in the compartments (Figures 7, 8, and 9). These similarities were also observed for the radiocarbon accumulation (Figure 6). The only exceptions to the above were the foliage compartments of the model *Storage: 0*, which were faster than in the other two models.

On the other hand, model structure had an indirect effect on the predictions of age and transit time, most likely because the addition of storage compartments impacted the outcome of the parameter estimation and these different parameter values then lead to different age and transit time predictions. An illustration of this is the fit of the models to the data (Appendix chapter 3, Fig. 5): Running the three models with the parameter set that gave the best fit for the model with 2 storage compartments hampered the fit of the model with no storage compartments to the woody and foliage C measurements. Thus, although the system had an external C input that could never be depleted because it was assumed to be a constant flux, the parameter estimation accounted for extra compartments by modifying the cycling rates to optimize the fit of the models to the data.

As expected, systems with ages distributed towards older values also have older transit time distributions. In fact, their correlation can be confirmed by observing the formulas once again. The calculation of these two properties depends on the matrix of transfer coefficients (\mathbf{B}), but there are other factors driving these two distributions. The additional factor driving

the mean age calculation is the relative amount of C stock at steady state; whereas the mean transit times depend on the C partitioning schemes ($\vec{\beta}$) (Metzler and Sierra, 2018). So, the mean transit time calculation is only limited by the rates of C transfer, while the mean age of C in the system also depends on its mass. This is why the mean age of C in vegetation is determined by the age of the compartment where the majority of the mass is stored, which in this case is Wood. We further explored this relation in the scatter plot in (Figure 10), where the distribution of the points below the 1:1 line indicate that the three models have mean ages greater than their mean transit times. This means that they have big masses of old carbon, but they also have highly dynamic compartments through which carbon transits very fast.

We also diagnosed the model performance by comparing the predicted ages for the storage compartments (Figure 3.9) with the mean age of NSC measured in previous empirical studies (Richardson *et al.*, 2013). The mean age of NSCs from red maple cores obtained at Harvard forest, was 7.2 ± 7.7 yr; for the fast cycling storage compartments of the models *Storage: 1* and *Storage: 2*, it was 1.25 and 1.55 yr respectively, and 13.25 yr for the slow cycling storage. Clearly, the mean ages of fast storage compartments are smaller than the mean value calculated empirically, but given the uncertainty of the measurements, they are still within the observed range. Furthermore, the density distributions of these storage compartments show that even though they are well-mixed, their C do not have the same age. Thus, it is also likely to find C between 0-5 yr and 0-50 yr in the fast and slow cycling storage compartments, respectively. This resonates with the fact that although stemwood NSC is highly dynamic on seasonal time-scales, it can also be surprisingly old (Richardson *et al.*, 2013). Then, the two hypothesis regarding C mixing -inward mixing of younger and older C in one compartment (Trumbore *et al.*, 2015), and 2 compartments (young and old) that mix (Richardson *et al.*, 2013)- converge in the concept of age distributions because C is simultaneously been fixed and removed from the compartments at different times, a process that results in C age distributions. We can think about these dynamics in the context of a stochastic process. The total amount of C that enters and leaves each compartment is fixed and given by the deterministic model, but the time that each C particle stays in a compartment varies stochastically within them. So, the age distribution of C particles in each compartment is a mix of new and old carbon, with distribution functions emerging from the deterministic model (equation 3.2).

Another important observation regarding the mean age predictions is the fact that these calculations were performed under the assumption that the system, in this case the forest, was in steady state. Since the C stocks in Harvard forest continue growing, the calculated mean ages and transit times should be interpreted as predictions of the mean age that the carbon may have in this forest once it is in steady state. Based on this, the time that this forest will take to reach the steady state is highly divergent among the three models. As an example, the model

with two storage compartments would predict 20 yr more of growth to reach a steady-state close to that of the model with no compartments.

In case of systems that are driven by environmental variables and result in time dependencies of inputs (GPP) and process rates, the mean ages and transit time distributions would also change over time. To calculate the means of these time-dependent distributions one would need to know the complete history of inputs and cycling rates for the duration of the simulation (Rasmussen *et al.*, 2016), information that is not available for Harvard forest. Nonetheless, we can predict that if there were external factors influencing the simulations, there would be a different prediction of mean ages and transit times at each time step, but the model structure (C allocation scheme in particular) would play a major role determining the shape of these distributions.

It is also noteworthy that what we assume to be a compartment, e.g. Wood, does not necessarily meet the well mixed assumption, so its particles may not have the same probability to leave the compartment at all times. Richardson *et al.* (2015) found a low concentration of old NSC in old rings of stemwood, and a high concentration of old NSC in coarse roots and fine roots of pine. Additionally, they found young and old C in roots. These dynamics were interpreted as poor C mixing and reserves that cycle on different timescales (Richardson *et al.*, 2015), but they may also obey to physiological constraints. For example, the parenchyma in heartwood is thought to be dead, so NSC trapped in there may no longer be accessible to the plant (Richardson *et al.*, 2015). So, to study the physiological significance of these findings with models, we might have to include such details regarding tree physiology. The important point we want to emphasize however, is that mixing of carbon in different vegetation compartments results in C age distributions that have been little studied previously. Our results are a first attempt to obtain these distributions using a number of assumptions, but in the future other analysis with more complex models and explicit formulas for time-dependent age distributions would help to obtain better predictions of ages and transit times as affected by specific physiological processes.

Although there are still knowledge gaps regarding plant physiology, and current C-dating methods only measure mean age of C rather than age distributions (Richardson *et al.*, 2013), we expect our results to motivate future work, particularly in the use of isotope tracers and their time evolution to approximate age distributions. Biosphere models can be enhanced with structural adjustments and the uncertainties in the parameter values can be reduced by constraining them with age and transit time distributions. These improved models could then be used to test hypotheses regarding physiological questions, and assess the sustainability of current terrestrial C sinks, given changes in environmental forcing.

Model equifinality (identifiability)

Model equifinality (Medlyn *et al.*, 2005) was evident from the fact that despite having different number of compartments and values of cycling rates, all of the three models had similar simulations of C stocks (Figures 3.3 and 3.4). Along with model equifinality, we obtained a high collinearity between some parameters, implying that they are non-identifiable, i.e., they cannot be uniquely estimated from the given data sets (Soetaert and Petzoldt, 2010). Thus, for these particular models, the time-course measurements from only 2 out of 4-6 vegetation compartments is not sufficient to estimate the values of 7-10 parameters.

Model equifinality as well as the impossibility to uniquely identify certain parameters (parameter non-identifiability) is expressed as high correlations between the parameter sets. Positive parameter correlations, may indicate *practical non-identifiability*, where the insufficiency or poor quality of data is not a good constrain for the parameters. In addition, a negative parameter correlation can be a symptom of *structural non-identifiability*, which is the result of a redundant parameterization (Raue *et al.*, 2009; Timmer, 2011; Raue *et al.*, 2012; Cressie *et al.*, 2009). Thus, the three models had practical and structural non-identifiabilities, which means that they need to be constrained with more and better data, and they need to be restructured in order to avoid compensation of fluxes into and out of the compartments.

Since this study was limited by the availability of relevant empirical data, the parameter values that we used are only one of many possible outcomes of parameter estimations using the same data sets. Therefore, it is possible that none of these models accurately depict the C cycle in the Harvard Forest. However, these problems experienced with parameter non-identifiability are not an isolated case; the process of finding unknown rates of C sequestration by fitting biosphere models to empirical data (Luo *et al.*, 2003) is often hampered by parameter non-identifiability (Schaber and Klipp, 2011). This is a real problem because parameters such as those that correspond to carbon turnover explain most of the variation in the response of terrestrial vegetation to future climate and CO₂ (Friend *et al.*, 2014) and are highly important in determining C age and transit times.

Conclusions

We obtained age and transit times distributions of carbon for simple vegetation models with contrasting carbon allocation schemes. Our results show that mixing of carbon in different vegetation compartments results in C age distributions not explored before in previous studies. The shape of these distributions depends largely on model structure, and in particular on how carbon allocation is represented in models.

Models with none or one storage compartment may fail to explain the mixing of ages found in different vegetation compartments, but they are more parsimonious than the model with 2 storage compartments. Nonetheless, parameter collinearity and model equifinality were persistent problems that might be solved if more constraints are added, since the time series of C in foliage and wood are not enough to parameterize a full vegetation model.

Although all models predicted similar C stocks in vegetation compartments, the inclusion of a carbon storage compartment resulted in very different predictions of age, transit time distributions, C release, and isotopic composition. Thus C ages and transit times, which can be indirectly measured using isotope tracers, can be used to improve biosphere models via examination of their structure and estimation of parameter values, which then can be used to assess the strength of C sources or sinks from vegetation.

Finally, it is advantageous to consider age and transit times as distributions, rather than only mean values; with their distributions we obtain additional insights on the temporal dynamics of carbon use, storage, and allocation, which not only depends on the rate at which C flows into and out of the compartments, but also on the stochastic nature of the process itself.

Source and sink limits on carbon allocation in vegetation: A dynamical system perspective

Vegetation is to a large extent resilient to changing environmental conditions by its ability to use storage reserves or to remobilize carbon and nutrients, therefore adjusting carbon transfers among compartments. Some environmental stressors can limit the strength of C sources and sinks in vegetation, but the interplay between these limits has not been analyzed yet from a theoretical perspective. We employed a simplified analytical model of carbon allocation to predict the vegetation response to source and sink limitation scenarios. With this, we ventured to answer three questions: (i) What model structure can represent the central role of non-structural C in vegetation functioning? (ii) Do the source and/or sink limitations alter the ratio between C stocks in equilibria? (iii) Are there alternative equilibria? How do they change under different source and/or sink strengths? We represented the central role of non-structural C in vegetation functioning with two compartments: a soluble sugars compartment that had a dual source/sink capacity, and a reserves compartment. Our model predictions were in line with empirical observations of vegetation growing under source and, or sink limitation. We found that strong sink limitations can lead to oscillations in the model solutions and shifts in the ratio between C stocks in equilibria. Our findings challenge the idea of NSC as a mere ‘overflow’ or ‘buffer’ compartment.

Introduction

Plants experience strong changes in environmental conditions while maintaining their sessile condition. This is possible by making adjustments whose impact transcend physiological processes, and could affect regional and even global energy and element fluxes (Keenan *et al.*,

2014). One of the ways in which plants cope with a changing environmental stimuli is by adjusting the partitioning of photoassimilates from sources (donors) to sinks (recipients). In fact, the remobilization of non-structural carbon (NSC) (from reserves to other sinks) is what allows plants to recover from periods of non lethal drought (Hartmann *et al.*, 2013), extreme temperatures (Hoch and Körner, 2003), shade (Kobe, 1997), tissue loss (Würth *et al.*, 2005), among others.

In this sense, vegetation can be considered as a system of C sources and sinks. The major C source in vegetation is the C supply gained through photosynthesis. After their assimilation, the photoassimilates are transported to plant sinks (compartments) such as leaves and woody tissues. Moreover, some sinks (e.g. NSC) can also become C sources, when they replenish the C of other sinks, such as the case when vegetation recovers from environmentally induced stress. While the importance of this source-sink interplay in vegetation functioning has motivated several studies, the identification of C transport between tree parts, and the characterization of the specific mechanisms that regulate carbon gain and distribution in vegetation are still unknown.

Quantifying C transport between tree parts has indeed been an elusive task, but Klein and Hoch (2015) were able to make an approximation using a C balance approach. They combined measurements of C exchange between the tree and its environment with the partitioning of sequestered C among tree compartments. Important progress has also been made with regard to the identification of the mechanisms regulating C gain and distribution (carbon allocation). Empirical findings have lead to the characterization of four factors that limit carbon allocation, which Hartmann *et al.* (2018) summarized as follows: (i) source strength, (ii) rate of translocation of C via phloem, (iii) sink strength, and (iv) sink priority.

Source strength refers to the strength of the C supply from photosynthesis and/or remobilization of storage to other C sinks. Therefore, this strength depends on environmental factors such as light, CO₂ and water availability. The *rate of translocation of C via phloem* determines the speed of C transport between plant parts, and is influenced by processes such as osmoregulation. The *sink strength* is defined as the maximum potential of C import rate of a sink; e.g. the maximum amount of C that a compartment can import for growth. Finally, the *sink priority* refers to the preference of a given sink over competing sinks to be supplied with photosynthate. This preference can respond to an established hierarchy such as the following: maintenance respiration > growth of the canopy and fruit development > stem cambium > root growth. Storage is considered to have the lowest priority. Changes in sink priority have also been attributed to phenology (Epron *et al.*, 2012); for example, Epron *et al.* (2011) observed a competition between the ¹³C partitioned to soil CO₂ efflux and the aboveground growth in late spring, as well as the storage in late summer, for a 20-year old beech stand. The sink priority

can also respond to the sink proximity to sources, or by the genetic regulation of proteins that affect phloem loading and unloading in sink tissues.

These four factors are represented in the figure 4.1. The limitation on source strength is symbolized with the function $\zeta(t)$, and the limitation on above and belowground sink strength is symbolized with the functions $\alpha(t)$ and $\rho(t)$, respectively. The array of vertical and horizontal fluxes represent the sink priority in response to the sink proximity to sources. The horizontal distribution of the compartments -reserves, soluble sugars, structural compartment- represents the rule: “last in, first out” (Lacointe *et al.*, 1993), since the structural compartments only receive the old C from the reserves if it is remobilized through the soluble sugars (which consists mostly of newly fixed C). Additionally, the C used for respiration also comes from the soluble sugars compartments, although the respiration is also proportional to the amount of living structural biomass. This scheme was intuitively designed based on plant physiology, and resembles the scheme used by Klein and Hoch (2015) in their carbon balance approach.

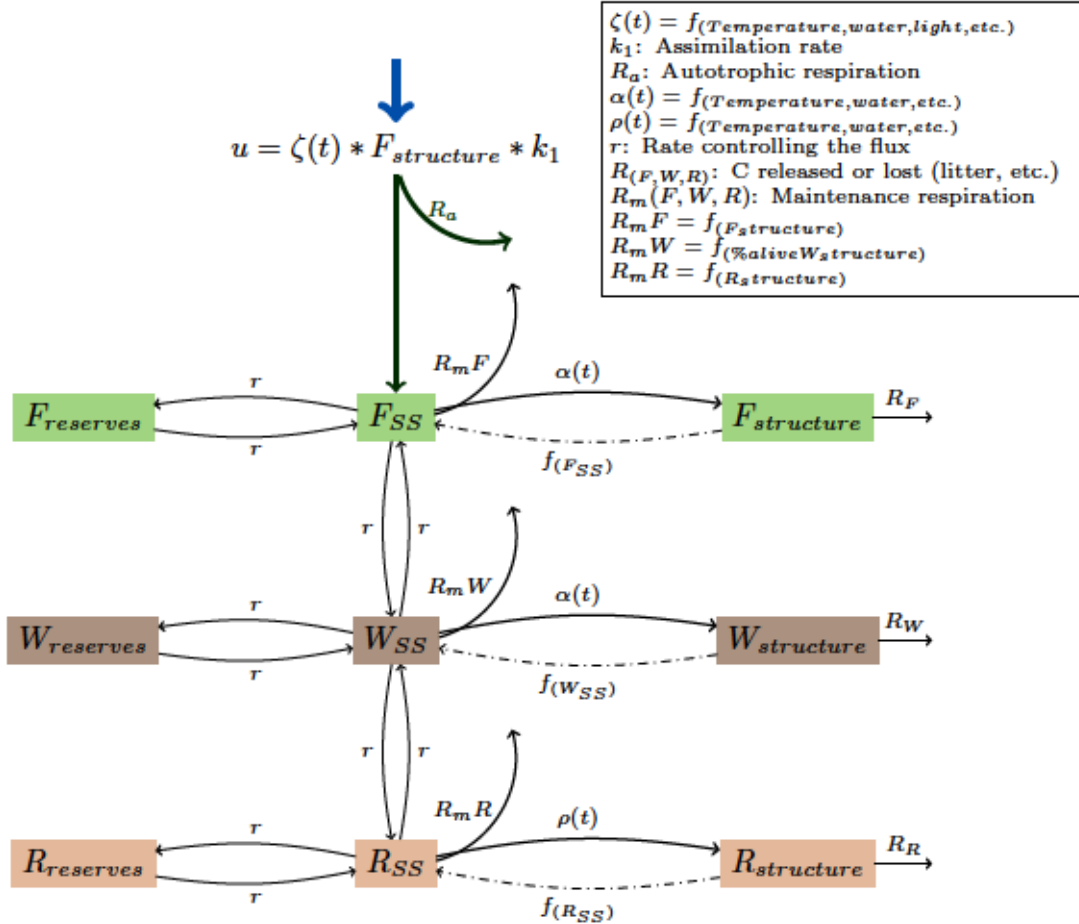


Figure 4.1: Carbon allocation scheme based on (Hartmann *et al.*, 2018). The figure shows a system of nine vegetation compartments -blocks- with C fluxes among them -arrows-. F, W and R stand for foliage, wood and roots, respectively. Each of these plant parts has a structural, soluble sugars and reserves compartment. The arrows point in the direction of the C flow, and the symbols associated to them represent the rates at which these fluxes occur. ζ, α, ρ are functions that modify the flux associated to them, thus indicating source, aboveground and belowground limitation, respectively; they are functions of environmental variables (e.g. some environmental controls of photosynthesis are light, temperature, nutrient and water availability, among others (Kozłowski and Keller, 1966)). u is a scalar function of system input (C assimilation via photosynthesis). $f_{(F,W,R)ss}$ is a function controlling the C flux from structural compartments to soluble sugars, it depends on the amount of soluble sugars.

Figure 4.2 represents the interplay of two of the four limiting conditions: source and sink strength limitation. These schemes can also be viewed as hypothesis for model predictions; for example, figure 4.2(a), (b), and (c) shows predictions of system behavior under (i) source limitation, (ii) prolonged or stronger source limitation, and (iii) sink limitation, respectively.

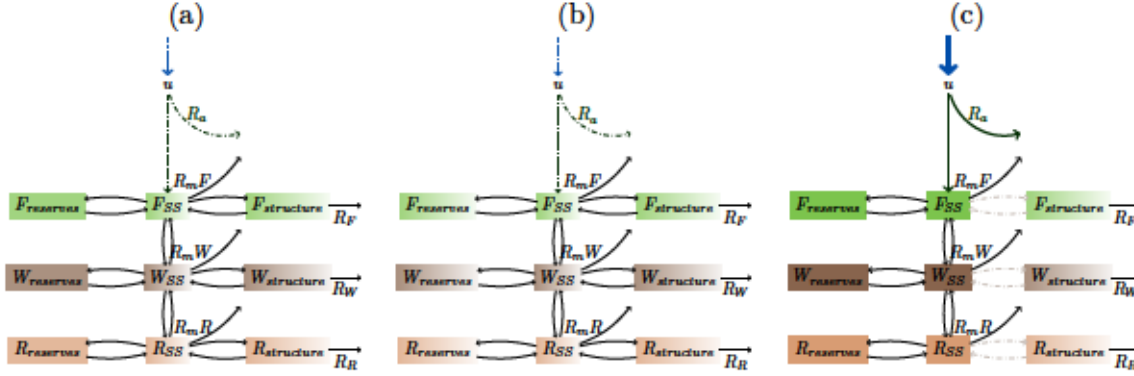


Figure 4.2: Schematic representation of limits of C allocation based on (Hartmann *et al.*, 2018). The figure shows a system of nine vegetation compartments under four different circumstances. F, W and R stand for foliage, wood and roots, respectively. Each of these organs has a structural, soluble sugars and reserves compartment. When the translocation and sink strength are not limiting, the rate of C partitioning to the sinks is a function of source strength and sink priority. (a) When there are environmental constraints on source strength -photosynthesis- e.g. low $[CO_2]$ and lack of light, which do not affect growth directly, the C fluxes are reduced, and so is the C in soluble sugars. This reduces the C flow to structural compartments and potentially induce the conversion of structural C to soluble sugars. (b) If the source limitation continues for an extended time, or takes place in close intervals, the vegetation will start using older C reserves. (c) If the translocation and source strength are not limiting, but there is a sink limitation (could be caused by low temperature, non-lethal drought), C is partitioned to the structural compartments until it reaches the limit of the sink, decreasing the cycling rate of C to these compartments. This results in the accumulation of soluble sugars and reserves.

The four factors that limit the carbon allocation in vegetation have been studied mostly separately, or without explicit relation to carbon allocation. As an example, Minchin and Lacoite (2005) proposed a mechanistic model that combined the transport-resistant approach with phloem loading dynamics. Other studies evaluate the effect of a few environmental variables on one or two of the factors that limit C allocation. One of the most studied environmental variables is water availability; e.g. McDowell *et al.* (2013) examined the model-based understanding of drought-induced vegetation mortality, and Fatichi *et al.* (2016) modelled the plant-water interactions in an ecohydrological overview from the cell to the global scale. Other modeling and empirical approaches have also focused on the interplay between water availability and carbon allocation, under elevated CO_2 conditions (Fatichi and Leuzinger, 2013). Perhaps the closest and most recent approach on combining the knowledge obtained from empirical findings and modelling to tackle the ‘long-standing puzzle’ of *sink limitation* has been the data assimilation approach of Mahmud *et al.* (2018). However, the model implemented in that work lacked explicit formulas for source and sink limitation.

Those studies are generally motivated by the question of whether the vegetation will be able to survive projected climatic conditions or not. Other studies revolve around the concept of *safe operating space* (Scheffer *et al.*, 2015) whose boundaries are acceptable levels of environmental

stressors. Manzoni *et al.* (2014), for example, proposed a minimal plant hydraulic model and found a bifurcation in the hydraulic failure, where some environmental parameters trigger the loss of a “physiologically sustainable equilibrium”. The term *equilibrium* leads us to another interesting topic: Given that plants adjust to drastic changes in environmental forcing via *acclimation*, they can have more than one stable state –or equilibrium, or fixed point, all these terms will be used interchangeably throughout this text. Bryla *et al.* (1997) found that citrus plants can acclimate to changes in water levels and temperature by shifting to higher or lower respiration rates. How easily can they shift between alternative steady states? Are there points of no return?

Evidently plant growth depends on factors that control the conversion of carbohydrates to new tissues (e.g. nutrient availability, temperature and cell turgor (Kozlowski and Keller, 1966; Körner, 2015)). Nonetheless, the prevailing assumption amongst models is that plant growth is primarily controlled by the C supply from photosynthesis i.e., source strength, thus ignoring sink strength limitation on growth. Here, a simplified analytical model of carbon allocation in vegetation is employed with explicit formulas for source and sink limitation. Three main questions were addressed: (i) What model structure can represent the central role of non-structural C in vegetation functioning? (ii) Do the source and/or sink limitations alter the ratio between C stocks in equilibria? (iii) Are there alternative equilibria? How do they change under different source and/or sink strengths?

Methods

Working definitions

The dual role of non-structural carbohydrates, in particular the soluble sugars (*SS*) as sinks and sources may generate confusion when the term *sink* or *source* strength (or in the opposite case, limitation) is used in this work. This is why it is important to distinguish them; in this context:

- *Source strength* only refers to the C supply from photosynthesis –*SS* are the sink of the photosynthetic source.
- *Sink strength* refers to the maximum C import rate of the structural sinks (foliage, wood and roots) for their growth –*SS* are the source of C for the structural compartments.

Model description

The model description follows the ODD (Overview, Design concepts, and Details) protocol (Grimm *et al.*, 2006, 2010).

1. Purpose

This model is a process based representation of the central role of non-structural C in vegetation functioning, particularly in the context of source and sink limitations on carbon allocation. Figure 4.3 shows the vegetation compartments considered and the fluxes between them. The carbon fluxes modelled are constrained by mass balance and are calculated using a set of ordinary differential equations 4.1-4.5. Despite the nonlinearities of some of these fluxes (see equation 4.1), the simplicity of the model facilitates the identification of fixed points.

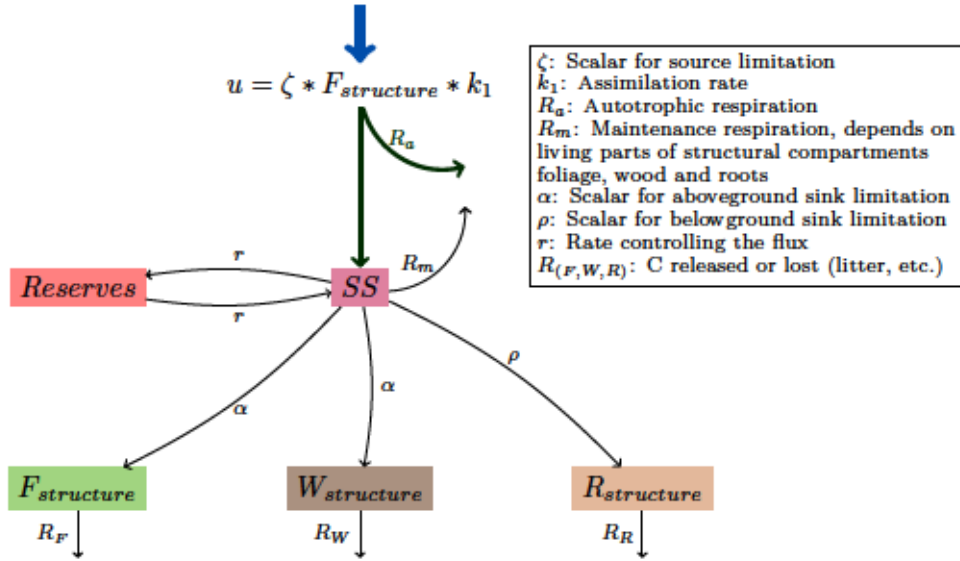


Figure 4.3: Schematic representation of the model. The model is a system of five vegetation compartments -blocks- with C fluxes among them -arrows-. F , W and R stand for foliage, wood and roots, respectively; together, they constitute the structural part of the vegetation. The non-structural carbon is divided in two compartments: soluble sugars (SS) and Reserves (starch, lipids, etc.). The arrows point in the direction of the C flow, and the symbols associated to them represent the rates at which these fluxes occur. u is a scalar function of system input (C assimilation via photosynthesis). All the photosynthesized C is first collected in the SS compartment, and from there it is transferred to the structural compartments and the Reserves. The C stored as reserves may also be converted to soluble sugars. ζ, α, ρ are scalars that modify the rates of the fluxes associated to them, thus indicating source, aboveground and belowground limitation, respectively; they can have values between 0 and 1. The flux from structural compartments to soluble sugars is neglected.

2. Entities, state variables and scales

The model consists of five state variables, i.e., vegetation compartments: soluble sugars (SS), reserves (Res), and structural foliage, wood and roots (F_{struc} , W_{struc} , and R_{struc} , respectively). Other parameters used in the model are described in the table 4.1.

3. Process overview and scheduling

The vegetation system modelled here consists of a photosynthetic input that enters via the soluble sugars and from there it is distributed to other compartments. This central position of soluble sugars guarantees its priority, which means that the other compartments can only obtain C when there are soluble sugars. This is in agreement with empirical findings where

Table 4.1: Variables and parameters of the model.

Symbol	Description	Value	Unit
SS	Soluble sugars (soluble NSC)	15	$kgC \cdot m^{-2}$
Res	Carbon in reserves (non-soluble NSC)	15	$kgC \cdot m^{-2}$
F_{struc}	Structural carbon in foliage	15	$kgC \cdot m^{-2}$
W_{struc}	Structural carbon in wood (wood of stem, branches, and roots)	150	$kgC \cdot m^{-2}$
R_{struc}	Structural carbon in fine roots	90	$kgC \cdot m^{-2}$
rm	Maintenance respiration scalar	1000.0	kgC^{-1}
α	Scalar for aboveground sink limitation	1	
η	Proportion of photosynthetically fixed carbon partitioned to SS	0.5	
γ_{12}	Flux rate of carbon from Res to SS	0.0015	day^{-1}
γ_{21}	Flux rate of carbon from SS to Res	0.001	day^{-1}
γ_F	Rate in which carbon leaves from F_{struc} to the exterior (e.g. litter)	0.01	day^{-1}
γ_R	Rate in which carbon leaves from R_{struc} to the exterior	0.0005	day^{-1}
γ_W	Rate in which carbon leaves from W_{struc} to the exterior	0.0001	day^{-1}
k_1	Atmospheric C absorption rate	1	day^{-1}
$liveWood$	Percentage of W_{struc} that is still alive	0.1	
max_{31}	Max. flux rate of carbon from SS to F_{struc}	$\frac{1}{100}$	day^{-1}
max_{41}	Max. flux rate of carbon from SS to W_{struc}	$\frac{1}{1000}$	day^{-1}
max_{51}	Max. flux rate of carbon from SS to R_{struc}	$\frac{1}{1000}$	day^{-1}
ρ	Scalar for belowground sink limitation	1	
ζ	Scalar for source limitation	1	
γ_{31}	Flux rate of carbon from SS to F_{struc}	$\alpha \cdot max_{31}$	day^{-1}
γ_{41}	Flux rate of carbon from SS to W_{struc}	$\alpha \cdot max_{41}$	day^{-1}
γ_{51}	Flux rate of carbon from SS to R_{struc}	$\alpha \cdot max_{51}$	day^{-1}
R_m	Rate of maintenance respiration	$\frac{F_{struc} + R_{struc} + (liveWood \cdot W_{struc})}{rm}$	day^{-1}

Values for SS , Res , F_{struc} , W_{struc} , and R_{struc} correspond to initial C stocks.

Values for ζ , α , and ρ varied according to the scenarios from figures 4.9 and 11.

reserve formation was prioritized over growth (Chapin *et al.*, 1990). Carbon continuously flows into and out of the compartments, with a rate of change computed with the set of differential equations 4.1-4.5. The model was implemented using the Python 3 package bgc-md¹. For this implementation, the set of ODEs 4.1-4.5 was transformed into its matrix representation (see table 4.2), according to the framework described in chapter 2.

$$\dot{SS} = F_{struc} \cdot \eta k_1 \cdot \zeta + Res \cdot \gamma_{12} + SS \cdot \left(-\alpha \cdot max_{31} - \alpha \cdot max_{41} - \gamma_{21} - max_{51} \cdot \rho - \frac{F_{struc} + R_{struc} + W_{struc} \cdot liveWood}{rm} \right) \quad (4.1)$$

$$\dot{Res} = -Res \cdot \gamma_{12} + SS \cdot \gamma_{21} \quad (4.2)$$

$$\dot{F}_{struc} = -F_{struc} \cdot \gamma_F + SS \cdot \alpha \cdot max_{31} \quad (4.3)$$

$$\dot{W}_{struc} = SS \cdot \alpha \cdot max_{41} - W_{struc} \cdot \gamma_W \quad (4.4)$$

$$\dot{R}_{struc} = -R_{struc} \cdot \gamma_R + SS max_{51} \rho \quad (4.5)$$

¹<https://github.com/MPIBGC-TEE/bgc-md>

Table 4.2: Matrix representation of the model

Name	Description	Expression
x	vector of states for vegetation	$x = \begin{bmatrix} SS \\ Res \\ F_{struc} \\ W_{struc} \\ R_{struc} \end{bmatrix}$
u	scalar function of photosynthetic inputs	$u = F_{struc} \cdot k_1 \cdot \zeta$
β	vector of partitioning coefficients of photosynthetically fixed carbon	$\beta = \begin{bmatrix} \eta \\ 0 \\ 0 \\ 0 \\ 0 \end{bmatrix}$
B	matrix of cycling rates	$B = \begin{bmatrix} -\gamma_{21} - \gamma_{31} - \gamma_{41} - \gamma_{51} - R_m & \gamma_{12} & 0 & 0 & 0 \\ \gamma_{21} & -\gamma_{12} & 0 & 0 & 0 \\ \gamma_{31} & 0 & -\gamma_F & 0 & 0 \\ \gamma_{41} & 0 & 0 & -\gamma_W & 0 \\ \gamma_{51} & 0 & 0 & 0 & -\gamma_R \end{bmatrix}$
f_v	the right-hand side of the ODE	$f_v = u(x) \cdot \beta + B(x) \cdot x$

4. Design concepts

- **Basic principles:** Here we assume that the functions that determine source and sink limitation have solutions in the range from 0 to 1, where 1 is a scalar that does not change the flux when multiplied by it, i.e. it indicates no limitation. This simplification has two important advantages. First, it avoids potential biases that result from the representation of processes with different levels of detail (Govingjee, 2009). In fact, the inner transport mechanisms and processes behind sink limitation are not as well known as the ones related to photosynthesis, thus the functions related to source limitation can and has been described in more detail than the ones related to sink limitation (Hilbert and Reynolds, 1991; King, 1993; Potter *et al.*, 1993; Foley *et al.*, 1996; Murty and McMurtrie, 2000; Arora and Boer, 2005; Williams *et al.*, 2005; DeAngelis *et al.*, 2012; Luo *et al.*, 2012). And second, the use of scalars multiplying particular fluxes facilitates the control of the target of the limitation, and thus the attribution of the observed dynamics to a particular treatment. Otherwise, it would be extremely difficult to discern between effects of variables that have a role in contrasting processes, such as temperature, water availability, etc.
- **Emergence:** The C input (photosynthetically fixed C) of the vegetation system modelled depends on the amount of C stored as structural foliage (F_{struc}), thus, any changes in the size of this compartment have an impact on the system's input.
- **Interaction:** The C exchange between vegetation compartments and between the vegetation and its surroundings is represented by the arrows in figure 4.3. The C used for maintenance respiration of the whole vegetation system is extracted from the soluble sugars (SS), but depends on the current biomass, i.e., the amount of C in the living tissues of structural compartments -foliage, wood and roots. This

results in a nonlinear flux.

5. Initialization

All the initial carbon stocks and parameter values used for the model runs are summarized in table 4.1, unless otherwise noted.

6. Input data

Given that the model proposed here is autonomous, i.e. is not driven by external time-dependent variables such as environmental drivers, no input data is required to run it.

Stability analysis

We based the stability analysis of the proposed model on the well established theory for dynamical autonomous systems (Jacquez and Simon, 1993; Strogatz, 2014). First, we computed the analytical solution of the system in steady state, i.e., we calculated the fixed points, which are points where the C input and output of each compartment cancel out. For this, we set the ordinary differential equations 4.1 - 4.5 to 0, and then solved them analytically, using the Python package SymPy (Meurer *et al.*, 2017).

Second, we assessed the stability of each fixed point by calculating the eigenvalues from the Jacobian matrix for each of them, using the Python 3 package, bgc-md (see link in subsection 4 Model description - Process overview and scheduling). The eigenvalues provide useful information regarding the qualitative behaviour of the solutions (Sierra and Müller, 2015); from them one can mainly infer whether the solutions of the modelled system would eventually converge to a given fixed point or not. The eigenvalues can also indicate whether the system solutions will approach the fixed points oscillating or not, because for complex eigenvalues of the form $\lambda = \epsilon + -i\kappa$, ϵ controls the rate of exponential decay and κ the oscillation frequency (Sierra and Müller, 2015). Thus, the ratio between these real and imaginary parts (i.e. damping ratio, ϕ) indicates whether the system oscillates indefinitely, i.e. $\phi = 0$, or decays exponentially, $\phi = 1$. The damping coefficient (ϕ) can be calculated using the equation (Lallement and Inman, 1995) :

$$\phi = \frac{-\epsilon}{\sqrt{\epsilon^2 + \kappa^2}} \quad (4.6)$$

Code availability

All of the simulations and figures for this work can be reproduced using the code and data provided in the supplementary material.

Results

Stability analysis

We found two fixed points by setting the ODE system (right-hand side of equations 4.2 - 4.5) to 0, and solved equations 4.2 to 4.5 for each state variable, thus the solutions were in terms of SS and the dimensionality of our five dimension system was reduced to one dimension. We replaced the state variables in the equation 4.1 with these solutions, which could then be solved, i.e., we found the solution of SS in steady state (equation 4.1 = 0). This solution could then be computed into the remaining ODEs to find the solutions of the other state variables in steady state. Aside from the fixed point $[0, 0, 0, 0, 0]$, the non-zero fixed point has as solution the following set of equations:

$$SS^* = \frac{2.5 \cdot 10^{-7} \alpha \zeta - 5.5 \cdot 10^{-9} \alpha - 5.0 \cdot 10^{-10} \rho}{1.0 \cdot 10^{-9} \alpha + 1.0 \cdot 10^{-9} \rho} \quad (4.7)$$

$$Res^* = \frac{1.66667 \cdot 10^{-7} \alpha \zeta - 3.66667 \cdot 10^{-9} \alpha - 3.33333 \cdot 10^{-10} \rho}{1.0 \cdot 10^{-9} \alpha + 1.0 \cdot 10^{-9} \rho} \quad (4.8)$$

$$F_{struc}^* = \frac{5.0 \cdot 10^{-5} \alpha (0.005 \alpha \zeta - 0.00011 \alpha - 1.0 \cdot 10^{-5} \rho)}{1.0 \cdot 10^{-9} \alpha + 1.0 \cdot 10^{-9} \rho} \quad (4.9)$$

$$W_{struc}^* = \frac{0.0005 \alpha (0.005 \alpha \zeta - 0.00011 \alpha - 1.0 \cdot 10^{-5} \rho)}{1.0 \cdot 10^{-9} \alpha + 1.0 \cdot 10^{-9} \rho} \quad (4.10)$$

$$R_{struc}^* = \frac{0.0001 \rho (0.005 \alpha \zeta - 0.00011 \alpha - 1.0 \cdot 10^{-5} \rho)}{1.0 \cdot 10^{-9} \alpha + 1.0 \cdot 10^{-9} \rho} \quad (4.11)$$

Notice that equations 4.7 to 4.11 are written in terms of the limitation parameters ζ , α and ρ , which would allow us to test how the fixed point changes with respect to limitation scenarios. Note also that none of these equations is quadratic (or higher order), so the model can only have maximum two fixed points for each parameter set, the fixed point with the empty system and the fixed point determined by the equations (4.7) to (4.11). This means that there are no potential bifurcations or tipping points (Strogatz, 2014).

The eigenvalues for the fixed point $[0, 0, 0, 0, 0]$ in the case all limitations are removed ($\zeta = \alpha = \rho = 1$) were: $[-0.0001, -0.0005, -0.0822, 0.0592, -0.0015]$. All but one of these eigenvalues are real negative numbers, which indicates that this fixed point is unstable, and solutions that start close to this value are repelled from this point (Strogatz, 2014).

And for the second fixed point, calculated with equations 4.7-4.11 with $\zeta = \alpha = \rho = 1$, the complex eigenvalues were the following: $[\lambda_1 : -0.50832, \lambda_2 : -1.5641 \times 10^{-3} + 0.0011i, \lambda_3 : -1.5641 \times 10^{-3} - 0.0011i, \lambda_4 : -1.2745 \times 10^{-4}, \lambda_5 : -1.5201 \times 10^{-3}]$. Their negative real parts indicate that this fixed point is stable, and the complex conjugate λ_2 and λ_3 indicates that solutions that start close to this fixed point converge to it through oscillations (Strogatz, 2014). Indeed, when we calculated the eigenvalues for this fixed point under different limitation scenarios, and their respective damping coefficients, we found that under certain conditions

(mainly when the aboveground sink limitation (α) = 0.01) the damping coefficient of eigenvalues λ_2 and λ_3 is the closest to 0 (see figure 4.4 (b)). As a reminder, when the damping coefficients = 0, the system oscillates indefinitely (Lallement and Inman, 1995; Sierra and Müller, 2015). This was further explored with the complex planes, i.e., plots of Real Vs. Imaginary parts of the eigenvalues (figures 4.5 and 4.6). The complex plane in figure 4.6(a) for eigenvalues λ_2 and λ_3 shows that when the aboveground sink limitation increases, so does the absolute value of the imaginary part of the eigenvalues, while the absolute value of the real part decreases. This trajectories follow a semicircle. In contrast, the eigenvalues λ_1 and λ_5 always have imaginary parts in the neighborhood of 0, independent of the limitation scenario.

The oscillations in the model solutions, which result from a strong aboveground limitation, can be seen in figure 4.7 (b) and (c). The spirals can be observed in the phase planes (C stocks in compartments plotted against each other) of the columns (b) and (c) of figure 4.8. In contrast, the eigenvalues for the same model run with a constant photosynthetic input (u no longer depends on the state variable F_{struc}) only had real parts, thus there were no oscillations (see figures 12 and 13).

Simulation of carbon allocation limits in steady state

We calculated the C stocks in steady state using the equilibria equations 4.7 to 4.11 under different limitation scenarios (represented by combinations of the scalars ζ , α , and ρ) see figure 4.9. Thus, the C stocks plotted should not be interpreted as ‘transient’ states of C limitation, they are the amount of C that each compartment would have when they reach the equilibrium, given a limitation condition and any initial C stock. For these simulations, all the parameters were kept as in table 4.1, except for the limiting scalars (ζ , α , or ρ), which varied according to the limitation scenario. The results shown in figure 4.9 will be described in more detail in the following subsections:

Source limitation: The simulations of C stocks in steady state is in agreement to the hypothesis from figure 4.2 (a) and (b). The constraint in source strength resulted in reduced C stocks (see figure 4.9(a)), and all of the compartments were equally affected. As the source limitation approached its maximum strength, i.e. as $\zeta \rightarrow 0$, the sensitivity of the steady-state carbon stocks increased.

Aboveground sinks limitation: When the strength of the aboveground sinks (structural foliage and wood) was reduced, their C stocks decreased smoothly with the decreasing sink strength, and accelerated when $\alpha \rightarrow 0$ (figure 4.9(b)). The reduction in the C content of the rest of the sinks (soluble sugars, reserves and roots) decreased in a smaller proportion, which could have been the result of an unintentional source limitation given by the input dependency on structural foliage –which was under sink limitation. This explanation can be confirmed by the

belowground sink limitation simulations and the predictions of the fixed-input version of the model (see figure 11(b)).

Belowground sink limitation: When the amount of C partitioned to the roots was limited, the C content in this compartment was shortly reduced at first, but dramatically declined when $\rho \rightarrow 0$. All of the four remaining compartments had slow increases in their C stocks, proportional to the sink limitation (see figure 4.9(c)).

Above and belowground sink limitation: The combination of the two former limitations, i.e. the sink limitation on the structural compartments foliage, wood and roots, resulted in similar reductions in the affected sinks (see figure 4.9(d)). On the contrary, the soluble sugars and reserves had small proportional increases and, under certain sink strengths (e.g. $\zeta = 1, \alpha < 0.1, \rho < 0.25$) the C stocks of non-structural carbon was higher than the structural compartments. This change in the NSC:structural C ratio can be explained by the sink limitation hypothesis (figure 4.2(c)), where a restriction in the flow of sugars to the structural compartments, results in their accumulation in the source compartments.

Source and sink limitation: This dual limitation can be interpreted as the representation of drought-induced stress, leaving aside the effect that it has on the entire C transport; in the early stages of drought the source strength is barely impacted, the aboveground sinks strength is affected the most, and the belowground sinks are slightly buffered by the water content that remains in the soil, so it is not as heavily impacted as the aboveground sinks (see figure 4.9(e)). Under these two limitations the C stocks in steady state were reduced, following the trends predicted for the individual above and belowground sink limitation scenarios, but with smaller C stocks. The sugars and reserves were the least affected by the limitations. Interestingly, there was a slight bump in the trend, possibly when the NSC accumulation slightly counteracted the sink limitations ($\zeta = 1, \alpha = 0.05, \rho = 0.1$).

Discussion

Representing the central role of non-structural C in vegetation functioning with an analytical model

We developed a simple analytical model of carbon allocation to predict the vegetation response to source and sink limitation scenarios. Our model representation not only satisfies the need for the inclusion of a non-structural C (NSC) compartment to capture vegetation growth under limited source or sink conditions as previously observed in empirical studies (Mahmud *et al.*, 2018), but it also portrays the multi-functional nature of NSCs, which can act as *cash flow* and reserves –among other roles (Martínez-Vilalta *et al.*, 2016). Perhaps the most important feature of this model is that the soluble sugars compartment is an intermediary between the

photosynthetic input and the structural C sinks, thus representing the central role of NSC in vegetation functioning.

The soluble sugars have very important and diverse roles in the entire plant functioning as summarized by Hartmann and Trumbore (2016). Soluble sugars are the products from photosynthesis, but since they are rapidly converted to reserves, the most highlighted quality of NSCs in general has been its *buffering* capacity. In fact, C reserves can “buffer any asynchrony of supply and demand” (Hartmann and Trumbore, 2016), and in certain cases this buffering capacity can cover C deficits over several growing seasons (Muhr *et al.*, 2016). Thus, the amount of C stored in a tree indicates its actual C-supply status, which reflects its capital for flushing and reproduction or to replace lost tissue (Würth *et al.*, 2005). However, these reserves can also be transformed back into soluble sugars to perform other tasks or to be used for growth, which is probable the reason why they have a dual behaviour: they act as a C sink with respect to the photoassimilates, and as a major C source with respect to reserves and structural compartments (see *SS* in figure 4.3).

Overall, the vegetation representation proposed in this work challenges two persisting views of carbon allocation in global vegetation models: 1. The role of non-structural C is far beyond what has been represented in models, where it has reached to a point where they are only determined by the imbalance between source strength (net assimilation) and the sink strength (growth of structural compartments) (Hartmann *et al.*, 2018). 2. With the inclusion of a sink limitation to growth, it highlights the fact that growth is not necessarily a C source-limited process, because what limits the biomass formation is the rate at which carbohydrates are converted to new tissues, as it has been observed, in an individual scale, in cambial growth (Kozlowski and Keller, 1966). This will be discussed in the next subsection.

Source and/or sink limitation can lead to changes in equilibria and alter the ratio between C stocks

This analysis was mainly focused on the effect that C allocation limitation can have on the stable state or equilibrium of a vegetation system. Thus, it is imperative to contextualize our results in the stability analysis of dynamical system theory. Here we proposed an **autonomous non-linear** model, which in principle means that it could potentially reach one or more fixed points (equilibria). Contrarily, the solutions of non-autonomous models, i.e., models driven by time-dependent variables, do not converge to a fixed steady state (Jacquez and Simon, 1993), but may instead be attracted to a particular region, which increases the complexity of their stability analysis (Müller and Sierra, 2017). In contrast, one of the simplest types of models whose stability analysis can be performed are the autonomous linear models with constant input, which are models that can only have one fixed point (Strogatz, 1994). This fixed point

is not zero, because a fixed point where all C stocks are 0 can only occur when the C input depends on a state variable. An example is the model proposed here, whose photosynthetic input depends on structural foliage (F_{struc}); if the C stock of F_{struc} reaches 0 no input can be generated, and all compartments will decay until no C remains in them. In addition to the fixed point 0, the nonlinearities of the model proposed here could potentially lead to more than one fixed point, because their steady state equations may have variables with orders of magnitude higher than 1, e.g. a quadratic equation. Yet, the model proposed here only had two fixed points, one of them zeros.

This non-zero fixed point represents the C stocks predicted by the model in equilibrium, and can vary depending on the degree of C allocation limitation, just as it has been observed in empirical studies (Bryla *et al.*, 1997). Certainly, increasing source and/or sink limitation resulted in smooth changes in the equilibrium, and the keyword is *smooth* because these adjustments were not drastic or catastrophic, i.e. there were no tipping points. Instead, some limitation scenarios had an effect on the way that model solutions approached the equilibrium, because very strong source and/or sink limitation lead to an increase in the nature of oscillations as captured by the damping ratio (see figure 4.7). There has been oscillations documented during *in situ* $^{13}\text{CO}_2$ pulse labelling studies in 20-year-old beech trees (Plain *et al.*, 2009), in a boreal pine forest (Subke *et al.*, 2009), in the soil CO_2 efflux of a temperate, 15-year old oak stand (in September) (Epron *et al.*, 2011), and on the stem CO_2 of a northern white-cedar (Powers and Marshall, 2011).

The C allocation limitation scenarios also influenced the predictions of vegetation functioning. Decreasing levels of source strength resulted in proportionally lower accumulation of C in all compartments (see figure 4.9 (a)). This is not only in agreement with our intuitive predictions, but also with empirical findings where reducing just the source -not the sink- strength resulted in decreased C in the vegetation compartments. An example is the decrease in NSC of trees growing in source-limitation conditions, observed at the individual level in an experiment designed to test drought-induced tree mortality in piñon pine trees (Sevanto *et al.*, 2014). Likewise, at the forest stand level, an extended drought lead to a reduction of root NSC of mature longleaf pine (Sword Sayer and Haywood, 2005). In contrast, NSC accumulated when source strength increased to a higher extent than the sink strength (growth became a limiting factor), in 32-to 35-m-tall trees of a deciduous forest exposed to elevated CO_2 (Körner *et al.*, 2005).

In fact, when the strength of structural sinks such as foliage, wood and roots is reduced, the carbohydrates not used for growth accumulate in reserves and soluble sugars (see figure 4.9 (c)-(e)). These findings are in agreement with empirical studies where the NSC increased at the expense of root growth in low temperatures (Alvarez-Uria and Körner, 2007), and leaf growth under limiting N availability (Cheng and H Fuchigami, 2003). Sink limitation has also

been attributed to the altitudinal tree limit, where low temperatures affected the sink activity -not the photosynthetic capacity- at the tree line and the surplus C was stored in the reserves (osmotically inactive) (Hoch and Körner, 2003, 2012).

Interestingly, if the sink limitation is strong enough (e.g. $\alpha < 0.01$, $\rho < 0.05$, see figure 4.9 (b), (d) and (e)), the ratios between C stocks shift, with NSC even higher than wood C (in the case of aboveground sink limitation). Thus, sink priorities change not by directly increasing the rate at which C is transferred to a particular compartment, but by a strong decrease in C transfer to other compartments (sink limitation), which then leads to the accumulation of C in the source compartments –soluble sugars and reserves.

The strong sink limitation also affected the predictions of C age. As discussed in chapter 3, the time that a C particle remains in a compartment since its entrance, i.e. C compartmental age, depends on the probability of C particles entering this compartment and then leaving after a certain period. Since this probability increases with faster cycling rates, fast cycling compartments tend to have younger mean ages than slower ones. In this context, when cycling rates are reduced by multiplying them by a coefficient < 1 , the probability of particles leaving the involved compartment decreases, and this results in the prediction of older compartmental mean ages (see figure 14). This effect was mainly observed when there was a very strong source and sink limitation (see figure 14 (a),(b), (d) and (e)), but the limitation impact was noticeably reduced when the same age calculations were performed with a fixed-input version of the model (figure 15) and almost disappeared for the linear version (figure 16). This means that the nonlinearities in the model proposed here magnified the effect that the carbon allocation limitations had on predicted mean ages.

Implications for C cycle modelling

With the simplified representation of source and sink limits on C allocation proposed here it has been demonstrated that the C source-sink dynamics are a defining characteristic of vegetation functioning. As an example, the model predicts that strong source and sink limitations can affect the C age and the sink capacity of vegetation with respect to the atmosphere, because ecosystems that have reached steady state under these limiting conditions accumulate less mass and have older mean ages than those with stronger C source and sink capacities. This behaviour has been observed in environmental gradients and contrasting ecosystems such as the rain forest and the dry forest, but the fact that both responses were only significantly predicted by the nonlinear model can be an indication that the nonlinearities may increase the model performance.

Overall, the model simulations explored here could steer the improvement of more detailed

models, where the limitation scalars (ζ, α, ρ) could be replaced with functions driven by environmental variables, and parameters estimated through the assimilation of experimental or observational data.

Conclusions

Our simple model was able to display qualitative behaviours of source and sink limitation that have been encountered in a wide range of scales: from single plants to forests. We found that the central role of non-structural C in vegetation functioning can be represented with two compartments: a soluble sugars compartment that acts as an intermediary between the photosynthetic input and the rest of the compartments (it has a dual source/sink capacity), and a reserves compartment, where the osmotically inactive compounds are stored.

In addition we found that strong sink limitations can lead to oscillations in the model solutions, and shifts in the ratio between C stocks in equilibria. These shifts result from the fact that the impairment of C flow for the growth of some sinks lead to the C accumulation in the source compartments (soluble sugars). Thus, under different source and/or sink strengths there are smooth changes in the equilibrium states, where not limited compartments accumulate more carbon than the limited ones.

All of our findings support the empirical inferences that challenge the idea of NSC as an ‘overflow’ or ‘buffer’ compartment that has been perpetuated in most dynamic global vegetation models. It is clear that, given its involvement in all aspects of vegetation functioning, NSC has a central role in C allocation in vegetation, and its accumulation when there are constraints on growth of structural tissues is only an effect of its dual role as a sink of photosynthetic input and source of the structural C compartments. Improving the representation of NSC in models could enhance model predictions of the vegetation response to source or sink limitation scenarios under changing environmental stressors.

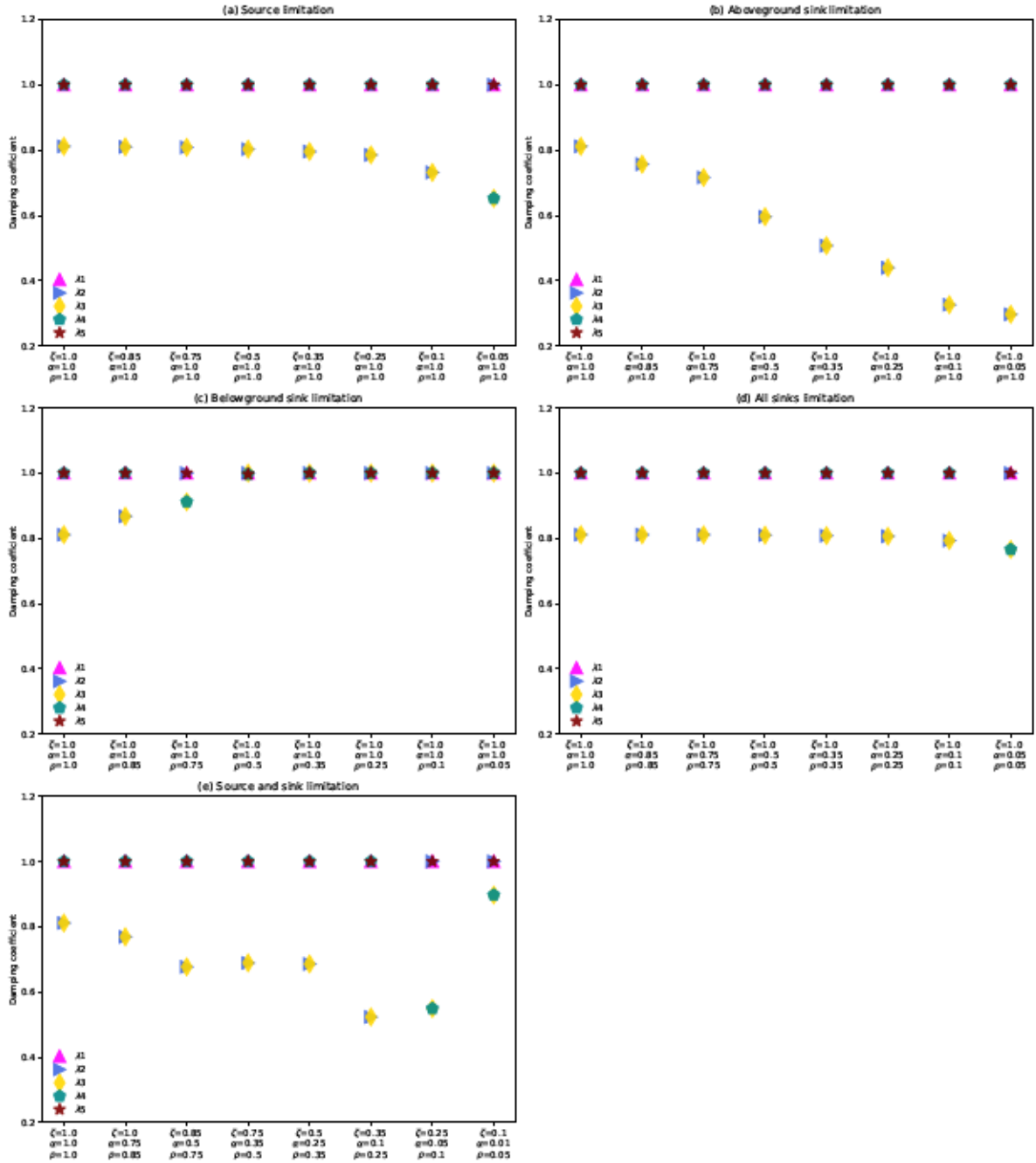


Figure 4.4: Damping coefficients under the different limitation scenarios. When there is no limitation, the damping coefficient of all the eigenvalues are in the neighborhood of 1, and most of them remain there even under different C allocation limitation scenarios. In contrast, λ_2 and λ_3 have slightly smaller values. They are also the only two eigenvalues whose damping coefficients start to drop under stronger limitation scenarios, especially under strong aboveground limitation (b) and a combined source and sink limitation (e). Another eigenvalue with an interesting response is λ_4 , whose damping ratio increases with increasing belowground sink limitation (c), and decreases when the combined source and sink limitation is the strongest (e).

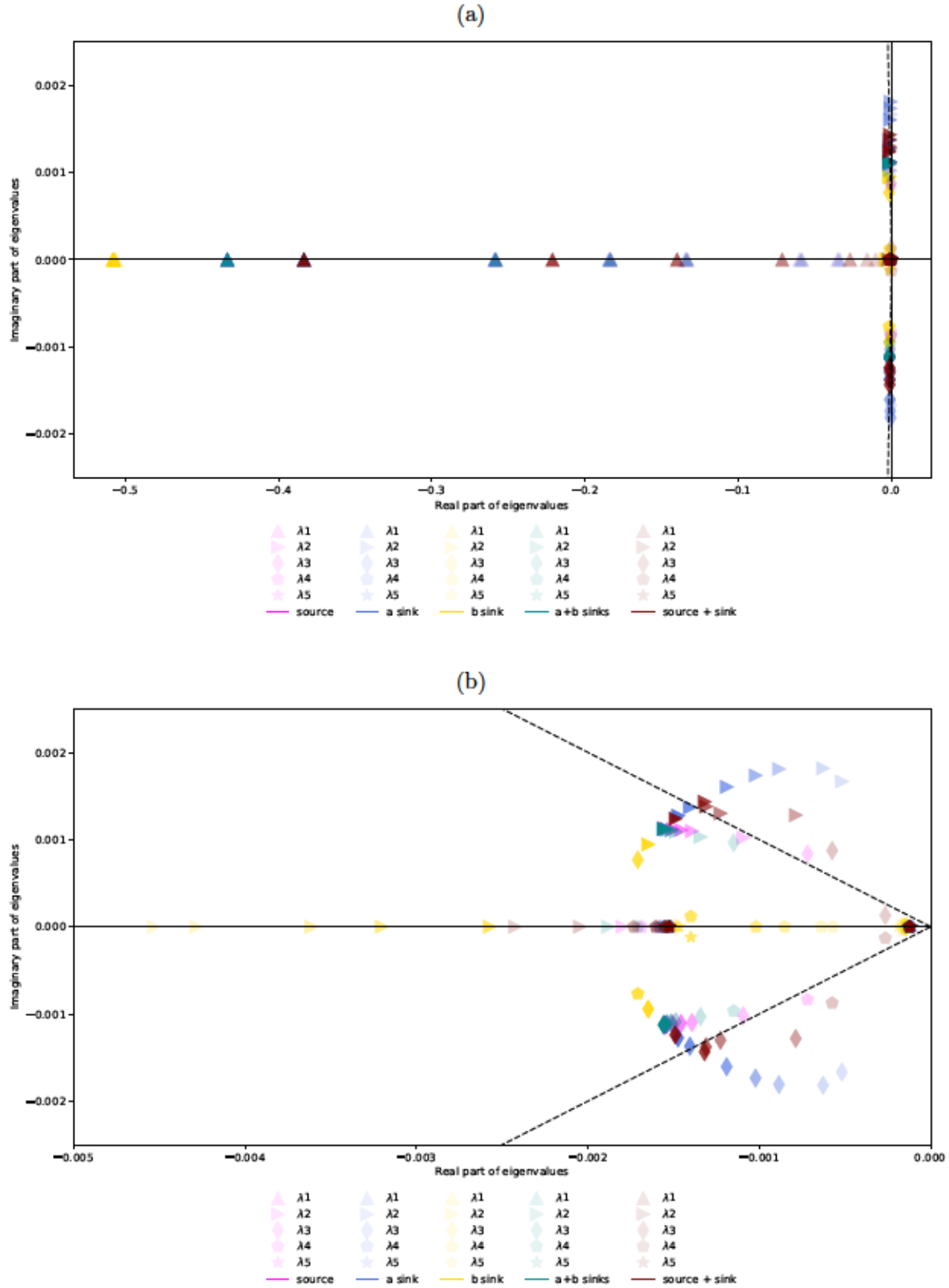


Figure 4.5: Complex planes for the model under different limitation scenarios. (a) All of the eigenvalues -see marker symbols- plotted for all of the limitation scenarios -see colors-. (b) Same plot, but zoomed into the smallest values of real parts. The color gradient indicates the strength of the C source or sink; the lighter color, the stronger the limitation.

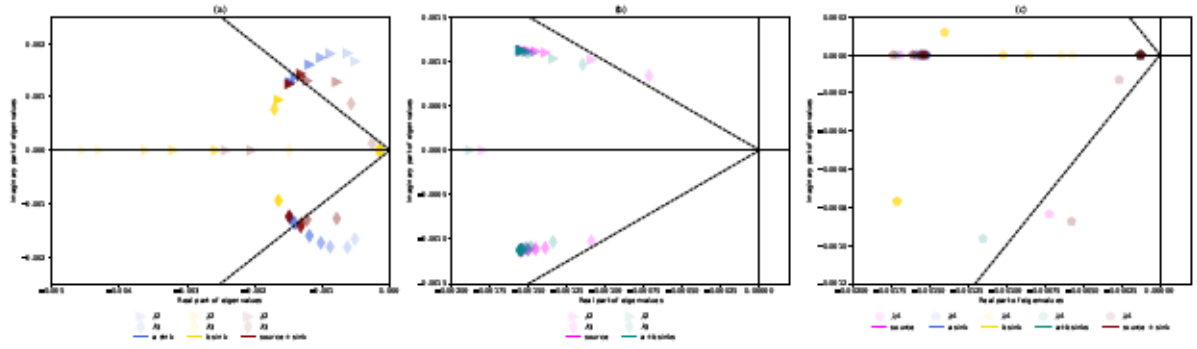


Figure 4.6: Complex plane for a selection of eigenvalues and limitation scenarios. (a) The only eigenvalues plotted are λ_2 and λ_3 —see marker symbols—in three limitation scenarios: aboveground sink limitation -a sink-, belowground sink limitation -b sink-, and source and sink limitation -source + sink-. The scenarios are color coded, and the color gradient indicates the strength of the C source or sink; the lighter color, the stronger the limitation. (b) Plot of eigenvalues λ_2 and λ_3 under source limitation -source-, and both sinks limitation -a+b sinks- scenarios. (c) Real Vs. Imaginary parts of eigenvalue λ_4 for all scenarios.

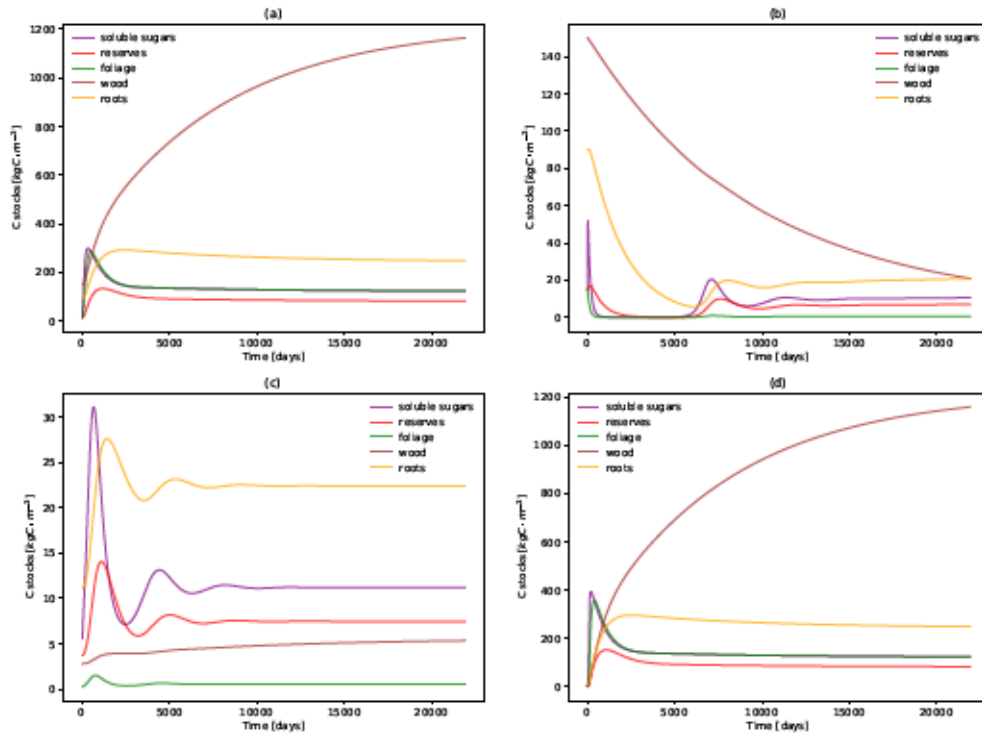


Figure 4.7: Carbon stocks with respect to time. (a) Model solutions with initial C stocks and parameter values as specified in table 4.1, no C allocation limitations. (b) Model simulations with same initial C stocks and parameters as before, but with strong aboveground sink limitation: $\alpha = 0.05$. (c) Model solutions with initial C stocks in the neighborhood of the steady state calculated with $\alpha = 0.05$; this parameter value was also used for the simulations. (d) Model simulations with same initial C stocks as in (c) but initial parameter values (no limitation).

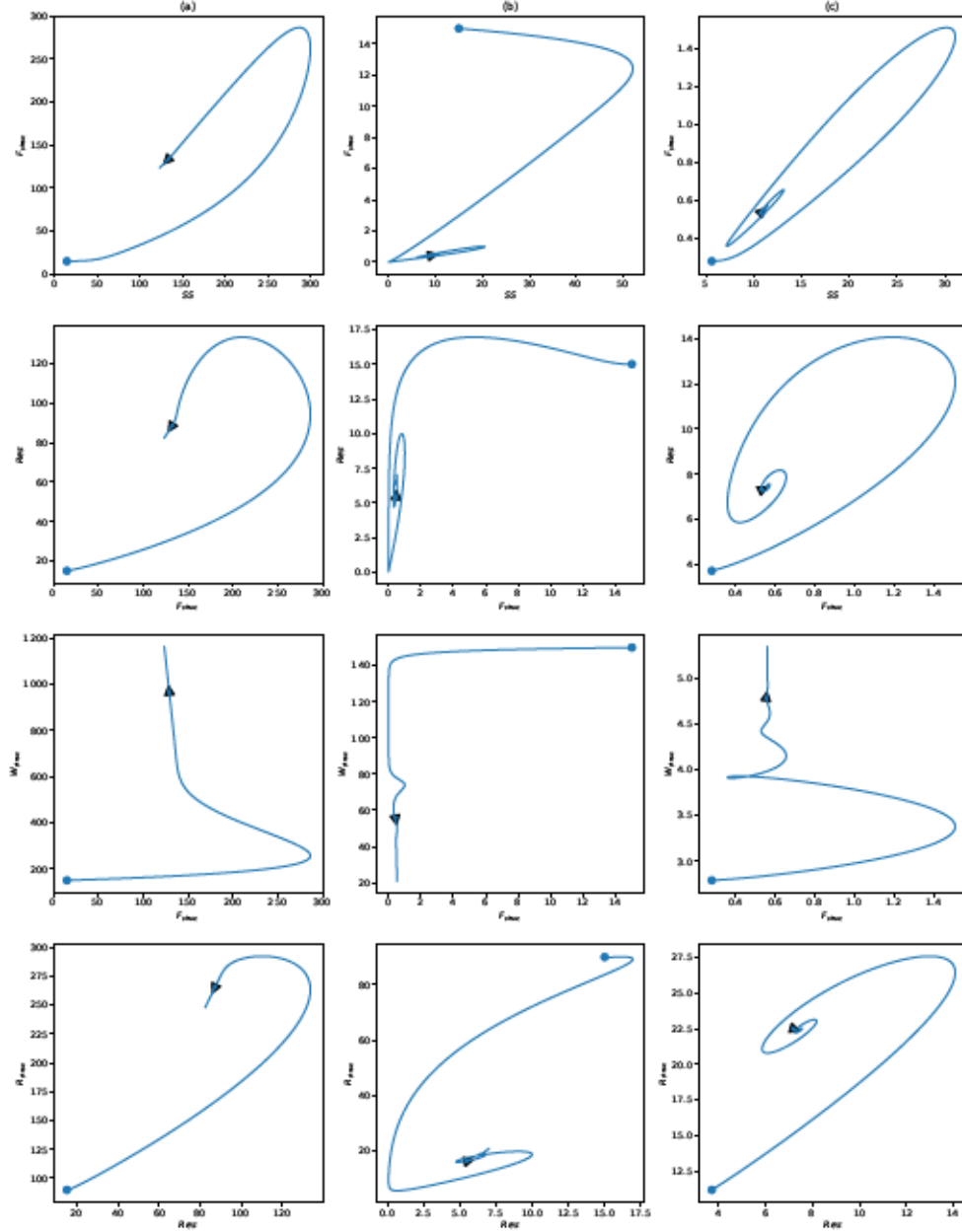


Figure 4.8: Phase planes of different combinations of vegetation compartments. The column (a) corresponds to model runs with initial conditions as in table 4.1 (see figure 4.7 (a)). The plots in column (b) correspond to model runs with the same initial C stocks as in (a), but with a strong aboveground sink limitation: $\alpha = 0.05$ (see figure 4.7 (b)). Finally, column (c) contains the plots from model runs with $\alpha = 0.05$ and initial C stocks in the neighborhood of the steady state calculated with this parameter value (see figure 4.7 (c)). Interestingly, the spirals of columns (b) and (c) occur in different planes. Additionally, the spiral for the phase plane of F_{struc} Vs. W_{struc} only appears when the simulations start in the neighborhood of the steady state calculated with $\alpha = 0.05$ column (c).

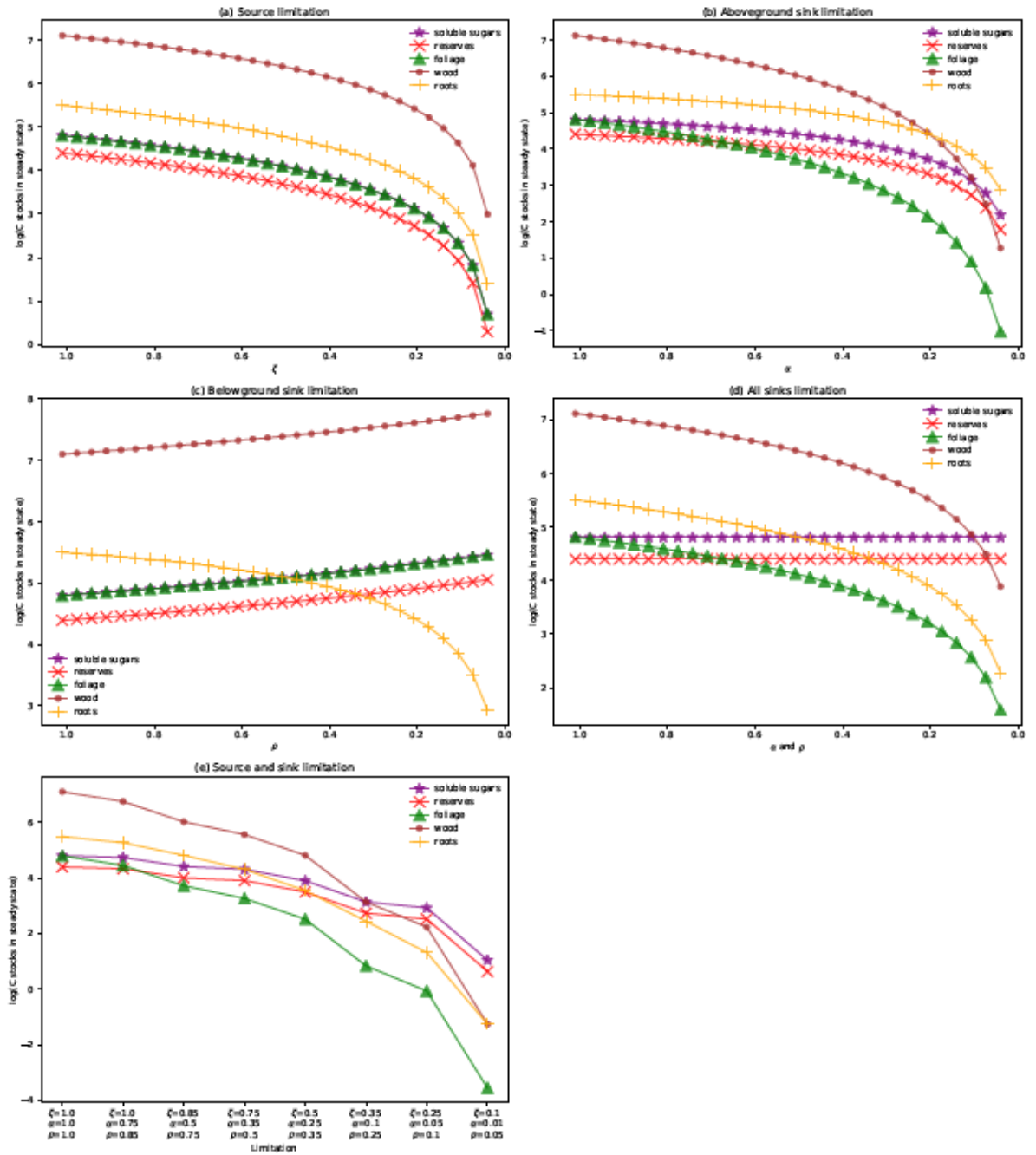


Figure 4.9: Carbon stocks of each compartment under different limitation scenarios; (a) source limitation only $-\zeta$, (b) aboveground sinks limitation $-\alpha$, (c) belowground sinks limitation $-\rho$, (d) above and belowground limitation $-\alpha, \rho$, and (e) Source and sink limitation $-\zeta, \alpha, \rho$. The highest source or sink strength is achieved when the respective scalar is equal to 1. For clarity, the C stocks are expressed in logarithmic scale. Note that under certain conditions, the ratio from wood to other compartments decreases, even to the point where the C content in the woody tissue is surpassed by the other compartments.

Concluding remarks and outlook

Our understanding of the influence of the terrestrial biosphere on the global carbon balance has improved, and we have been able to predict possible scenarios for ecosystems in a climate change context thanks to the development of global models of terrestrial biogeochemistry (Cramer *et al.*, 1999). A key comparison of 17 of these models categorized them as follows: 1) remote sensing based models, 2) models of seasonal biogeochemical fluxes, and 3) models of process and pattern, which are capable of predicting the response of vegetation to climate change (Cramer *et al.*, 1999). This thesis on *Nonlinearities in carbon allocation and vegetation functioning* focused on process based models, and aimed at enhancing our holistic understanding of the process of carbon allocation in vegetation, using for this purpose concepts from the well studied theory of dynamical systems. This theoretical approach had the advantage of building up on the knowledge that has already been encapsulated in the ecosystem models, whose development has put together the information gained in empirical studies as pieces of a puzzle.

Evidently, carbon allocation in vegetation is a multi scale process, and as such, many empirical studies have aimed at shedding light on some of its details at diverse scales. For example, at a small scale, some studies have focused on phloem physiology and the long distance carbon transport (Minchin and Lacoïnte, 2005; Furze *et al.*, 2018), as well as the carbon partitioning to defense and storage in wheat (Huang *et al.*, 2017). At a larger time-scale, other studies have assessed the seasonal variations of belowground carbon transfer in trees (Epron *et al.*, 2011), the allocation dynamics of vegetation in response to increasing temperatures and drought (Blessing *et al.*, 2015), and they even dug into the mechanisms behind tree mortality as a result of drought and other stressful conditions (McDowell and Sevanto, 2010; Sevanto *et al.*, 2014). Other processes such as the carbon source–sink balance and the effect of limitation on the partitioning of carbon into growth and storage, have been studied in small scales (i.e. trees (Wiley *et al.*, 2013)) and in a global scale (Hoch and Körner, 2012; Mahmud *et al.*, 2018). In

such bigger scales meteorological data and fluxes calculated via eddy covariance towers and field measurements are used in combination with modeling to simulate forest productivity and response to changing environmental conditions (Ueyama *et al.*, 2010; Marthews *et al.*, 2012; De Kauwe *et al.*, 2014; Gea-Izquierdo *et al.*, 2015; Koven *et al.*, 2015). And all these studies have been carried out in vegetation at different ontological stages (e.g. seedlings, saplings and mature trees), leading to reviews that have questioned the validity on the inference of carbon allocation mechanisms for mature trees based on experiments in seedlings (Hartmann *et al.*, 2018).

All this information available at different scales must be combined in order to facilitate the continuous assessments of carbon fluxes (Hartmann *et al.*, 2018), and has been used to infer the general mechanisms that are the backbone of ecosystem models. This means that with every new observed behaviour and elucidated mechanism the ecosystem models become more complex, to the point where it is hard to imagine that they were once as simple as box diffusion models (Oeschger *et al.*, 1975). Paradoxically, given that models still need to be simple enough so that they can remain computationally efficient, the complexity of the observed processes is not fully portrayed in ecosystem models, and this leaves room for diverse interpretations of empirical findings. Therefore, just as there is a need for a systematic review protocol to compare methods for measuring and assessing carbon stocks in terrestrial carbon pools (Petrokofsky *et al.*, 2012), it is also necessary to have protocols that can allow us to systematically compare models. The framework developed in this thesis can help to achieve this goal, and this is supported by answering the three research questions proposed in this thesis.

1. Is there a robust framework in the realm of dynamical systems that can be used to identify key aspects of carbon allocation linked to model uncertainties?

While dynamic vegetation models have been a powerful tool for enhancing our understanding of the carbon allocation process as a whole, their representation of carbon allocation often differs in the formulated strategies. This is important because, although some models underperform because of wrong parameter values (Rogers *et al.*, 2017), it has been claimed that alternative carbon allocation strategies are the reason why seven models had divergent projections of terrestrial carbon uptake in response to elevated atmospheric CO₂ concentration (Walker *et al.*, 2015). Indeed, Model–Data Synthesis projects have shown that model uncertainty can be reduced by identifying and evaluating the main assumptions causing differences among models (Medlyn *et al.*, 2015). Considering that these different model assumptions are represented with different mathematical formulations, the framework proposed in this PhD thesis emerges as a powerful tool to identify and evaluate these differences, since it synthesizes the carbon allocation strategies that have been proposed in published model descriptions, and represents them in a

compact form using the same programming and mathematical language. This common language for describing models also offers a great advantage to researchers that are just familiarizing with ecosystem models and want to compare several of them systematically, because it eliminates the intermediate steps of searching for the right set of equations in scripts written in different programming languages, and then *translating* them back to the ecosystem processes that they were meant to portray.

This leads us to another important feature of this framework: the division of the carbon allocation process into components of biogeochemical relevance (input: u , partitioning: $\vec{\beta}$, and cycling: B). The complex conceptual design used in some models to represent the entire carbon allocation process in vegetation can then be arranged into smaller objects of interest that can be individually explored in detail. This is specially relevant for studies that aim at punctual aspects of the global carbon cycle as it is commonly done in empirical studies such as the study performed by Malhi *et al.* (2015), where they assessed the linkages between photosynthesis, productivity, growth and biomass in lowland Amazonian forests using the largest data set assembled to that date. These empirical studies are crucial when trying to constrain terrestrial carbon cycle projections (Mystakidis *et al.*, 2016), but it is important to know how to interpret the observation-based carbon flux estimates and incorporate them into models whose structure are a reflection of the observed carbon allocation strategies.

It is in this particular matter where the framework proposed in this work can be of great use. For instance, when comparing the partitioning component of the models in this framework, it became clear that the models used for global predictions often used fixed coefficients in order to partition the photosynthetically fixed carbon among the vegetation compartments, i.e. they have a fixed partitioning scheme. In contrast, models used for simulations in smaller scales often had a dynamic partitioning of the photosynthetic input, evidenced by the fact that the elements of their $\vec{\beta}$ vector had functions instead of coefficients. Naturally, these two schemes have important consequences for the simulated response of vegetation to changing conditions in models; while with the fixed coefficients the vegetation compartments will always receive the same proportion of photosynthetic input, with a dynamic partitioning scheme the proportion of photosynthetically fixed carbon that goes to each compartment may change in response to external variables (e.g. temperature, water availability, among others) or to state variables (the amount of carbon in each compartment at a given time). This clear distinction can further help in the selection of model properties that can better represent the response mechanisms inferred from observations or boost the improvement of current models.

These improved models can be used to guide field experiments by providing *a priori* predictions of the ecosystem response to treatments (Medlyn *et al.*, 2016). In addition, models can be used to explore questions such as the prioritization of carbon partitioning under various

environmental conditions (Guillemot *et al.*, 2015). For example, is non-structural carbon an “overflow” compartment that only receives the C that remains after partitioning it to other compartments? Or, does it have a more important role and is therefore prioritized under stressful conditions such as drought and low $[\text{CO}_2]$? For the reasons explained in the previous paragraph, these questions cannot be explored using a model that has fixed coefficients as a partitioning scheme.

Furthermore, within the proposed framework, the models are generalized in a matrix form that benefits from the general language of dynamical systems and can accommodate nonlinearities, providing an optimal common ground for the comparison of model structures. Essentially, with this matrix representation important interactions within the elements of the model become conspicuous, for example, nonlinear interactions among state variables, and model dependencies on variables whose value can change with time. In this way, it facilitates the classification of models depending on their autonomy, i.e. non-autonomous models are driven by external variables that depend on time, whereas autonomous models do not, and according to their linearity, i.e. as linear and nonlinear models.

Nonlinearities are the result of strong interactions (such as feedback loops) between compartments, and as such they can only be observed in models with non-diagonal compartmental matrices where the off-diagonal values of the matrix also have state variables because the C transfer rates depend on them. In these kind of models the compartments may also exchange C, in which case it is also likely that they have at least one non-structural C compartment that can act as an intermediary in the C exchange. One of the most common nonlinear interactions is between the foliage-dependent photosynthetic input and the dynamic partitioning: $u(x, t) \cdot b(x, t)$. This is a positive feedback loop that assures the increase in photosynthesis with an increase in foliage, which might explain the rapid loss and replenishment of foliage in deciduous forests.

The above mentioned model classification with respect to their mathematical formulation is also important because there are some model properties that can be predicted from their structure. One of these properties is the stability of the system. A stability analysis can inform us, for example, whether the modelled system could potentially reach a steady state, i.e., if each state variable in the model can converge to a fixed point in time, where its inputs and outputs are cancelled out. This is an interesting property because, even though it is highly debated whether the ecosystems can reach such a steady state, it is an assumption that has to be done in order to use some methods to diagnose the model performance.

2. What diagnostics can be used to assess model performance?

As discussed above, the difference in the formulation of carbon allocation strategies in models can influence their capacity to predict empirically observed dynamics, thus affecting

their performance. Model performance is commonly diagnosed using different methods, some of which require that the system is in steady state. So, models that abide by this requirement portray a vegetation system in equilibrium. Naturally, whether ecosystems can indeed reach this equilibrium or what would this equilibrium be like is subject of discussion. Ecosystem processes are regulated by external drivers that change with time, e.g. light, temperature, water availability, as well as by endogenous heterogeneity (e.g. age, birth, death, etc.) (Moorcroft *et al.*, 2001). Given that vegetation undergo changes depending on daily and seasonal cycles, how can it reach an equilibrium? How does it look like? Do we have to set space/time boundaries within which it is possible to assume that there is an equilibrium? Some researchers assume that a certain equilibrium is reached when there are no longer drastic changes in the behaviour of the system, i.e., when a system behaves with a certain “periodicity”. So, assuming that the system of interest is in *equilibrium*, the performance of a model that can simulate it can be diagnosed using a method that has a steady state requirement, as long as an autonomous model (as opposed to a non-autonomous model that can not reach a steady state) is employed.

In this thesis three simple autonomous models were diagnosed using different mechanisms that required the systems to be in steady state; it was assessed how changes in model structure could impact the predictions of vegetation functioning. We concluded that the differences in carbon allocation strategies altered model performance, and from all the different performance diagnostics compared, the distribution of C ages and transit times emerged as the most sensible diagnostic. This is in agreement with a model intercomparison study where it was found that 63% of the variability in contemporary global vegetation C stocks across the 11 Earth system models involved in the Coupled Model Intercomparison Project phase 5 (CIMP5) was explained by differences in vegetation C residence time (Jiang *et al.*, 2015).

These results are a strong motivation for improvements in measurements of C dating that could lead to the measurement of age distributions and not just mean ages. One empirical approach in this subject is the relative quantification of radiocarbon, which has been used to infer cycling rates (e.g. pulse-labeling experiments using ^{14}C) and carbon mean ages (^{14}C), but this approach has limitations. Although it has been possible to develop robust models based on the available experimental evidence, some observations are not available at the same level of detail and, or spatio-temporal resolution as modelled processes. Indeed, most of the rates at which carbon exchange take place at the ecosystem level are not measurable (Trumbore, 2006) because of physical and experimental constraints. For example, given that radiocarbon experiments can only be performed in individuals, these results need to be upscaled to the whole ecosystem. Additionally, since the rates inferred from individuals-based experiments are not *universal*, multiple measurements have to take place in several species at different phenological and ontogenical stages in order to improve the upscaling. In fact, previous

studies have concluded that a better understanding and representation of plant phenology and physiology can improve predictions of gross primary productivity over time and space (Xia *et al.*, 2015). Another limitation is that some cycling rates can not be measured because, in an effort to formulate simple models, some artificial boundaries have been set in order to delimit compartments that do not exist in nature. Therefore, the design of future experiments should take this into account, and aim at an ecosystem level calculation of fluxes, carbon stocks and ages, preferably with a good resolution (time courses with multiple points).

The distribution of C ages and transit times was not only found to be a good diagnostic, but it also shed some light on the prevailing puzzle of the mixing of C ages in vegetation compartments. In this regard it was concluded that the temporal dynamics of carbon use, storage and allocation, not only depend on deterministic rates of carbon transfer, but also on the stochastic nature of the processes involved at a particle scale.

Towards the end of chapter 3 it was also briefly discussed about model equifinality and parameter identifiability. In this regard it was found that the three models had practical and structural non-identifiabilities, and as such the results could not be interpreted as accurate depictions of the C cycle in the Harvard Forest (site from which the data used to constrained the models was obtained). Some of these issues could potentially be solved in the future by using empirical measurements of carbon stocks, fluxes and ages, preferably obtained as time series where the measurement frequency and length is big enough to capture the C dynamics. The use of some measurements as proxies for carbon stocks and fluxes should also take into account potential pitfalls such as the delay between growth and stem diameter (Cuny *et al.*, 2015), and the correlation between fluxes such as the canopy photosynthesis and respiration obtained with eddy covariance methods (Baldocchi *et al.*, 2015). Finally, the parameter estimations could also be further constrained using boundaries for the parameter values that make ecological “common sense” (Bloom and Williams, 2015).

3. How can nonlinear interactions lead to the emergence of different patterns over time?

One of the main motivations behind the development of dynamic vegetation models is the possibility to predict ecosystem responses to global changes in climate (Schimel *et al.*, 2015; Seddon *et al.*, 2016). Amongst the effects that these changes have had is the reduction in the strength of carbon sources and sinks in vegetation (Guillemot *et al.*, 2015). Although studies on this topic have led to a “paradigm shift in plant growth control” (Fatichi *et al.*, 2014; Körner, 2015), the mechanisms behind the source and sink limitation of carbon allocation still remain unknown. This long lasting puzzle was approached in this thesis using a simple model, whose formulation was the result of a better understanding of key aspects of model structures found at the beginning of this thesis while performing the model synthesis.

Here it was found that strong sink limitations can lead to shifts in the C stocks ratio in equilibrium, and can also lead to changes in the way this equilibrium is approached by the system solution, i.e., they can even result in oscillations of the carbon stocks. Limitations on carbon allocation can also have implications for the predicted C mean ages, and these effects are enhanced by the nonlinear interactions. All of these model predictions can inspire new experimental designs to test them. Hence, a model whose parameters are fitted to a given system, i.e., the object of study (e.g. saplings of a given tree species), can be used to predict at what degree of sink limitation the oscillations in carbon stocks become apparent, and use this information to confirm the predicted dynamics in an experimental design that recreates the same limitation. Another experimental design can involve the comparison of the mean carbon ages of a couple of ecosystems that have grown in different sink limitation conditions (e.g. temperate Vs. tropical forests).

The structure of the proposed model corroborated the important role that non-structural carbon has on vegetation functioning. In previous studies, a labile carbohydrate store mediated the shift between the assimilation and growth, and in that way the C allocation could be better coupled to phenology (Haverd *et al.*, 2016). In the present study it became very clear that representing the non-structural carbon compartment as an independent pool that receives the carbon that overflows from the other compartments is not only an oversimplification, but also a misconception. It was concluded that, given the dual capacity of non-structural carbon as a source and a sink, it would be more accurate to represent this compartment as a central pool that receives the photosynthetic input and redistributes it to the structural compartments and reserves. This could be one of the changes that are needed to improve the core structure of current dynamic global vegetation models, as previously suggested by Fatichi *et al.* (2014). This model structure can also be a good candidate to further explore the hypothesis of the prioritization of storage under stressful conditions (Palacio *et al.*, 2014). For example, it can help distinguish between cases where the results are a reflection of the mass balance approach of the model (e.g. non-structural carbon cannot be fully drained to feed the other compartments because if this happens the system will collapse), or some compartments are indeed prioritized over others (e.g. if there is a restriction in the flux from non-structural carbon to the structural compartments, or if the reserves compartment is favoured over the structural compartments) as it has been suggested in some empirical studies where the prioritization of belowground sinks have helped the trees to recover from drought (Hagedorn *et al.*, 2016).

Overall, this thesis addressed relevant aspects of current research performed on carbon allocation in vegetation in a manner that simplified the assessment of the effect that both, the models mathematical formulation and their conceptual design have on the stability of the system and the vegetation functioning, respectively. This approach can contribute to the understanding

of the holistic system behaviour, given that this mathematical framework is compact enough to ease the qualitative understanding of models, but its simplicity does not compromise the detail in the process representation (Sierra *et al.*, 2018).

Accordingly, the knowledge gained regarding the conceptual design of the models can help the modelers to select pertinent modeling approaches not only based on expected properties (e.g. stability), but also on their suitability to the experimental design. For example, given two models: a linear non-autonomous system, and a non-linear autonomous system, what model should be used for a data assimilation experiment, provided that they both have comparable outcomes? This choice depends on the experimental design. If the environmental conditions were kept constant, then they cannot be the model drivers, thus the non-linear, autonomous system would be more suitable.

Given that the framework and mathematical tool proposed here is part of a Python package that is now available to the public, it can be further enhanced and built on. Perhaps the next versions of the software can make it possible to implement individuals based models such as the one that deals with the ecosystems endogenous heterogeneity using partial differential equations (Moorcroft *et al.*, 2001), or the one that models tree growth taking into account C source and sink limitations (Hayat *et al.*, 2017). The new functionalities could further explore long lasting questions in an automated way. One of these questions concerns the relation between model complexity and the size of the space/time scale, which is expected to be inversely proportional. Another relation that can be explored is the one between model complexity, in terms of number of variables and parameters, and the level of detail in which processes are described. Additionally, the common language used in this tool is a crucial base to find a metric of model similarity that could even lead to the generation of cladograms.

With this thesis it has been demonstrated that the holistic understanding of carbon allocation in vegetation can be achieved through the inference of general mechanisms from empirical observations and experiments, and integrating this information into broader overarching hypotheses formulated in ecosystem models. These proposed hypotheses, or ways in which carbon allocation have been interpreted, can be further explored to achieve a further generalization. This can be done in three steps: 1) synthesizing the mathematical formulation of ecosystem models and testing whether their formulation is in agreement with the intended conceptual design, as well as identifying important properties from model structures e.g. linearity and autonomy; 2) diagnosing the model performance using sensitive methods whose requirements are in line with the model properties e.g. stability of the system; and 3) developing improved models with structures that truly reflect the biological concepts that inspired their design, and using them to predict the response of vegetation to alternative scenarios in the context of climate change. See Fig. 5.1 for a schematic representation.

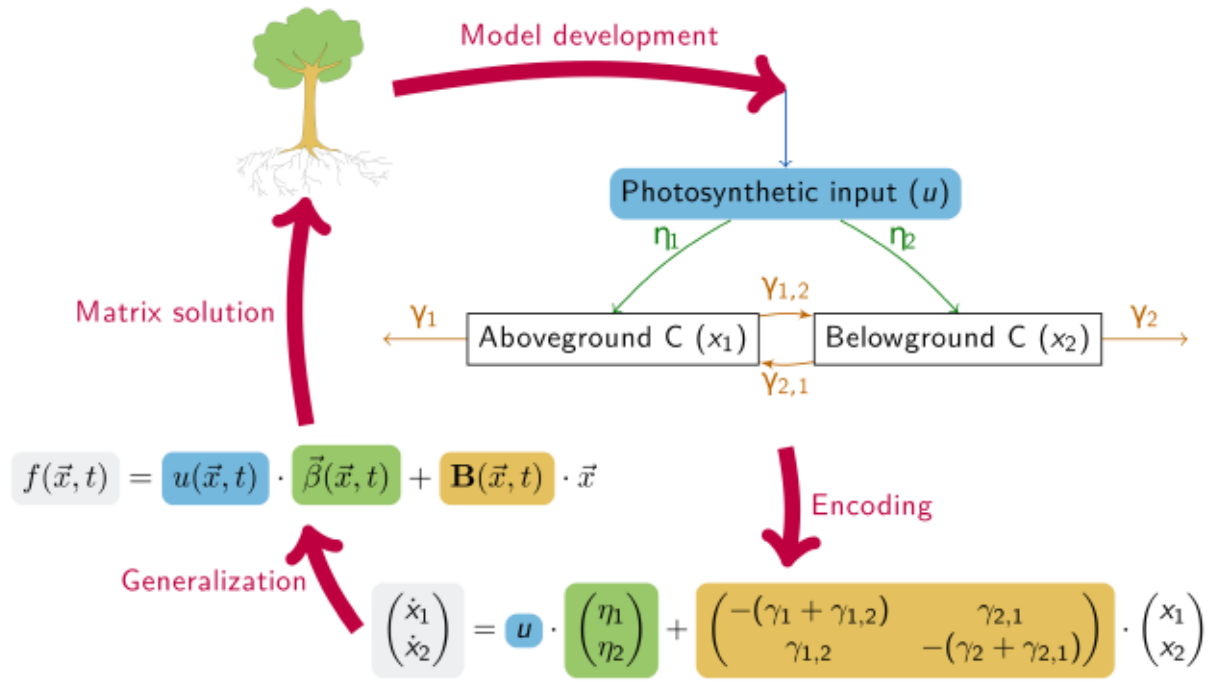


Figure 5.1: Mathematical tool and conceptual framework to study carbon cycle modeling. These equations are fully described in chapter 2. Models are developed from the overarching mechanisms inferred from empirical observations and experiments. These models are then encoded using ordinary differential equations. These equations can be written in the form of a matrix that generalizes them into components of biogeochemical relevance. These models can be adjusted to particular vegetation systems by estimating their parameters (η_i, γ_i) to field measurements of carbon stocks and fluxes. Once parameterized, the performance of the models can be diagnosed using methods whose application requirements are met by the model's properties; the latter two steps are not represented in the figure. The validated models can finally be used to predict the vegetation response to environmental forcing over time and other queries.

Finally, from the present work it was concluded that, while linear structures are the prevalent modelling approach in the dynamic global vegetation models, nonlinear models have also been proposed. For this reason, it would be interesting to test whether these nonlinearities indeed improve the model performance with respect to empirical observations. Another hypothesis that could be tested in the future is whether these nonlinearities are relevant for predictions obtained with global dynamic vegetation models enriched with soil compartments and coupled to climate, and see if the nonlinear interactions, which have so far been ignored by some models, have an impact on the prediction of the sustainability of terrestrial carbon sequestration under changing climate regimes. Perhaps more importantly, improved models in combination with further research on the relationship between the ecosystems resilience and the stability of the models can help us identify the *safe operating space* of each ecosystem and develop strategies that can better prevent their collapse in the future.

Bibliography

- Alvarez-Uria, P. and Körner, C. (2007). Low temperature limits of root growth in deciduous and evergreen temperate tree species. *Functional Ecology*, 21(2):211–218.
- Anderson, D. H. (1983). *Compartmental modeling and tracer kinetics*, volume 50. Springer Science & Business Media.
- Arora, V. K. and Boer, G. J. (2005). A parameterization of leaf phenology for the terrestrial ecosystem component of climate models. *Global Change Biology*, 11(1):39–59.
- Baldocchi, D., Sturtevant, C., and FLUXNET Contributors (2015). Does day and night sampling reduce spurious correlation between canopy photosynthesis and ecosystem respiration? *Agricultural and Forest Meteorology*, 207:117 – 126.
- Blessing, C. H., Werner, R. A., Siegwolf, R., and Buchmann, N. (2015). Allocation dynamics of recently fixed carbon in beech saplings in response to increased temperatures and drought. *Tree Physiology*.
- Bloom, A. A. and Williams, M. (2015). Constraining ecosystem carbon dynamics in a data-limited world: Integrating ecological "common sense" in a model–data fusion framework. *Biogeosciences*, 12(5):1299–1315.
- Bolin, B. and Rodhe, H. (1973). A note on the concepts of age distribution and transit time in natural reservoirs. *Tellus*, 25(1):58–62.
- Box, G. E. P. (1976). Science and statistics. *Journal of the American Statistical Association*, 71(356):791–799.
- Bryla, D. R., Bouma, T. J., and Eissenstat, D. M. (1997). Root respiration in citrus acclimates to temperature and slows during drought. *Plant, Cell & Environment*, 20(11):1411–1420.
- Canadell, J. G., Le Quéré, C., Raupach, M. R., Field, C. B., Buitenhuis, E. T., Ciais, P., Conway, T. J., Gillett, N. P., Houghton, R. A., and Marland, G. (2007). Contributions to

- accelerating atmospheric CO₂ growth from economic activity, carbon intensity, and efficiency of natural sinks. *Proceedings of the National Academy of Sciences*, 104(47):18866–18870.
- Carbone, M. S., Czimczik, C. I., McDuffee, K. E., and Trumbore, S. E. (2007). Allocation and residence time of photosynthetic products in a boreal forest using a low-level ¹⁴C pulse-chase labeling technique. *Global Change Biology*, 13(2):466–477.
- Castanho, A. D. A., Coe, M. T., Costa, M. H., Malhi, Y., Galbraith, D., and Quesada, C. A. (2013). Improving simulated amazon forest biomass and productivity by including spatial variation in biophysical parameters. *Biogeosciences*, 10(4):2255–2272.
- Chapin, F., Matson, P., and Mooney, H. (2002). *Principles of Terrestrial Ecosystem Ecology*. Principles of Terrestrial Ecosystem Ecology. Springer.
- Chapin, F. S., Schulze, E., and Mooney, H. A. (1990). The ecology and economics of storage in plants. *Annual Review of Ecology and Systematics*, 21(1):423–447.
- Chen, J.-L. and Reynolds, J. (1997). Geps: A generic plant simulator based on object-oriented principles. *Ecological modelling*, 94(1):53–66.
- Cheng, L. and H Fuchigami, L. (2003). Growth of young apple trees in relation to reserve nitrogen and carbohydrates. *Tree physiology*, 22:1297–303.
- Comins, H. N. and McMurtrie, R. E. (1993). Long-term response of nutrient-limited forests to CO₂ enrichment; equilibrium behavior of plant-soil models. *Ecological Applications*, 3(4):666–681.
- Cramer, W., Kicklighter, D. W., Bondeau, A., Iii, B. M., Churkina, G., Nemry, B., Ruimy, A., Schloss, A. L., and Intercomparison, T. P. O. T. P. N. M. (1999). Comparing global models of terrestrial net primary productivity (NPP): overview and key results. *Global Change Biology*, 5(S1):1–15.
- Cressie, N., Calder, C. A., Clark, J. S., Hoef, J. M. V., and Wikle, C. K. (2009). Accounting for uncertainty in ecological analysis: the strengths and limitations of hierarchical statistical modeling. *Ecological Applications*, 19(3):553–570.
- Crutzen, P. J. and Stoermer, E. F. (2000). “The Anthropocene”. *Global Change Newsletter*, pages 17–18.
- Cuny, H. E., Rathgeber, C. B. K., Frank, D. C., Fonti, P., Mäkinen, H., Prislan, P., Rossi, S., Martinez del Castillo, E., Campelo, F., Vavřík, H., Camarero, J. J., Bryukhanova, M. V., Jyske, T., Gričar, J., Gryc, V., de Luis, M., Vieira, J., Čufar, K., Kirdyanov, A. V., Oberhuber,

- W., Trembl, V., Huang, J.-G., Li, X., Swidrak, I., Deslauriers, A., Liang, E., Nöjd, P., Gruber, A. J., Nabais, C., Morin, H. M. A., Krause, C., King, G., and Fournier, M. (2015). Woody biomass production lags stem-girth increase by over one month in coniferous forests. *Nature plants*, 1:15160.
- Davidson, R. L. (1969). Effect of root/leaf temperature differentials on root/shoot ratios in some pasture grasses and clover. *Annals of Botany*, 33(3):561–569.
- De Kauwe, M. G., Medlyn, B. E., Zaehle, S., Walker, A. P., Dietze, M. C., Wang, Y. P., Luo, Y., Jain, A. K., El-Masri, B., Hickler, T., Wårlind, D., Weng, E., Parton, W. J., Thornton, P. E., Wang, S., Prentice, I. C., Asao, S., Smith, B., McCarthy, H. R., Iversen, C. M., Hanson, P. J., Warren, J. M., Oren, R., and Norby, R. J. (2014). Where does the carbon go? A model-data intercomparison of vegetation carbon allocation and turnover processes at two temperate forest free-air CO₂ enrichment sites. *New Phytologist*, 203(3):883–899.
- DeAngelis, D. L., Ju, S., Liu, R., Bryant, J. P., and Gourley, S. A. (2012). Plant allocation of carbon to defense as a function of herbivory, light and nutrient availability. *Theoretical Ecology*, 5(3):445–456.
- Dieleman, W. I. J., Vicca, S., Dijkstra, F. A., Hagedorn, F., Hovenden, M. J., Larsen, K. S., Morgan, J. A., Volder, A., Beier, C., Dukes, J. S., King, J., Leuzinger, S., Linder, S., Luo, Y., Oren, R., De Angelis, P., Tingey, D., Hoosbeek, M. R., and Janssens, I. A. (2012). Simple additive effects are rare: A quantitative review of plant biomass and soil process responses to combined manipulations of CO₂ and temperature. *Global Change Biology*, 18(9):2681–2693.
- Dietze, M. C., Sala, A., Carbone, M. S., I., C. C., Mantooth, J. A., Richardson, A. D., and Vargas, R. (2014). Nonstructural carbon in woody plants. *Annual Review of Plant Biology*, 65(1):667–687.
- Doughty, C. E., Metcalfe, D. B., Girardin, C. A., Amézquita, F. F., Cabrera, D. G., Huasco, W. H., Silva-Espejo, J. E., Araujo-Murakami, A., Da Costa, M. C., Rocha, W., Feldpausch, T. R., Mendoza, A. L., Da Costa, A. C., Meir, P., Phillips, O. L., and Malhi, Y. (2015). Drought impact on forest carbon dynamics and fluxes in Amazonia. *Nature*, 519(7541):78–82.
- Dufrene, E., Davi, H., Francois, C., le Maire, G., and Dantec, V. L. (2005). Modelling carbon and water cycles in a beech forest Part I: Model description and uncertainty analysis on modelled NEE. *Ecological modelling*, 185(2-4):407–436.
- Eglin, T., Francois, C., Michelot, A., Delpierre, N., and Damesin, C. (2010). Linking intra-seasonal variations in climate and tree-ring $\Delta^{13}\text{C}$: A functional modelling approach. *Ecological modelling*, 221(15):1779–1797.

- El-Masri, B., Barman, R., Meiyappan, P., Song, Y., and Liang, M. (2013). Carbon dynamics in the amazonian basin: Integration of eddy covariance and ecophysiological data with a land surface model. *Agricultural and forest meteorology*, 182(Sp. Iss. SI):156–167.
- Epron, D., Bahn, M., Derrien, D., Lattanzi, F. A., Pumpanen, J., Gessler, A., Höglberg, P., Maillard, P., Dannoura, M., Gérant, D., and Buchmann, N. (2012). Pulse-labelling trees to study carbon allocation dynamics: a review of methods, current knowledge and future prospects. *Tree Physiology*, 32(6):776–798.
- Epron, D., Ngao, J., Dannoura, M., Bakker, M. R., Zeller, B., Bazot, S., Bosc, A., Plain, C., Lata, J. C., Priault, P., Barthes, L., and Loustau, D. (2011). Seasonal variations of belowground carbon transfer assessed by *in situ* $^{13}\text{CO}_2$ pulse labelling of trees. *Biogeosciences*, 8(5):1153–1168.
- Ericsson, T., Rytter, L., and Vapaavuori, E. (1996). Physiology of carbon allocation in trees. *Biomass and Bioenergy*, 11(2):115–127.
- Farquhar, G. D., von Caemmerer, S., and Berry, J. A. (1980). A biochemical model of photosynthetic CO_2 assimilation in leaves of C_3 species. *Planta*, 149(1):78–90.
- Fatichi, S. and Leuzinger, S. (2013). Reconciling observations with modeling: The fate of water and carbon allocation in a mature deciduous forest exposed to elevated CO_2 . *Agricultural and forest meteorology*, 174:144–157.
- Fatichi, S., Leuzinger, S., and Körner, C. (2014). Moving beyond photosynthesis: from carbon source to sink-driven vegetation modeling. *New Phytologist*, 201(4):1086–1095.
- Fatichi, S., Pappas, C., and Ivanov, V. Y. (2016). Modeling plant–water interactions: an ecohydrological overview from the cell to the global scale. *Wiley Interdisciplinary Reviews: Water*, 3(3):327–368.
- Foley, J. A., Prentice, I. C., Ramankutty, N., Lewis, S., Pollard, D., Sitch, S., and Haxeltine, A. (1996). An integrated biosphere model of land surface processes, terrestrial carbon balance, and vegetation dynamics. *Global Biogeochemical Cycles*, 10(4):603–628.
- Fox, A., Williams, M., Richardson, A. D., Cameron, D., Gove, J. H., Quaife, T., Ricciuto, D., Reichstein, M., Tomelleri, E., Trudinger, C. M., and Wijk, M. T. V. (2009). The REFLEX project: Comparing different algorithms and implementations for the inversion of a terrestrial ecosystem model against eddy covariance data. *Agricultural and Forest Meteorology*, 149(10):1597 – 1615.

- Fox, G. (1992). The effect of time-varying mortality and carbon assimilation on models of carbon allocation in annual plants. *Evolutionary Ecology*, 6(6):500–518.
- Franklin, O., Johansson, J., Dewar, R. C., Dieckmann, U., McMurtrie, R. E., Brännström, A., and Dybzinski, R. (2012). Modeling carbon allocation in trees: A search for principles. *Tree Physiology*, 32(6):648–666.
- Friedlingstein, P., Cox, P., Betts, R., Bopp, L., Von Bloh, W., Brovkin, V., Cadule, P., Doney, S., Eby, M., Fung, I., Bala, G., John, J., Jones, C., Joos, F., Kato, T., Kawamiya, M., Knorr, W., Lindsay, K., Matthews, H. D., Raddatz, T., Rayner, P., Reick, C., Roeckner, E., Schnitzler, K. G., Schnur, R., Strassmann, K., Weaver, A. J., Yoshikawa, C., and Zeng, N. (2006). Climate-carbon cycle feedback analysis: Results from the C4MIP model intercomparison. *Journal of Climate*, 19(14):3337–3353.
- Friedlingstein, P., Meinshausen, M., Arora, V. K., Jones, C. D., Anav, A., Liddicoat, S. K., and Knutti, R. (2014). Uncertainties in CMIP5 climate projections due to carbon cycle feedbacks. *Journal of Climate*, 27(2):511–526.
- Friend, A. D., Lucht, W., Rademacher, T. T., Keribin, R., Betts, R., Cadule, P., Ciais, P., Clark, D. B., Dankers, R., Falloon, P. D., Ito, A., Kahana, R., Kleidon, A., Lomas, M. R., Nishina, K., Ostberg, S., Pavlick, R., Peylin, P., Schaphoff, S., Vuichard, N., Warszawski, L., Wiltshire, A., and Woodward, F. I. (2014). Carbon residence time dominates uncertainty in terrestrial vegetation responses to future climate and atmospheric CO₂. *Proceedings of the National Academy of Sciences of the United States of America*, 111(9):3280–5.
- Furze, M. E., Trumbore, S., and Hartmann, H. (2018). Detours on the phloem sugar highway: Stem carbon storage and remobilization. *Current Opinion in Plant Biology*, 43:89 – 95.
- Gea-Izquierdo, G., Guibal, F., Joffre, R., Ourcival, J. M., Simioni, G., and Guiot, J. (2015). Modelling the climatic drivers determining photosynthesis and carbon allocation in evergreen Mediterranean forests using multiproxy long time series. *Biogeosciences*, 12(12):3695–3712.
- Govingjee (2009). *Photosynthesis in silico. Understanding complexity from molecules to ecosystems*, volume 29. Springer.
- Grimm, V., Berger, U., Bastiansen, F., Eliassen, S., Ginot, V., Giske, J., Goss-Custard, J., Grand, T., Heinz, S., Huse, G., Huth, A., Jepsen, J., Jørgensen, C., Mooij, W., Müller, B., Pe’er, G., Piou, C., F. Railsback, S., M. Robbins, A., and Deangelis, D. (2006). A standard protocol for describing individual-based and agent based models. *Ecological Modelling*, 198:115–126.

- Grimm, V., Berger, U., Deangelis, D., Polhill, J., Giske, J., and F. Railsback, S. (2010). The ODD protocol: A review and first update. *Ecological Modelling*, 221:2760–2768.
- Gulke, N. E., Andersen, C. P., and Hogsett, W. E. (2001). Seasonal changes in above- and belowground carbohydrate concentrations of ponderosa pine along a pollution gradient. *Tree Physiology*, 21(2-3):173.
- Gu, F., Zhang, Y., Tao, B., Wang, Q., and Yu, G. (2010). Modeling the effects of nitrogen deposition on carbon budget in two temperate forests. *Ecological complexity*, 7(2, Sp. Iss. SI):139–148.
- Guillemot, J., Martin-StPaul, N. K., Dufrêne, E., François, C., Soudani, K., Ourcival, J. M., and Delpierre, N. (2015). The dynamic of the annual carbon allocation to wood in european tree species is consistent with a combined source–sink limitation of growth: Implications for modelling. *Biogeosciences*, 12(9):2773–2790.
- Hagedorn, F., Joseph, J., Peter, M., Luster, J., Pritsch, K., Nickel, U., Kerner, R., Molinier, V., Egli, S., Schaub, M., Liu, J., Li, M., Sever, K., Weiler, M., Siegwolf, R., Gessler, A., and Arend, M. (2016). Recovery of trees from drought depends on belowground sink control. *Nature Plants*, 2:16111.
- Hartmann, H., Adams, H. D., Hammond, W. M., Hoch, G., Landhäusser, S. M., Wiley, E., and Zaehle, S. (2018). Identifying differences in carbohydrate dynamics of seedlings and mature trees to improve carbon allocation in models for trees and forests. *Environmental and Experimental Botany*, 152:7 – 18.
- Hartmann, H., McDowell, N. G., and Trumbore, S. (2015). Allocation to carbon storage pools in Norway spruce saplings under drought and low CO₂. *Tree Physiology*, 35(3):243–252.
- Hartmann, H. and Trumbore, S. (2016). Understanding the roles of nonstructural carbohydrates in forest trees -from what we can measure to what we want to know. *New Phytologist*, 211(2):386–403.
- Hartmann, H., Ziegler, W., and Trumbore, S. E. (2013). Lethal drought leads to reduction in nonstructural carbohydrates in Norway spruce tree roots but not in the canopy. *Functional Ecology*, 27(2):413–427.
- Haverd, V., Smith, B., Raupach, M., Briggs, P., Nieradzik, L., Beringer, J., Hutley, L., Trudinger, C. M., and Cleverly, J. (2016). Coupling carbon allocation with leaf and root phenology predicts tree–grass partitioning along a savanna rainfall gradient. *Biogeosciences*, 13(3):761–779.

- Hayat, A., Hacket-Pain, A. J., Pretzsch, H., Rademacher, T. T., and Friend, A. D. (2017). Modeling tree growth taking into account carbon source and sink limitations. *Frontiers in Plant Science*, 8:182.
- Hilbert, D. W. and Reynolds, J. F. (1991). A model allocating growth among leaf proteins, shoot structure, and root biomass to produce balanced activity. *Annals of Botany*, 68(5):417–425.
- Hoch, G. and Körner, C. (2003). The carbon charging of pines at the climatic treeline: A global comparison. *Oecologia*, 135(1):10–21.
- Hoch, G. and Körner, C. (2012). Global patterns of mobile carbon stores in trees at the high-elevation tree line. *Global Ecology and Biogeography*, 21(8):861–871.
- Holling, C. S. (1973). Resilience and stability of ecological systems. *Annual Review of Ecology and Systematics*, 4:1–23.
- Huang, J., Hammerbacher, A., Forkelová, L., and Hartmann, H. (2017). Release of resource constraints allows greater carbon allocation to secondary metabolites and storage in winter wheat. *Plant, Cell & Environment*, 40(5):672–685.
- Huntingford, C., Cox, P. M., and Lenton, T. M. (2000). Contrasting responses of a simple terrestrial ecosystem model to global change. *Ecological modelling*, 134(1):41–58.
- Jacquez, J. A. and Simon, C. P. (1993). Qualitative theory of compartmental systems. *Siam Review*, 35(1):43–79.
- Jiang, L., Yan, Y., Hararuk, O., Mickle, N., Xia, J., Shi, Z., Tjiputra, J., Wu, T., and Luo, Y. (2015). Scale-dependent performance of CMIP5 Earth System Models in simulating terrestrial vegetation carbon. *Journal of Climate*, 28(13):5217–5232.
- Jost, J. (2005). *Dynamical systems: examples of complex behaviour*. Springer, Berlin; New York.
- Keenan, T., Gray, J., A. Friedl, M., Toomey, M., Bohrer, G., Hollinger, D., Munger, J., O’Keefe, J., Peter Schmid, H., Sue Wing, I., Yang, B., and Richardson, A. (2014). Net carbon uptake has increased through warming-induced changes in temperate forest phenology. *Nature Climate Change*, 4:598–604.
- Keenan, T. F., Davidson, E. A., Munger, J. W., and Richardson, A. D. (2013a). Rate my data: Quantifying the value of ecological data for the development of models of the terrestrial carbon cycle. *Ecological Applications*, 23(1):273–286.

- Keenan, T. F., Hollinger, D. Y., Bohrer, G., Dragoni, D., Munger, J. W., Schmid, H. P., and Richardson, A. D. (2013b). Increase in forest water-use efficiency as atmospheric carbon dioxide concentrations rise. *Nature*, 499(7458):324–327.
- King, D. A. (1993). A model analysis of the influence of root and foliage allocation on forest production and competition between trees. *Tree Physiology*, 12(2):119–135.
- Klein, T. and Hoch, G. (2015). Tree carbon allocation dynamics determined using a carbon mass balance approach. *New Phytologist*, 205(1):147–159.
- Kobe, R. K. (1997). Carbohydrate allocation to storage as a basis of interspecific variation in sapling survivorship and growth. *Oikos*, 80(2):226–233.
- Körner, C. (2015). Paradigm shift in plant growth control. *Current Opinion in Plant Biology*, 25:107 – 114.
- Körner, C. (2017). A matter of tree longevity. *Science*, 355(6321):130–131.
- Körner, C., Asshoff, R., Bignucolo, O., Hättenschwiler, S., Keel, S. G., Peláez-Riedl, S., Pepin, S., Siegwolf, R. T. W., and Zotz, G. (2005). Carbon flux and growth in mature deciduous forest trees exposed to elevated CO₂. *Science*, 309(5739):1360–1362.
- Koven, C. D., Chambers, J. Q., Georgiou, K., Knox, R., Negron-Juarez, R., Riley, W. J., Arora, V. K., Brovkin, V., Friedlingstein, P., and Jones, C. D. (2015). Controls on terrestrial carbon feedbacks by productivity vs. turnover in the CMIP5 Earth System Models. *Biogeosciences Discussions*, 12(8):5757–5801.
- Kozlowski, T. T. and Keller, T. (1966). Food relations of woody plants. *The Botanical Review*, 32(4):293–382.
- Lacointe, A. (2000). Carbon allocation among tree organs: A review of basic processes and representation in functional-structural tree models. *Annals of Forest Science*, 57(5-6):521–533.
- Lacointe, A., Kajji, A., Daudet, F.-A., Archer, P., Frossard, J.-S., Saint-Joanis, B., and Vandame, M. (1993). Mobilization of carbon reserves in young walnut trees. *Acta Botanica Gallica*, 140(4):435–441.
- Lallement, G. and Inman, D. J. (1995). A tutorial on complex eigenvalues. In *Proceedings-SPIE The International Society For Optical Engineering*, pages 490–490.
- Lazzarotto, P., Calanca, P., and Fuhrer, J. (2009). Dynamics of grass-clover mixtures-an analysis of the response to management with the productive grassland simulator (prograss). *Ecological modelling*, 220(5):703–724.

- Leuzinger, S., Luo, Y., Beier, C., Dieleman, W., Vicca, S., and Koerner, C. (2011). Do global change experiments overestimate impacts on terrestrial ecosystems? *Trends in Ecology & Evolution*, 26(5):236–241.
- Li, G., Harrison, S. P., Prentice, I. C., and Falster, D. (2014). Simulation of tree-ring widths with a model for primary production, carbon allocation, and growth. *Biogeosciences*, 11(23):6711–6724.
- Litton, C. M., Raich, J. W., and Ryan, M. G. (2007). Carbon allocation in forest ecosystems. *Global Change Biology*, 13(10):2089–2109.
- Luenberger, D. G. and Hill, R. L. (1979). *Introduction to dynamic systems : theory, models, and applications*. New York : Wiley.
- Luo, Y., Shi, Z., Lu, X., Xia, J., Liang, J., Jiang, J., Wang, Y., Smith, M. J., Jiang, L., Ahlström, A., Chen, B., Hararuk, O., Hastings, A., Hoffman, F., Medlyn, B., Niu, S., Rasmussen, M., Todd-Brown, K., and Wang, Y.-P. (2017). Transient dynamics of terrestrial carbon storage: Mathematical foundation and its applications. *Biogeosciences*, 14(1):145–161.
- Luo, Y., Weng, E., and Yang, Y. (2012). Ecosystem ecology. In Hastings, A. and Gross, L., editors, *Encyclopedia of Theoretical Ecology*, pages 219–229. University of California Press, Berkeley.
- Luo, Y., White, L. W., Canadell, J. G., DeLucia, E. H., Ellsworth, D. S., Finzi, A., Lichter, J., and Schlesinger, W. H. (2003). Sustainability of terrestrial carbon sequestration: A case study in duke forest with inversion approach. *Global Biogeochemical Cycles*, 17(1):n/a–n/a.
- Mahmud, K., Medlyn, B. E., Duursma, R. A., Campany, C., and De Kauwe, M. G. (2018). Inferring the effects of sink strength on plant carbon balance processes from experimental measurements. *Biogeosciences*, 15(13):4003–4018.
- Malhi, Y., Doughty, C., and Galbraith, D. (2011). The allocation of ecosystem net primary productivity in tropical forests. *Philosophical Transactions of the Royal Society B: Biological Sciences*, 366(1582):3225–3245.
- Malhi, Y., Doughty, C. E., Goldsmith, G. R., Metcalfe, D. B., Girardin, C. A. J., Marthews, T. R., del Aguila-Pasquel, J., Aragão, L. E. O. C., Araujo-Murakami, A., Brando, P., da Costa, A. C. L., Silva-Espejo, J. E., Farfán Amézquita, F., Galbraith, D. R., Quesada, C. A., Rocha, W., Salinas-Revilla, N., Silvério, D., Meir, P., and Phillips, O. L. (2015). The linkages between photosynthesis, productivity, growth and biomass in lowland amazonian forests. *Global Change Biology*, 21(6):2283–2295.

- Manzoni, S., Katul, G., and Porporato, A. (2014). A dynamical system perspective on plant hydraulic failure. *Water Resources Research*, 50(6):5170–5183.
- Manzoni, S. and Porporato, A. (2009). Soil carbon and nitrogen mineralization: Theory and models across scales. *Soil Biology and Biochemistry*, 41(7):1355–1379.
- Marthews, T., Malhi, Y., Girardin, C. A. J., Espejo, J. S., Aragão, L. E. O. C., Mercado, L. M., Galbraith, D. R., Metcalfe, D., Rapp, J., Fisher, R., Fisher, J., Revilla, N. S., Friend, A., Coupe, N. R., and Williams, R. (2012). Simulating forest productivity along a neotropical elevational transect: temperature variation and carbon use efficiency. *Global change biology*, 18(9):2882–98.
- Martínez-Vilalta, J., Sala, A., Asensio, D., Galiano, L., Hoch, G., Palacio, S., Piper, F. I., and Lloret, F. (2016). Dynamics of non-structural carbohydrates in terrestrial plants: A global synthesis. *Ecological Monographs*, 86(4):495–516.
- McDowell, N. G., Fisher, R. A., Xu, C., Domec, J. C., Hölttä, T., Mackay D., S., Sperry, J. S., Boutz, A., Dickman, L., Gehres, N., Limousin, J. M., Macalady, A., Martínez-Vilalta, J., Mencuccini, M., Plaut, J. A., Ogée, J., Pangle, R. E., Rasse, D. P., Ryan, M. G., Sevanto, S., Waring, R. H., Williams A., P., Yepez, E. A., and Pockman, W. T. (2013). Evaluating theories of drought-induced vegetation mortality using a multimodel-experiment framework. *New Phytologist*, 200(2):304–321.
- McDowell, N. G. and Sevanto, S. (2010). The mechanisms of carbon starvation: how, when, or does it even occur at all? *New Phytologist*, 186(2):264–266.
- Medlyn, B., Zaehle, S., De Kauwe, M., Walker, A., Dietze, M., Hanson, P., Hickler, T., Jain, A., Luo, Y., Parton, W., Prentice, I., E. Thornton, P., Wang, S., Wang, Y., Weng, E., Iversen, C., McCarthy, H., Warren, J., Oren, R., and Norby, R. (2015). Using ecosystem experiments to improve vegetation models. *Nature Climate Change*, 5:528–534.
- Medlyn, B. E., De Kauwe, M. G., Zaehle, S., Walker, A. P., Duursma, R. A., Luus, K., Mishurov, M., Pak, B., Smith, B., Wang, Y.-P., Yang, X., Crous, K. Y., Drake, J. E., Gimeno, T. E., Macdonald, C. A., Norby, R. J., Power, S. A., Tjoelker, M. G., and Ellsworth, D. S. (2016). Using models to guide field experiments: *a priori* predictions for the CO₂ response of a nutrient- and water-limited native Eucalypt woodland. *Global Change Biology*, 22(8):2834–2851.
- Medlyn, B. E., Robinson, A. P., Clement, R., and McMurtrie, R. E. (2005). On the validation of models of forest CO₂ exchange using eddy covariance data: Some perils and pitfalls. *Tree Physiology*, 25(7):839–857.

- Metzler, H. and Sierra, C. A. (2018). Linear autonomous compartmental models as continuous-time Markov chains: Transit-time and age distributions. *Mathematical Geosciences*, 50(1):1–34.
- Meurer, A., Smith, C. P., Paprocki, M., Čertík, O., Kirpichev, S. B., Rocklin, M., Kumar, A., Ivanov, S., Moore, J. K., Singh, S., Rathnayake, T., Vig, S., Granger, B. E., Muller, R. P., Bonazzi, F., Gupta, H., Vats, S., Johansson, F., Pedregosa, F., Curry, M. J., Terrel, A. R., Roučka, v., Saboo, A., Fernando, I., Kulal, S., Cimrman, R., and Scopatz, A. (2017). SymPy: symbolic computing in python. *PeerJ Computer Science*, 3:e103.
- Minchin, P. E. H. and Lacoite, A. (2005). New understanding on phloem physiology and possible consequences for modelling long-distance carbon transport. *New Phytologist*, 166(3):771–779.
- Moorcroft, P. R., Hurtt, G. C., and Pacala, S. W. (2001). A method for scaling vegetation dynamics: The ecosystem demography model (ED). *Ecological Monographs*, 71(4):557–586.
- Muhr, J., Messier, C., Delagrange, S., Trumbore, S., Xu, X., and Hartmann, H. (2016). How fresh is maple syrup? Sugar maple trees mobilize carbon stored several years previously during early springtime sap-ascent. *New Phytologist*, 209(4):1410–1416.
- Müller, M. and Sierra, C. A. (2017). Application of input to state stability to reservoir models. *Theoretical Ecology*, 10(4):451–475.
- Murty, D. and McMurtrie, R. (2000). The decline of forest productivity as stands age: A model-based method for analysing causes for the decline. *Ecological modelling*, 134(2-3):185–205.
- Mystakidis, S., Davin, E. L., Gruber, N., and Seneviratne, S. I. (2016). Constraining future terrestrial carbon cycle projections using observation-based water and carbon flux estimates. *Global Change Biology*, 22(6):2198–2215.
- Oeschger, H., Siegenthaler, U., Schotterer, U., and Gugelmann, A. (1975). A box diffusion model to study the carbon dioxide exchange in nature. *Tellus*, 27(2):168–192.
- Palacio, S., Hoch, G., Sala, A., Körner, C., and Millard, P. (2014). Does carbon storage limit tree growth? *New Phytologist*, 201(4):1096–1100.
- Parton, W. J., Hanson, P. J., Swanston, C., Torn, M., Trumbore, S. E., Riley, W., and Kelly, R. (2010). ForCent model development and testing using the Enriched Background Isotope Study experiment. *Journal of Geophysical Research: Biogeosciences*, 115(4).
- Pavlick, R., Drewry, D. T., Bohn, K., Reu, B., and Kleidon, A. (2013). The Jena Diversity-Dynamic Global Vegetation Model (JeDi-DGVM): A diverse approach to representing terres-

- trial biogeography and biogeochemistry based on plant functional trade-offs. *Biogeosciences*, 10(6):4137–4177.
- Petrokofsky, G., Kanamaru, H., Achard, F., Goetz, S. J., Joosten, H., Holmgren, P., Lehtonen, A., Menton, M. C., Pullin, A. S., and Wattenbach, M. (2012). Comparison of methods for measuring and assessing carbon stocks and carbon stock changes in terrestrial carbon pools. how do the accuracy and precision of current methods compare? A systematic review protocol. *Environmental Evidence*, 1(1):6.
- Plain, C., Gerant, D., Maillard, P., Dannoura, M., Dong, Y., Zeller, B., Priault, P., Parent, F., and Epron, D. (2009). Tracing of recently assimilated carbon in respiration at high temporal resolution in the field with a tuneable diode laser absorption spectrometer after *in situ* $^{13}\text{CO}_2$ pulse labelling of 20-year-old beech trees. *Tree Physiology*, 29(11):1433–1445.
- Potter, C. S., Randerson, J. T., Field, C. B., Matson, P. A., Vitousek, P. M., Mooney, H. A., and Klooster, S. A. (1993). Terrestrial ecosystem production: A process model based on global satellite and surface data. *Global Biogeochemical Cycles*, 7(4):811–841.
- Powers, E. M. and Marshall, J. D. (2011). Pulse labeling of dissolved ^{13}C -carbonate into tree xylem: developing a new method to determine the fate of recently fixed photosynthate. *Rapid Communications in Mass Spectrometry*, 25(1):33–40.
- Purves, D. and Pacala, S. (2008). Predictive models of forest dynamics. *Science*, 320(5882):1452–1453.
- Quaiser, T., Dittrich, A., Schaper, F., and Monnigmann, M. (2011). A simple work flow for biologically inspired model reduction—application to early JAK-STAT signaling. *BMC Syst Biol*, 5:30.
- Rasmussen, M., Hastings, A., Smith, M. J., Agosto, F. B., Chen-Charpentier, B. M., Hoffman, F. M., Jiang, J., Todd-Brown, K. E. O., Wang, Y., Wang, Y.-P., and Luo, Y. (2016). Transit times and mean ages for nonautonomous and autonomous compartmental systems. *J. Math. Biol.*, 73(6-7):1379–1398.
- Raue, A., Kreutz, C., Maiwald, T., Bachmann, J., Schilling, M., Klingmüller, U., and Timmer, J. (2009). Structural and practical identifiability analysis of partially observed dynamical models by exploiting the profile likelihood. *Bioinformatics*, 25(15):1923.
- Raue, A., Kreutz, C., Theis, F. J., and Timmer, J. (2012). Joining forces of bayesian and frequentist methodology: A study for inference in the presence of non-identifiability. *Philosophical Transactions of the Royal Society of London A: Mathematical, Physical and Engineering Sciences*, 371(1984).

- Reichstein, M., Richardson, A. D., Migliavacca, M., and Carvalhais, N. (2014). Plant–environment interactions across multiple scales. In Monson, R. K., editor, *Ecology and the Environment*, pages 1–27. Springer New York, New York, NY.
- Richardson, A. D., Carbone, M. S., Huggett, B. A., Furze, M. E., Czimczik, C. I., Walker, J. C., Xu, X., Schaberg, P. G., and Murakami, P. (2015). Distribution and mixing of old and new nonstructural carbon in two temperate trees. *New Phytologist*, 206(2):590–597.
- Richardson, A. D., Carbone, M. S., Keenan, T. F., Czimczik, C. I., Hollinger, D. Y., Murakami, P., Schaberg, P. G., and Xu, X. (2013). Seasonal dynamics and age of stemwood nonstructural carbohydrates in temperate forest trees. *New Phytologist*, 197(3):850–861.
- Richardson, A. D., Williams, M., Hollinger, D. Y., Moore, D. J. P., Dail, D. B., Davidson, E. A., Scott, N. A., Evans, R. S., Hughes, H., Lee, J. T., Rodrigues, C., and Savage, K. (2010). Estimating parameters of a forest ecosystem c model with measurements of stocks and fluxes as joint constraints. *Oecologia*, 164(1):25–40.
- Rockström, J., Steffen, W. L., Noone, K., Persson, Å., Chapin III, F. S., Lambin, E., Lenton, T. M., Scheffer, M., Folke, C., Schellnhuber, H. J., *et al.* (2009). Planetary boundaries: exploring the safe operating space for humanity. *Ecology and Society*, 14(2):32.
- Rogers, A., Serbin, S. P., Ely, K. S., Sloan, V. L., and Wullschleger, S. D. (2017). Terrestrial biosphere models underestimate photosynthetic capacity and CO₂ assimilation in the Arctic. *New Phytologist*, 216(4):1090–1103.
- Running, S. W. and Coughlan, J. C. (1988). A general model of forest ecosystem processes for regional applications I. Hydrologic balance, canopy gas exchange and primary production processes. *Ecological Modelling*, 42(2):125–154.
- Schaber, J. and Klipp, E. (2011). Model-based inference of biochemical parameters and dynamic properties of microbial signal transduction networks. *Current Opinion in Biotechnology*, 22(1):109–116.
- Scheffer, M., Barrett, S., Carpenter, S. R., Folke, C., Green, A. J., Holmgren, M., Hughes, T. P., Kosten, S., van de Leemput, I. A., Nepstad, D. C., van Nes, E. H., Peeters, E. T. H. M., and Walker, B. (2015). Creating a safe operating space for iconic ecosystems. *Science*, 347(6228):1317–1319.
- Scheffer, M., Carpenter, S. R., Foley, J. A., Folke, C., and Walker, B. (2001). Catastrophic shifts in ecosystems. *Nature*, 413(6856):591–596.

- Scheiter, S. and Higgins, S. I. (2009). Impacts of climate change on the vegetation of Africa: An adaptive dynamic vegetation modelling approach. *Global Change Biology*, 15(9):2224–2246.
- Schiestl-Aalto, P., Kulmala, L., Mäkinen, H., Nikinmaa, E., and Mäkelä, A. (2015). CASSIA – a dynamic model for predicting intra-annual sink demand and interannual growth variation in Scots pine. *New Phytologist*, 206(2):647–659.
- Schimel, D., House, J. I., Hibbard, K., Bousquet, P., Ciais, P., Peylin, P., Braswell, B. H., Apps, M. J., Baker, D., Bondeau, A., Canadell, J., Churkina, G., Cramer, W., Denning, A. S., Field, C. B., Friedlingstein, P., Goodale, C. L., Heimann, M., Houghton, R. A., Melillo, J. M., Moore III, B., D., M., Noble, I., Pacala, S., Prentice, I. C., Raupach, M. R., Rayner, P. J., Scholes, R., Steffen, W., and Wirth, C. (2001). Recent patterns and mechanisms of carbon exchange by terrestrial ecosystems. *Nature*, 414:169–172.
- Schimel, D., Stephens, B. B., and Fisher, J. B. (2015). Effect of increasing co2 on the terrestrial carbon cycle. *Proceedings of the National Academy of Sciences*, 112(2):436–441.
- Seddon, A., Macias-Fauria, M., Long, P., Benz, D., and J. Willis, K. (2016). Sensitivity of global terrestrial ecosystems to climate variability. *Nature*, advance online publication.
- Sevanto, S., McDowell, N. G., Dickman L., T., Pangle, R., and Pockman, W. T. (2014). How do trees die? A test of the hydraulic failure and carbon starvation hypotheses. *Plant, Cell & Environment*, 37(1):153–161.
- Sierra, C. A., Ceballos-Núñez, V., Metzler, H., and Müller, M. (2018). Representing and understanding the carbon cycle using the theory of compartmental dynamical systems. *Journal of Advances in Modeling Earth Systems*.
- Sierra, C. A. and Müller, M. (2015). A general mathematical framework for representing soil organic matter dynamics. *Ecological Monographs*, 85(4):505–524.
- Sierra, C. A., Müller, M., Metzler, H., Manzoni, S., and Trumbore, S. E. (2016). The muddle of ages, turnover, transit, and residence times in the carbon cycle. *Global Change Biology*, in print.
- Sierra, C. A., Müller, M., and Trumbore, S. E. (2012). Models of soil organic matter decomposition: The SoilR package, version 1.0. *Geoscientific Model Development*, 5(4):1045–1060.
- Sitch, S., Smith, B., Prentice, I. C., Arneth, A., Bondeau, A., Cramer, W., Kaplan, J. O., Levis, S., Lucht, W., Sykes, M. T., Thonicke, K., and Venevsky, S. (2003). Evaluation of ecosystem dynamics, plant geography and terrestrial carbon cycling in the LPJ dynamic global vegetation model. *Global Change Biology*, 9(2):161–185.

- Smallman, T. L., Exbrayat, J. F., Mencuccini, M., Bloom, A. A., and Williams, M. (2017). Assimilation of repeated woody biomass observations constrains decadal ecosystem carbon cycle uncertainty in aggrading forests. *Journal of Geophysical Research: Biogeosciences*.
- Soetaert, K., Hoffmann, M., Meire, P., Starink, M., and van Oevelen, D. (2004). Modeling growth and carbon allocation in two reed beds (*phragmites australis*) in the scheldt estuary. *Aquatic botany*, 79(3):211–234.
- Soetaert, K. and Petzoldt, T. (2010). Inverse modelling, sensitivity and monte carlo analysis in r using package FME. *Journal of Statistical Software*, 33(3).
- Strogatz, S. (2014). *Nonlinear Dynamics and Chaos: With Applications to Physics, Biology, Chemistry, and Engineering*. Studies in Nonlinearity. Westview Press.
- Strogatz, S. H. (1994). *Nonlinear dynamics and chaos: with applications to physics, biology, chemistry, and engineering*. Perseus publishing.
- Subke, J.-A., Vallack, H. W., Magnusson, T., Keel, S. G., Metcalfe, D. B., Högberg, P., and Ineson, P. (2009). Short-term dynamics of abiotic and biotic soil $^{13}\text{CO}_2$ effluxes after *in situ* $^{13}\text{CO}_2$ pulse labelling of a boreal pine forest. *New Phytologist*, 183(2):349–357.
- Sword Sayer, M. A. and Haywood, J. D. (2005). Fine root production and carbohydrate concentrations of mature longleaf pine (*Pinus palustris* P. Mill.) as affected by season of prescribed fire and drought.
- Thomas, R. Q. and Williams, M. (2014). A model using marginal efficiency of investment to analyze carbon and nitrogen interactions in terrestrial ecosystems (ACONITE version 1). *Geoscientific Model Development*, 7(5):2015–2037.
- Timmer, J. (2011). Addressing parameter identifiability by model-based experimentation. *IET Systems Biology*, 5:120–130(10).
- Trumbore, S., Czimczik, C. I., Sierra, C. A., Muhr, J., and Xu, X. (2015). Non-structural carbon dynamics and allocation relate to growth rate and leaf habit in california oaks. *Tree Physiology*, 35(11):1206.
- Trumbore, S., Gaudinski, J. B., Hanson, P. J., and Southon, J. R. (2002). Quantifying ecosystem-atmosphere carbon exchange with a ^{14}C label. *Eos, Transactions American Geophysical Union*, 83(24):265–268.
- Trumbore, S. E. (2006). Carbon respired by terrestrial ecosystems - recent progress and challenges. *Global Change Biology*, 12(2):141–153.

- Trumbore, S. E., Sierra, C. A., and Hicks Pries, C. E. (2016). Radiocarbon nomenclature, theory, models, and interpretation: Measuring age, determining cycling rates, and tracing source pools. In Schuur, A. E., Druffel, E., and Trumbore, E. S., editors, *Radiocarbon and Climate Change: Mechanisms, Applications and Laboratory Techniques*, pages 45–82. Springer International Publishing.
- Ueyama, M., Ichii, K., Hirata, R., Takagi, K., and Asanuma, J. (2010). Simulating carbon and water cycles of larch forests in East Asia by the BIOME-BGC model with AsiaFlux data. *Biogeosciences*, 7(3):959–977.
- Urbanski, S., Barford, C., Wofsy, S., Kucharik, C., Pyle, E., Budney, J., McKain, K., Fitzjarrald, D., Czikowsky, M., and Munger, J. W. (2007). Factors controlling CO₂ exchange on timescales from hourly to decadal at harvard forest. *Journal of Geophysical Research: Biogeosciences (2005–2012)*, 112(G2).
- Valentine, H. (1999). Estimation of the net primary productivity of even-aged stands with a carbon-allocation model. *Ecological modelling*, 122(3):139–149.
- Walker, A. P., Hanson, P. J., De Kauwe, M. G., Medlyn, B. E., Zaehle, S., Asao, S., Dietze, M., Hickler, T., Huntingford, C., Iversen, C. M., Jain, A., Lomas, M., Luo, Y., Mccarthy, H., Parton, W. J., Prentice, I. C., Thornton, P. E., Wang, S., Wang, Y.-p., Warlind, D., Weng, E., Warren, J. M., Woodward, F. I., Oren, R., and Norby, R. J. (2014). Comprehensive ecosystem model-data synthesis using multiple datasets at two temperate forest free-air CO₂ enrichment experiments: Model performance at ambient CO₂ concentration. *Journal of Geophysical Research: Biogeosciences*, 119(5):937–964.
- Walker, A. P., Zaehle, S., Medlyn, B. E., De Kauwe, M. G., Asao, S., Hickler, T., Parton, W., Ricciuto, D. M., Wang, Y.-P., Wärlind, D., and Norby, R. J. (2015). Predicting long-term carbon sequestration in response to CO₂ enrichment: How and why do current ecosystem models differ? *Global Biogeochemical Cycles*, 29(4):476–495.
- Wang, Y. P., Law, R. M., and Pak, B. (2010). A global model of carbon, nitrogen and phosphorus cycles for the terrestrial biosphere. *Biogeosciences*, 7(7):2261–2282.
- Waring, R. and Running, S. (1998). *Forest Ecosystems: Analysis at Multiple Scales*. Number v. 1 in *Forest Ecosystems: Analysis at Multiple Scales*. Academic Press.
- Wiley, E., Huepenbecker, S., Casper, B. B., and Helliker, B. R. (2013). The effects of defoliation on carbon allocation: can carbon limitation reduce growth in favour of storage? *Tree Physiology*, 33(11):1216–1228.

- Williams, M., Schwarz, P. A., Law, B. E., Irvine, J., and Kurpius, M. R. (2005). An improved analysis of forest carbon dynamics using data assimilation. *Global Change Biology*, 11(1):89–105.
- Wofsy, S., Goulden, M., Munger, J., Fan, S.-M., Bakwin, P., Daube, B., Bassow, S., and Bazzaz, F. (1993). Net exchange of CO₂ in a mid-latitude forest. *Science*, 260(5112):1314–1317.
- Würth, M. K. R., Peláez-Riedl, S., Wright, S. J., and Körner, C. (2005). Non-structural carbohydrate pools in a tropical forest. *Oecologia*, 143(1):11–24.
- Xia, J., Luo, Y., Wang, Y. P., and Hararuk, O. (2013). Traceable components of terrestrial carbon storage capacity in biogeochemical models. *Global Change Biology*, 19(7):2104–2116.
- Xia, J., Niu, S., Ciais, P., Janssens, I. A., Chen, J., Ammann, C., Arain, A., Blanken, P. D., Cescatti, A., Bonal, D., Buchmann, N., Curtis, P. S., Chen, S., Dong, J., Flanagan, L. B., Frankenberg, C., Georgiadis, T., Gough, C. M., Hui, D., Kiely, G., Li, J., Lund, M., Magliulo, V., Marcolla, B., Merbold, L., Montagnani, L., Moors, E. J., Olesen, J. E., Piao, S., Raschi, A., Rouspard, O., Suyker, A. E., Urbaniak, M., Vaccari, F. P., Varlagin, A., Vesala, T., Wilkinson, M., Weng, E., Wohlfahrt, G., Yan, L., and Luo, Y. (2015). Joint control of terrestrial gross primary productivity by plant phenology and physiology. *Proceedings of the National Academy of Sciences*, 112(9):2788–2793.
- Xia, J., Yuan, W., Wang, Y.-P., and Zhang, Q. (2017). Adaptive carbon allocation by plants enhances the terrestrial carbon sink. *Scientific Reports*, 7(3341).
- Yizhao, C., Jianyang, X., Zhengguo, S., Jianlong, L., Yiqi, L., Chengcheng, G., and Zhaoqi, W. (2015). The role of residence time in diagnostic models of global carbon storage capacity: Model decomposition based on a traceable scheme. *Scientific Reports*, 5(16155).
- Zaehle, S. and Friend, A. D. (2010). Carbon and nitrogen cycle dynamics in the O-CN land surface model: 1. Model description, site-scale evaluation, and sensitivity to parameter estimates. *Global Biogeochemical Cycles*, 24(1):1–13.
- Zaehle, S., Medlyn, B. E., De Kauwe, M. G., Walker, A. P., Dietze, M. C., Hickler, T., Luo, Y., Wang, Y. P., El-Masri, B., Thornton, P., Jain, A., Wang, S., Warlind, D., Weng, E., Parton, W., Iversen, C. M., Gallet-Budynek, A., McCarthy, H., Finzi, A., Hanson, P. J., Prentice, I. C., Oren, R., and Norby, R. J. (2014). Evaluation of 11 terrestrial carbon-nitrogen cycle models against observations from two temperate Free-Air CO₂ Enrichment studies. *New Phytologist*, 202(3):803–822.

Zobeley, J., Lebiedz, D., Kammerer, J., Ishmurzin, A., and Kummer, U. (2005). A new time-dependent complexity reduction method for biochemical systems. In *Transactions on Computational Systems Biology I*, pages 90–110. Springer.

Selbständigkeitserklärung

Ich erkläre, dass ich die vorliegende Arbeit selbständig und nur unter Verwendung der angegebenen Hilfsmittel, persönlichen Mitteilungen und Quellen angefertigt habe.

.....

Ort, Datum Verónica Ceballos-Núñez

Curriculum Vitae

Personal information

First name: Verónica
Family name: Ceballos Núñez
Date of birth: December 10th, 1987
Place of birth: Cali, Valle del Cauca, Colombia

Professional experience

01.2015-12.2018 **PhD researcher**; Max Planck Institute for Biogeochemistry (Jena)
Thesis title:
Nonlinearities in Carbon Allocation and Vegetation Functioning
Main advisor: Dr. Carlos A. Sierra

09.2016 - 12.2016 **Research stay**; Richardson Lab: Terrestrial Ecosystems and Global Change.
Department of Organismic & Evolutionary Biology,
Harvard University, Cambridge, MA, USA

10.2013 - 12.2013 **Visitor student**; Mathematical Modeling and Systems Biology.
Max-Planck-Institut für Molekulare Pflanzenphysiologie, Potsdam, Germany

10.2013 - 12.2013 **SABIO RK, core maintenance**; HITS gGmbHs. Heidelberg, Germany

4.2009 - 2.2012 **Researcher**; Laboratory of Molecular Biology and Pathogenesis.
Universidad del Valle, Colombia

10.2009 **Monitor in the area of Genetics**; Science Fair 'Carpa de Melquíades',
XV Pacific Book Fair, Universidad del Valle, Colombia

Education and training

- 10.2012 - 9.2014** **MSc, Molecular Biosciences**; Major: Systems Biology
 Ruprecht-Karls-Universität Heidelberg, Germany
 Thesis title:
Hormone-based signaling networks controlling metabolic changes in plants during insect herbivory
 Major advisors: Dr. Emmanuel Gaquerel, Prof. Dr. Ursula Kummer
- 10.2012 - 11.2012** **In Silico Methods in Biochemistry**; Ursula Kummer, Sven Sahle, Katharina Beuke, Jennifer Levering, Nadine Veith, Andreas Weidemann.
 Ruprecht-Karls-Universität Heidelberg, Germany
- 2.2006 - 11.2012** **BSc, Biology**; Universidad del Valle, Colombia
 Thesis title:
Genomic and functional characterization of genes associated with Preeclampsia
 Major advisors: Dr. Felipe García Vallejo, Dr. José María Satizábal S.

Awards, oral presentations and publications

Verónica Ceballos-Núñez, Henrik Hartmann, Carlos A. Sierra. (In prep.). Sink and source limits on carbon allocation in vegetation: A dynamical system perspective.

Verónica Ceballos-Núñez, Markus Müller, Carlos A. Sierra. (In review). Towards better representations of carbon allocation in vegetation: A conceptual framework and mathematical tool. *Ecological Modelling*.

Carlos A. Sierra, **Verónica Ceballos-Núñez**, Holger Metzler, Markus Müller. (2018). Representing and Understanding the Carbon Cycle Using the Theory of Compartmental Dynamical Systems. *Journal of Advances in Modeling Earth Systems*.

Verónica Ceballos-Núñez, Andrew Richardson, Carlos A. Sierra. (2018). Ages and transit times as important diagnostics of model performance for predicting carbon dynamics in terrestrial vegetation models. *Biogeosciences*, 15:1607–1625.

Verónica Ceballos-Núñez, Andrew Richardson, Carlos A. Sierra. (2017). Measurements of carbon age distribution could revolutionize the terrestrial vegetation models. Poster in New Phytologist Next Generation Scientists Meeting. Norwich, UK.

Verónica Ceballos-Núñez, Andrew Richardson, Carlos A. Sierra. (2017). Ages and transit times predicted by ecosystem models with different carbon allocation schemes. Oral in Session BG2.20 - Carbon allocation in plants and ecosystems: mechanisms, responses and biogeochemical implications. EGU General Assembly

Verónica Ceballos-Núñez, Holger Metzler, Markus Müller, Carlos A. Sierra. (2016). Nonlinearities in Carbon Allocation and Vegetation Functioning: The Model Database. Poster in Session BG2.2 - Carbon allocation in plants and ecosystems: mechanisms, responses and biogeochemical implications. EGU General Assembly

Appendix chapter 2

Variables, parameters and matrix representation of the models used for the example in chapter 2.

1. Autonomous linear model

Name	Description	Units	Values
State variables			
C_f	Carbon in foliage	$kgC \cdot m^{-2}$	15
C_{NSC}	Non Structural Carbohydrates	$kgC \cdot m^{-2}$	15
C_w	Carbon in wood (wood of stem, branches, and roots)	$kgC \cdot m^{-2}$	150
C_r	Carbon in fine roots	$kgC \cdot m^{-2}$	90
Photosynthesis parameters			
k_1	Absorption rates (light, CO2, water...)	day^{-1}	2
Partitioning rates			
η_f	Flux rate of photosynthetically fixed carbon from foliage to foliage	day^{-1}	1
η_{NSC}	Flux rate of photosynthetically fixed carbon from foliage to Non Structural Carbohydrates	day^{-1}	0.016
η_w	Flux rate of photosynthetically fixed carbon from Non Structural Carbohydrates to wood	day^{-1}	0.001
η_r	Flux rate of photosynthetically fixed carbon from Non Structural Carbohydrates to roots	day^{-1}	0.003
Internal cycling rates			
γ_{fNSC}	Flux rate of carbon from C_{NSC} to foliage	day^{-1}	0.01
Release rates			
γ_f	Rate in which carbon leaves from C_f to the exterior (respiration, litter, etc.)	day^{-1}	0.01
γ_w	Rate in which carbon leaves from C_w to the exterior (respiration, litter, etc.)	day^{-1}	0.0001
γ_r	Rate in which carbon leaves from C_r to the exterior (respiration, litter, etc.)	day^{-1}	0.0005

Table 1: Variables and parameters of the linear model.

Table 2: Matrix representation of the Autonomous Linear Model, see variables and parameters in table 1

Name	Description	Expression
x	vector of states for vegetation	$x = \begin{bmatrix} C_f \\ C_{NSC} \\ C_w \\ C_r \end{bmatrix}$
u	scalar function of photosynthetic inputs	$u = k_1$
β	vector of partitioning coefficients of photosynthetically fixed carbon	$\beta = \begin{bmatrix} \eta_f \\ 0 \\ 0 \\ 0 \end{bmatrix}$
B	matrix of cycling rates	$B = \begin{bmatrix} -\eta_{NSC} - \gamma_f & \gamma_{fNSC} & 0 & 0 \\ \eta_{NSC} & -\eta_r - \eta_w - \gamma_{fNSC} & 0 & 0 \\ 0 & \eta_w & -\gamma_w & 0 \\ 0 & \eta_r & 0 & -\gamma_r \end{bmatrix}$
f_v	the righthandside of the ode	$f_v = u \cdot \beta + B \cdot x$

2. Autonomous nonlinear model

Name	Description	Units	Values
State variables			
C_f	Carbon in foliage	$kgC \cdot m^{-2}$	15
C_{NSC}	Non Structural Carbohydrates	$kgC \cdot m^{-2}$	15
C_w	Carbon in wood (wood of stem, branches, and roots)	$kgC \cdot m^{-2}$	150
C_r	Carbon in fine roots	$kgC \cdot m^{-2}$	90
Photosynthesis parameters			
k_1	Absorption rates (light, CO2, water...)	day^{-1}	0.5
Other rates			
k_1	Michaelis-Menten parameter	200	
k_2	Michaelis-Menten parameter	560	
v_1	Michaelis-Menten parameter	1	
v_2	Michaelis-Menten parameter	0.01	
Partitioning rates			
η_f	Flux rate of photosynthetically fixed carbon from foliage to foliage	1	day^{-1}
η_{NSC}	Flux rate of photosynthetically fixed carbon from foliage to Non Structural Carbohydrates	$\eta_{NSC} = \frac{v_1}{k_1 + C_{NSC}}$	day^{-1}
η_w	Flux rate of photosynthetically fixed carbon from Non Structural Carbohydrates to wood	day^{-1}	0.001
η_r	Flux rate of photosynthetically fixed carbon from Non Structural Carbohydrates to roots	day^{-1}	0.003
Internal cycling rates			
γ_{fNSC}	Flux rate of carbon from C_{NSC} to foliage	$\gamma_{fNSC} = \frac{v_2}{k_2 + C_f}$	day^{-1}
Release rates			
γ_f	Rate in which carbon leaves from C_f to the exterior (respiration, litter, etc.)	day^{-1}	0.01
γ_w	Rate in which carbon leaves from C_w to the exterior (respiration, litter, etc.)	day^{-1}	0.0001
γ_r	Rate in which carbon leaves from C_r to the exterior (respiration, litter, etc.)	day^{-1}	0.0005

Table 3: Variables and parameters of the nonlinear model.

Table 4: Matrix representation of the Autonomous Nonlinear Model, see variables and parameters in table 3

Name	Description	Expression
x	vector of states for vegetation	$x = \begin{bmatrix} C_f \\ C_{NSC} \\ C_w \\ C_r \end{bmatrix}$
u	scalar function of photosynthetic inputs	$u = k_1 \cdot \frac{C_f}{C_{NSC}}$
β	vector of partitioning coefficients of photosynthetically fixed carbon	$\beta = \begin{bmatrix} \eta_f \\ 0 \\ 0 \\ 0 \end{bmatrix}$
B	matrix of cycling rates	$B = \begin{bmatrix} -\eta_{NSC} - \gamma_f & \gamma_f NSC & 0 & 0 \\ \eta_{NSC} & -\eta_r - \eta_w - \gamma_f NSC & 0 & 0 \\ 0 & \eta_w & -\gamma_w & 0 \\ 0 & \eta_r & 0 & -\gamma_r \end{bmatrix}$
f_v	the righthandside of the ode	$f_v = u(x) \cdot \beta + B(x) \cdot x$

Appendix chapter 3

Table 5: Number of positive and negative correlations between parameters. Only R^1 values < -0.1 and > 0.1 were assumed to account for correlations.

Model	Positive correlations	Negative correlations	Possible combinations
<i>Storage: 0</i>	5	9	21
<i>Storage: 1</i>	10	15	28
<i>Storage: 2</i>	12	21	45

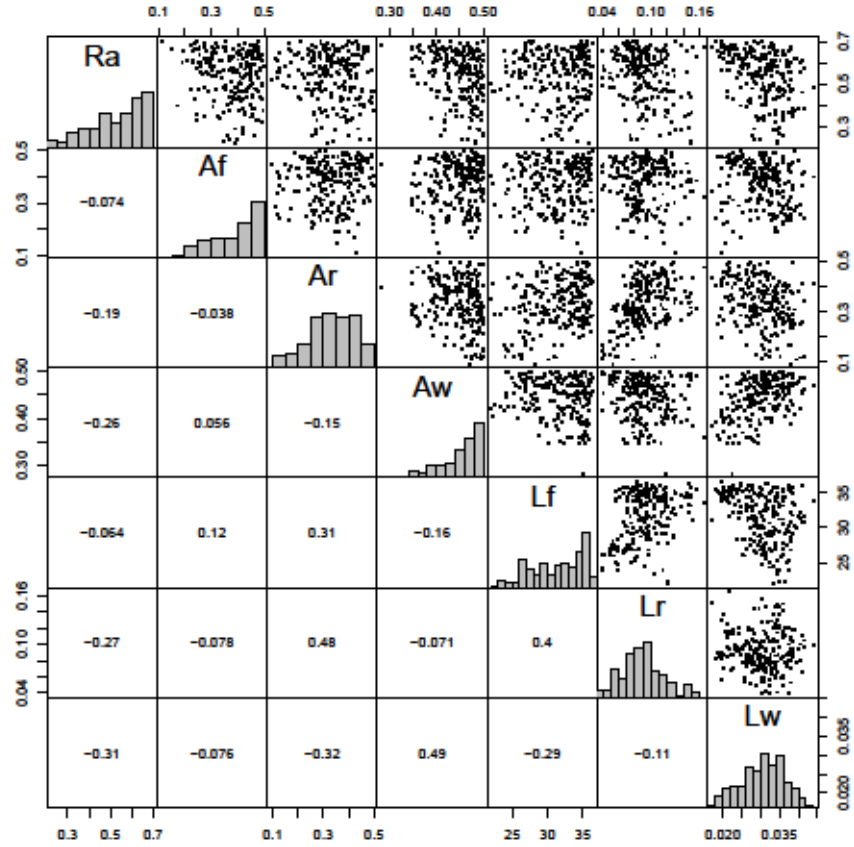
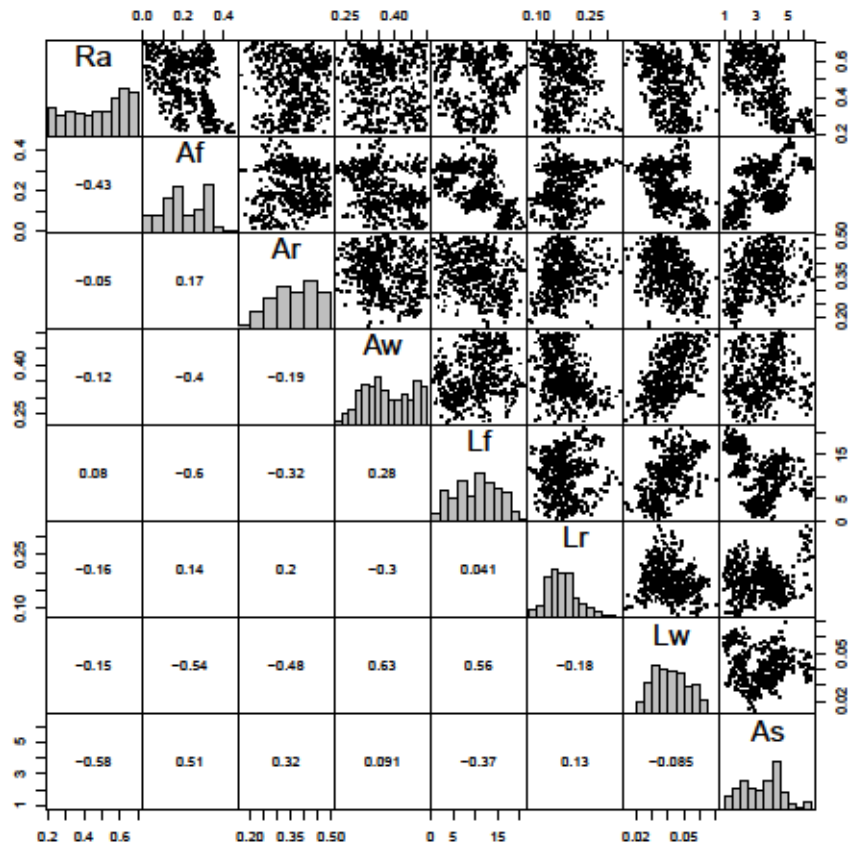


Figure 2: Pairwise plots of sensitivity functions for the model *Storage: 0*

Figure 3: Pairwise plots of sensitivity functions for the model *Storage: 1*

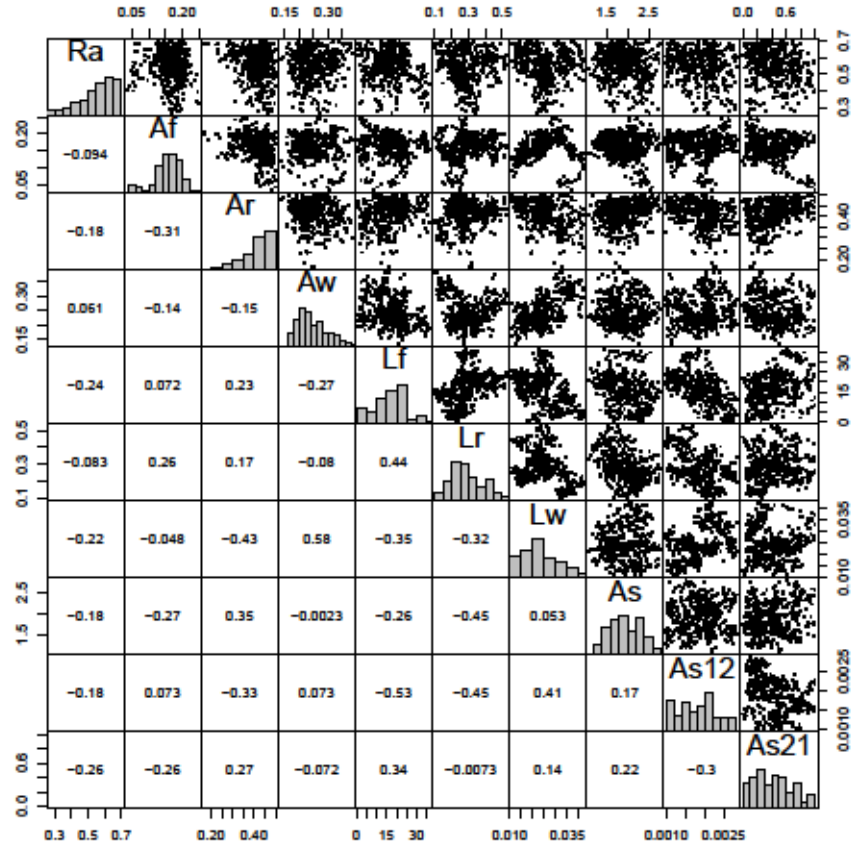


Figure 4: Pairwise plots of sensitivity functions for the model *Storage: 2*

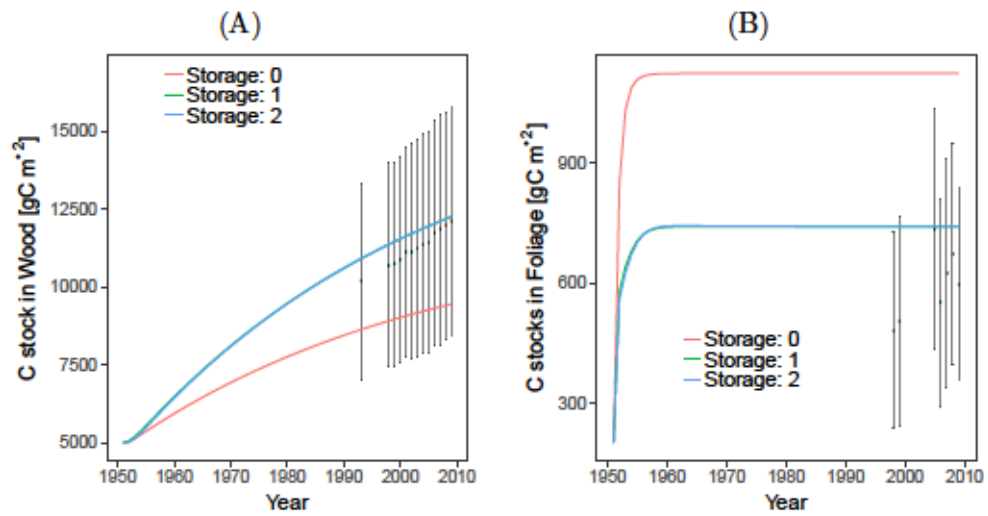


Figure 5: Carbon stocks estimated for each model, comparing the observed data and the model predictions of C stocks in Wood (A) and Foliage (B). The C stocks from models *Storage: 0* and *2* overlap. The three models were run using the same parameter set.

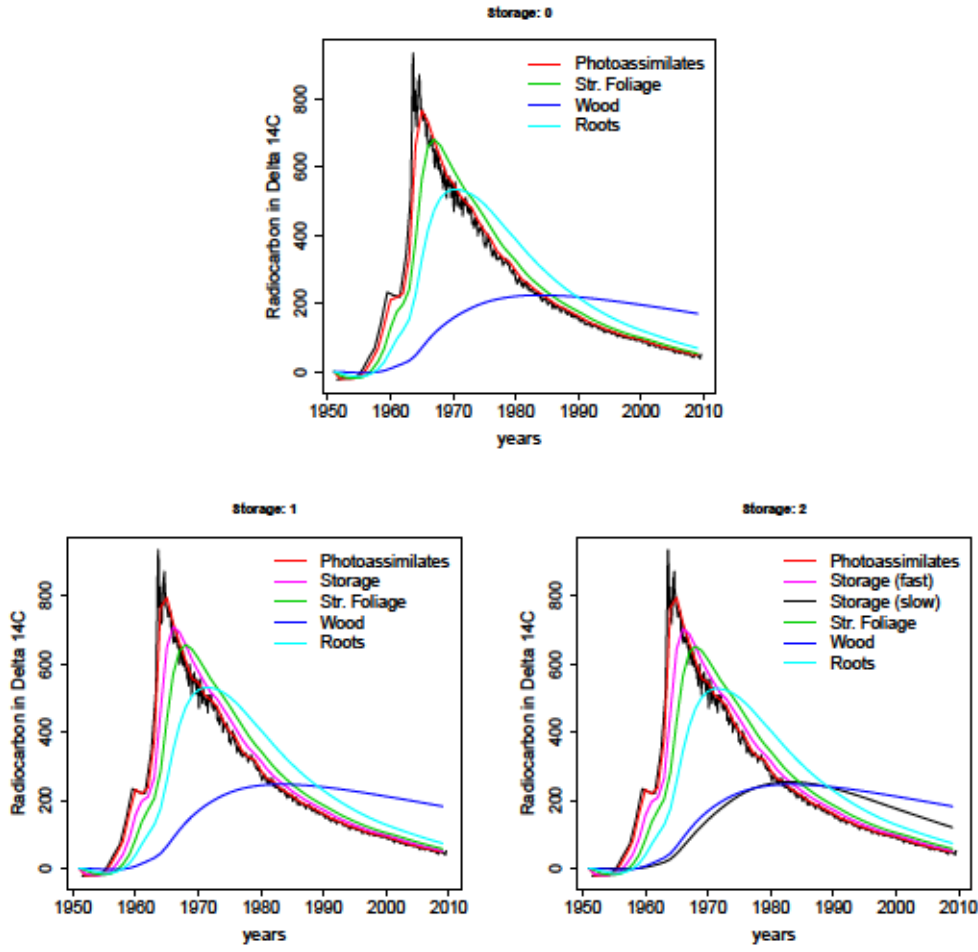


Figure 6: Radiocarbon simulations for the three models. The three models were run using the same parameter set. The black curve corresponds to the $\delta^{14}C$ accumulation in the atmosphere, and the other colors depict the vegetation compartments.

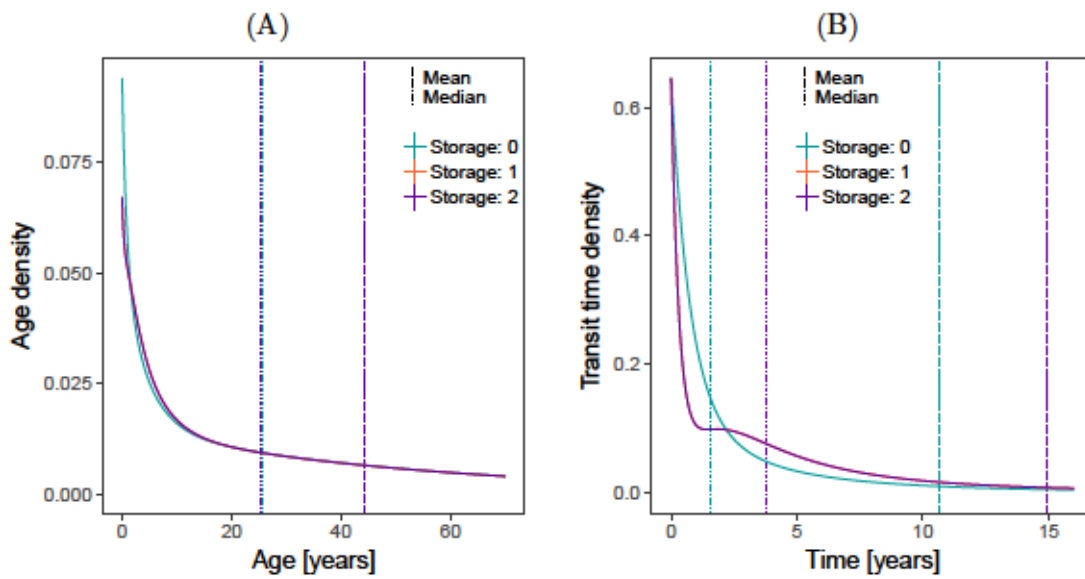


Figure 7: System ages and transit times. (A) Age and transit time (B) distributions calculated for each of the three models using the same parameter set; the dashed and dotted lines mark the mean and median ages, respectively. Some of the lines may be overlapping others.

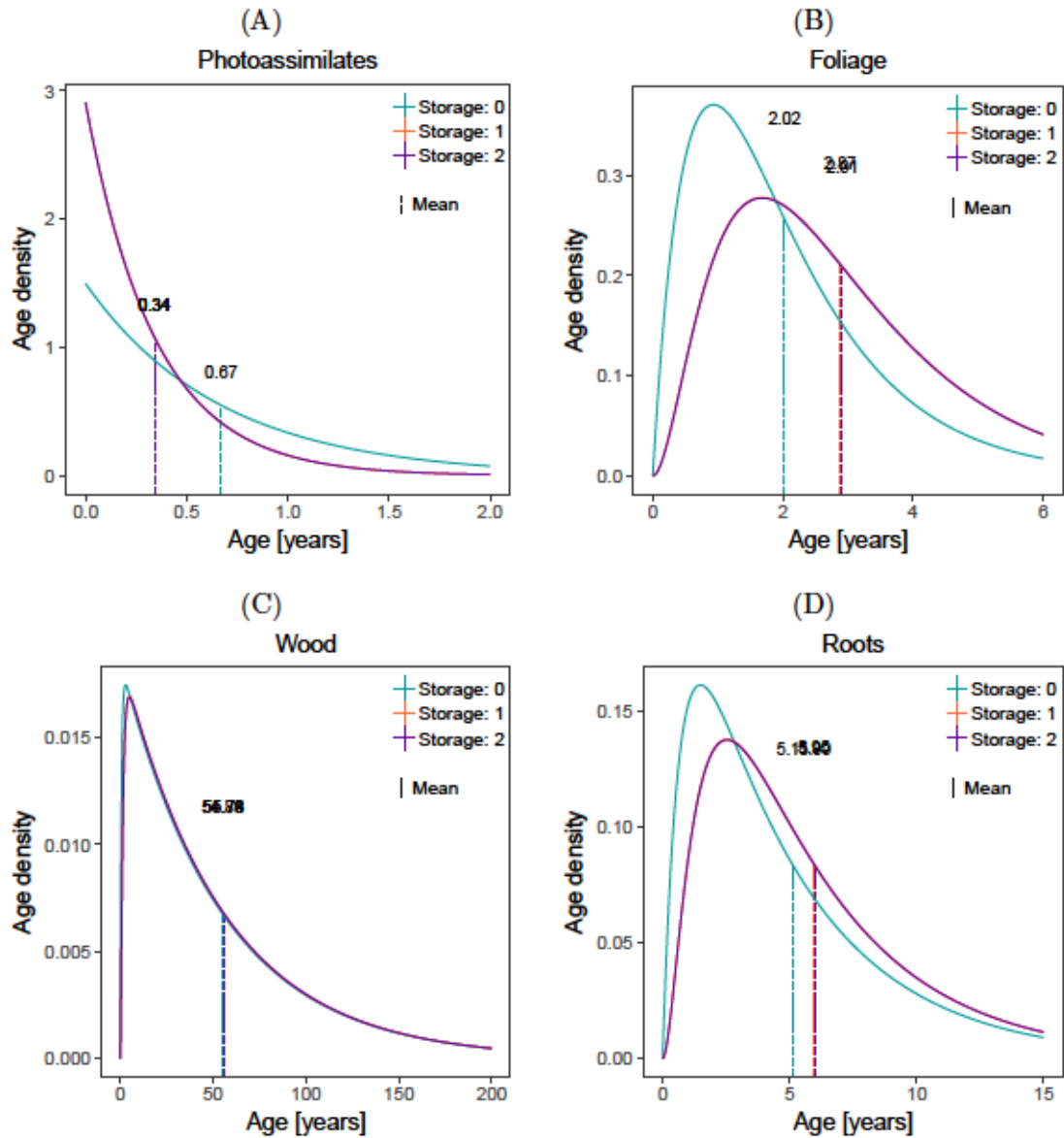


Figure 8: Age densities simulated for the compartments: (A) Photoassimilates, (B) Str. Foliage, (C) Wood and (D) Roots. The three models were run using the same parameter set. Each model is depicted in a different color. The dashed lines correspond to the mean ages of each model for each compartment.

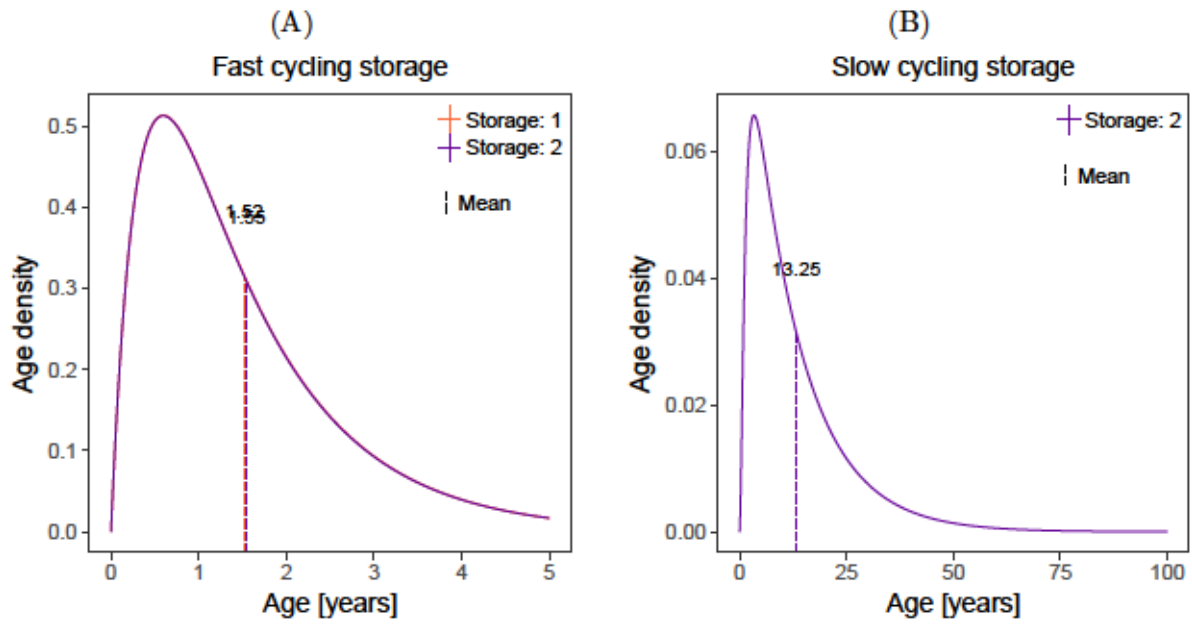


Figure 9: Age densities simulated for the models with storage compartments; the models were run using the same parameter set. (A) Fast cycling compartment of models *Storage: 0* and *Storage: 2*. (B) Slow cycling storage of the only model with 2 storage compartments.

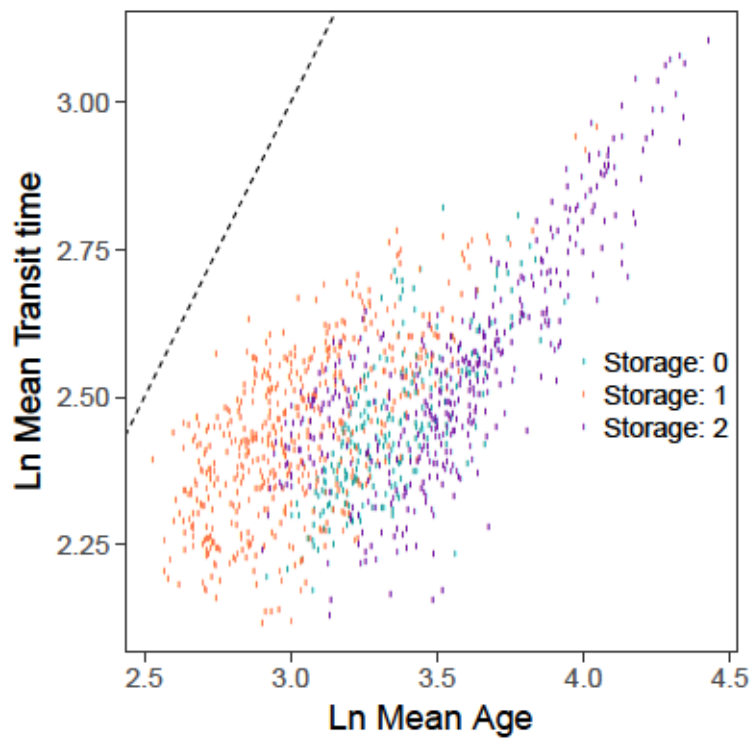


Figure 10: Scatter plot of mean age Vs. mean transit times in log scale. The three models have distributions below the 1:1 line.

Appendix chapter 4

Impact of C allocation limitation scenarios on the predictions of a model with fixed photosynthetic input

The model proposed in this work has a photosynthetic input that depends on the state variable structural foliage ($u = k_1 \cdot \zeta \cdot F_{struc}$); in order to determine whether this dependency could affect the impact of the limitation scenarios on diverse model simulations, we developed another version with fixed-input. This new version is summarized in the table 6 and was used to calculate the impact of source and sink strength on the predicted C stocks in steady state (figure 11), the transient C accumulation in each compartment (figure 12), the phase planes (figure 13), and the mean ages for the system compartments (figure 15).

Table 6: Matrix representation of the model with fixed photosynthetic input (u no longer depends on foliage)

Name	Description	Expression
x	vector of states for vegetation	$x = \begin{bmatrix} SS \\ Res \\ F_{struc} \\ W_{struc} \\ R_{struc} \end{bmatrix}$
u	scalar function of photosynthetic inputs	$u = k_1 \cdot \zeta$
β	vector of partitioning coefficients of photosynthetically fixed carbon	$\beta = \begin{bmatrix} \eta \\ 0 \\ 0 \\ 0 \\ 0 \end{bmatrix}$
B	matrix of cycling rates	$B = \begin{bmatrix} -\gamma_{21} - \gamma_{31} - \gamma_{41} - \gamma_{51} - R_m & \gamma_{12} & 0 & 0 & 0 \\ \gamma_{21} & -\gamma_{12} & 0 & 0 & 0 \\ \gamma_{31} & 0 & -\gamma_F & 0 & 0 \\ \gamma_{41} & 0 & 0 & -\gamma_W & 0 \\ \gamma_{51} & 0 & 0 & 0 & -\gamma_R \end{bmatrix}$
f_v	the right-hand side of the ode	$f_v = u \cdot \beta + B(x) \cdot x$

Impact of limitation scenarios on predicted mean ages of a linear model

The initial model proposed in this work has two sources of nonlinearities: a photosynthetic input that depends on a state variable ($u(x)$), and the multiplication between the state variable soluble sugars (SS) and the maintenance respiration rate that depends on other state variables $R_m = \frac{F_{struc} + R_{struc} + (liveWood \cdot W_{struc})}{rm}$. In order to determine whether these nonlinearities modified the impact of the limitation scenarios on predicted compartment mean ages, we developed a linear version of the model proposed in this work. The linear version is summarized in the table 7 and the predicted mean ages for the compartments of this model are in figure 16.

Table 7: Matrix representation of the linear model with constant photosynthetic input and constant maintenance respiration ($R_m = rm$)

Name	Description	Expression
x	vector of states for vegetation	$x = \begin{bmatrix} SS \\ Res \\ F_{struc} \\ W_{struc} \\ R_{struc} \end{bmatrix}$
u	scalar function of photosynthetic inputs	$u = k_1 \cdot \zeta$
β	vector of partitioning coefficients of photosynthetically fixed carbon	$\beta = \begin{bmatrix} \eta \\ 0 \\ 0 \\ 0 \\ 0 \end{bmatrix}$
B	matrix of cycling rates	$B = \begin{bmatrix} -\gamma_{21} - \gamma_{31} - \gamma_{41} - \gamma_{51} - R_m & \gamma_{12} & 0 & 0 & 0 \\ \gamma_{21} & -\gamma_{12} & 0 & 0 & 0 \\ \gamma_{31} & 0 & -\gamma_F & 0 & 0 \\ \gamma_{41} & 0 & 0 & -\gamma_W & 0 \\ \gamma_{51} & 0 & 0 & 0 & -\gamma_R \end{bmatrix}$
f_v	the right-hand side of the ode	$f_v = u \cdot \beta + B \cdot x$

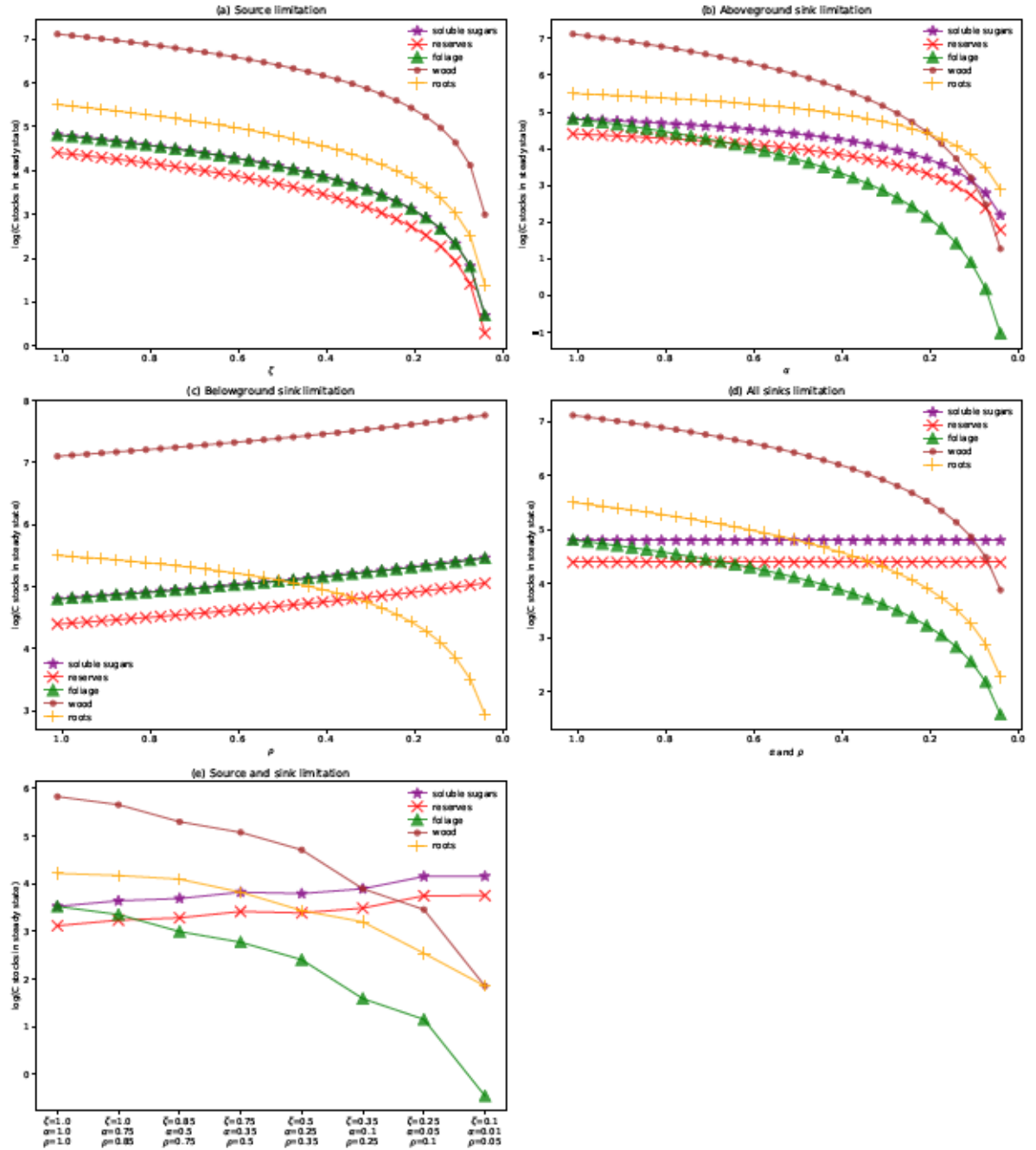


Figure 11: Carbon stocks of each compartment under different limitation scenarios; (a) source limitation only $-\zeta$, (b) aboveground sinks limitation $-\alpha$, (c) belowground sinks limitation $-\rho$, (d) above and belowground limitation $-\alpha, \rho$, and (e) Source and sink limitation $-\zeta, \alpha, \rho$. For these simulations the photosynthetic input was kept constant, i.e., it was no longer dependent on foliage.

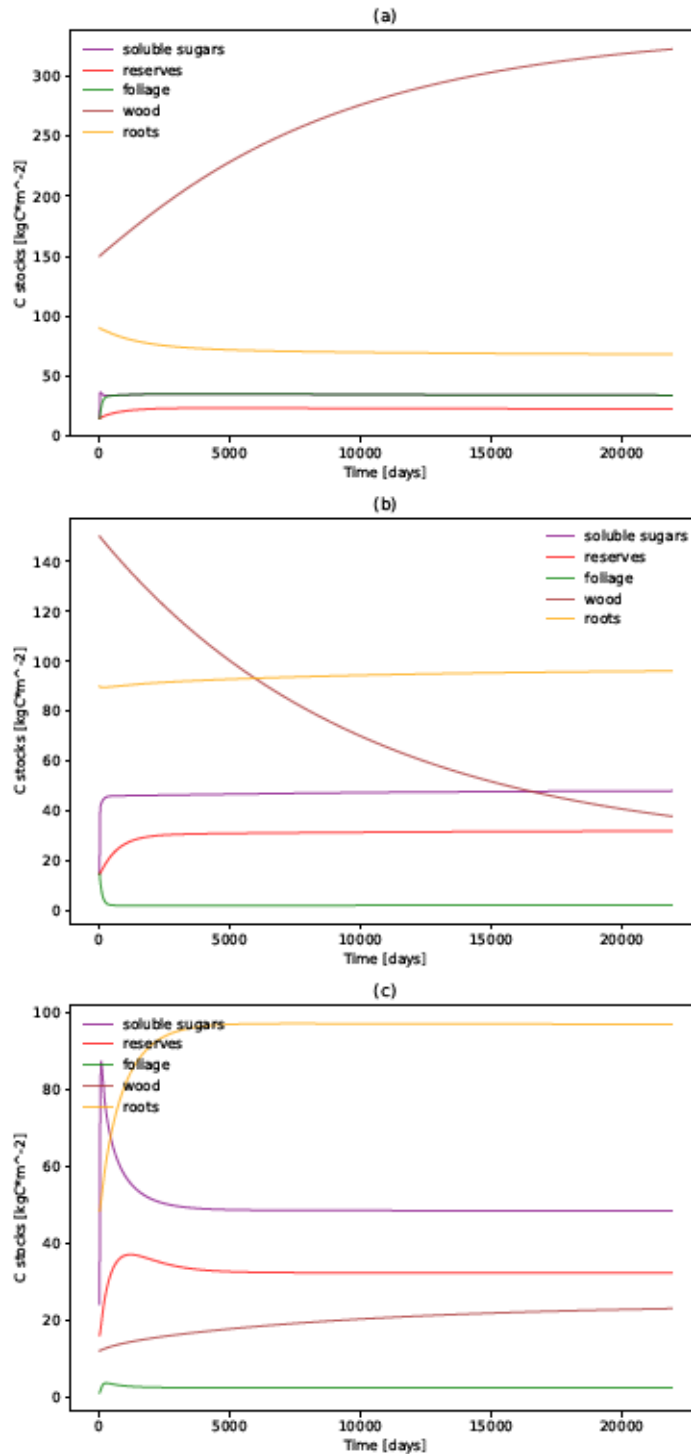


Figure 12: Carbon stocks with respect to time for a model with constant photosynthetic input. (a) Model solutions with initial C stocks and parameter values as specified in table 4.1, no C allocation limitations. (b) Model simulations with same initial C stocks and parameters as before, but with strong aboveground sink limitation: $\alpha = 0.05$. (c) Model solutions with initial C stocks in the neighborhood of the steady state calculated with $\alpha = 0.05$; this parameter value was also used for the simulations.

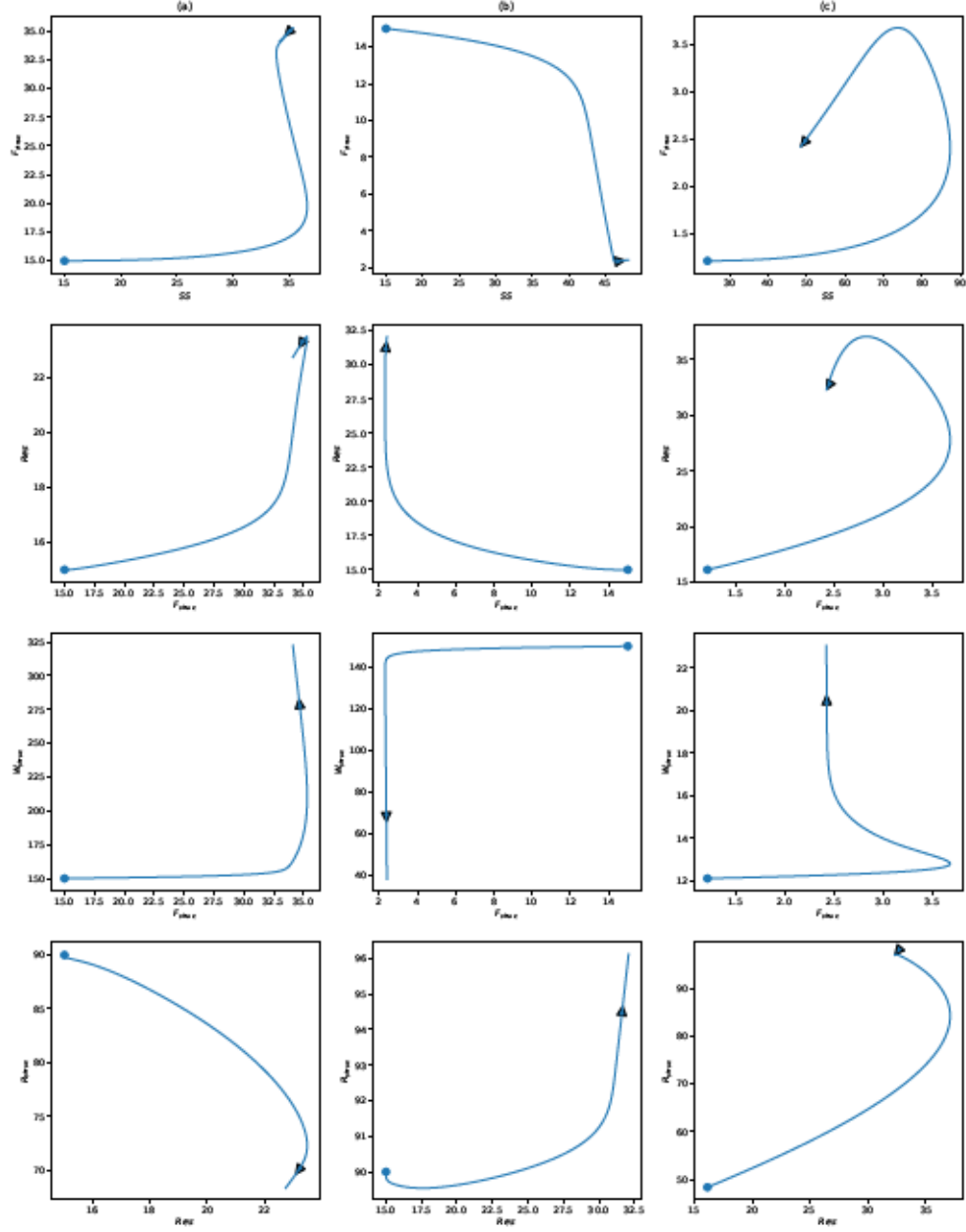


Figure 13: Phase planes of different combinations of vegetation compartments for a model with constant photosynthetic input. The column (a) corresponds to model runs with initial conditions as in table 4.1. The plots in column (b) correspond to model runs with the same initial C stocks as in (a), but with a strong aboveground sink limitation: $\alpha = 0.05$. Finally, column (c) contains the plots from model runs with $\alpha = 0.05$ and initial C stocks in the neighborhood of the steady state calculated with this parameter value.

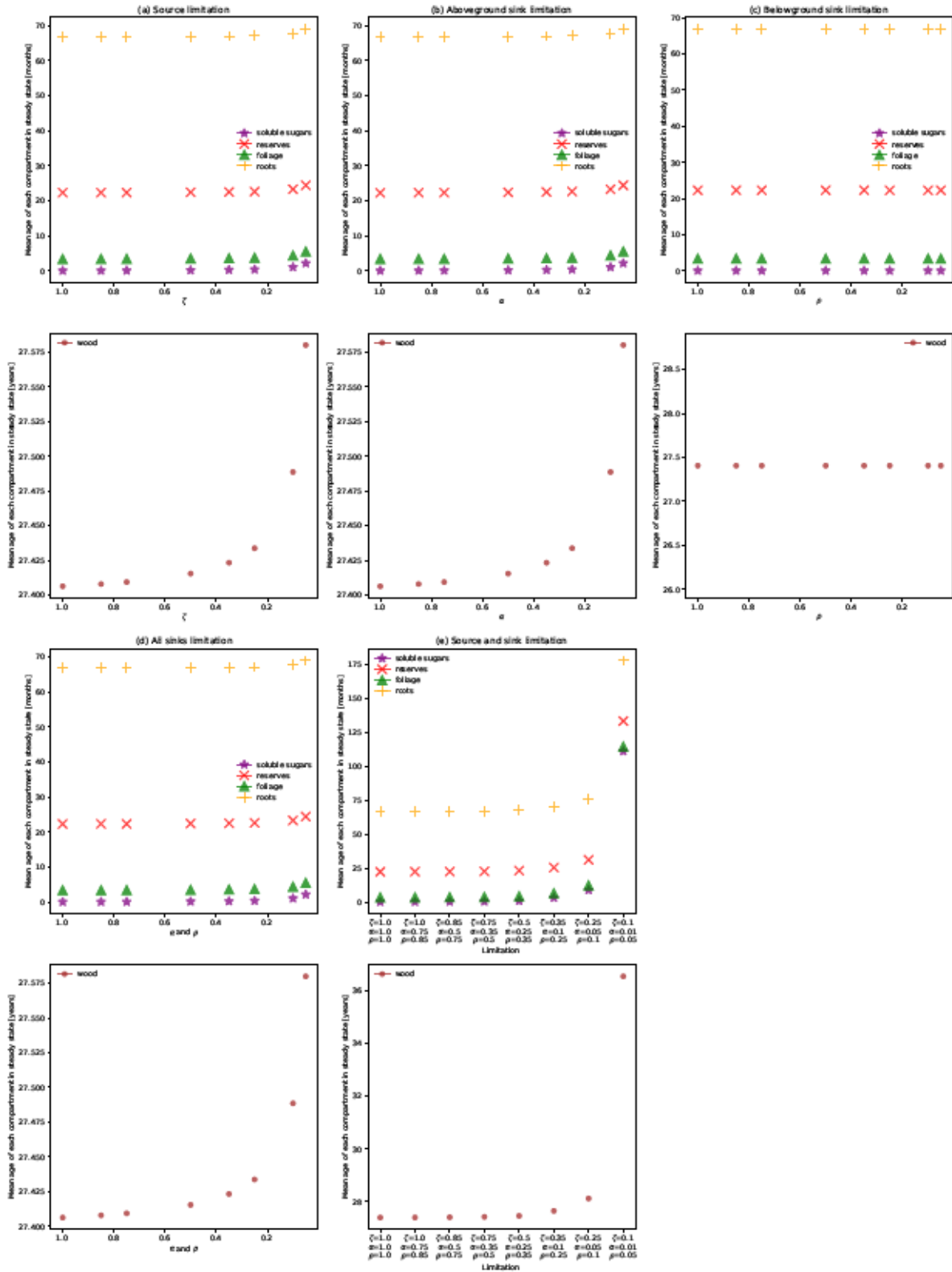


Figure 14: Mean ages predicted for the initial model proposed in this work, in steady state under different limitation conditions; (a) source limitation only $-\zeta$, (b) aboveground sinks limitation $-\alpha$, (c) belowground sinks limitation $-\rho$, (d) above and belowground limitation $-\alpha, \rho$, and (e) Source and sink limitation $-\zeta, \alpha, \rho$. The highest source or sink strength is achieved when the respective scalar is equal to 1.

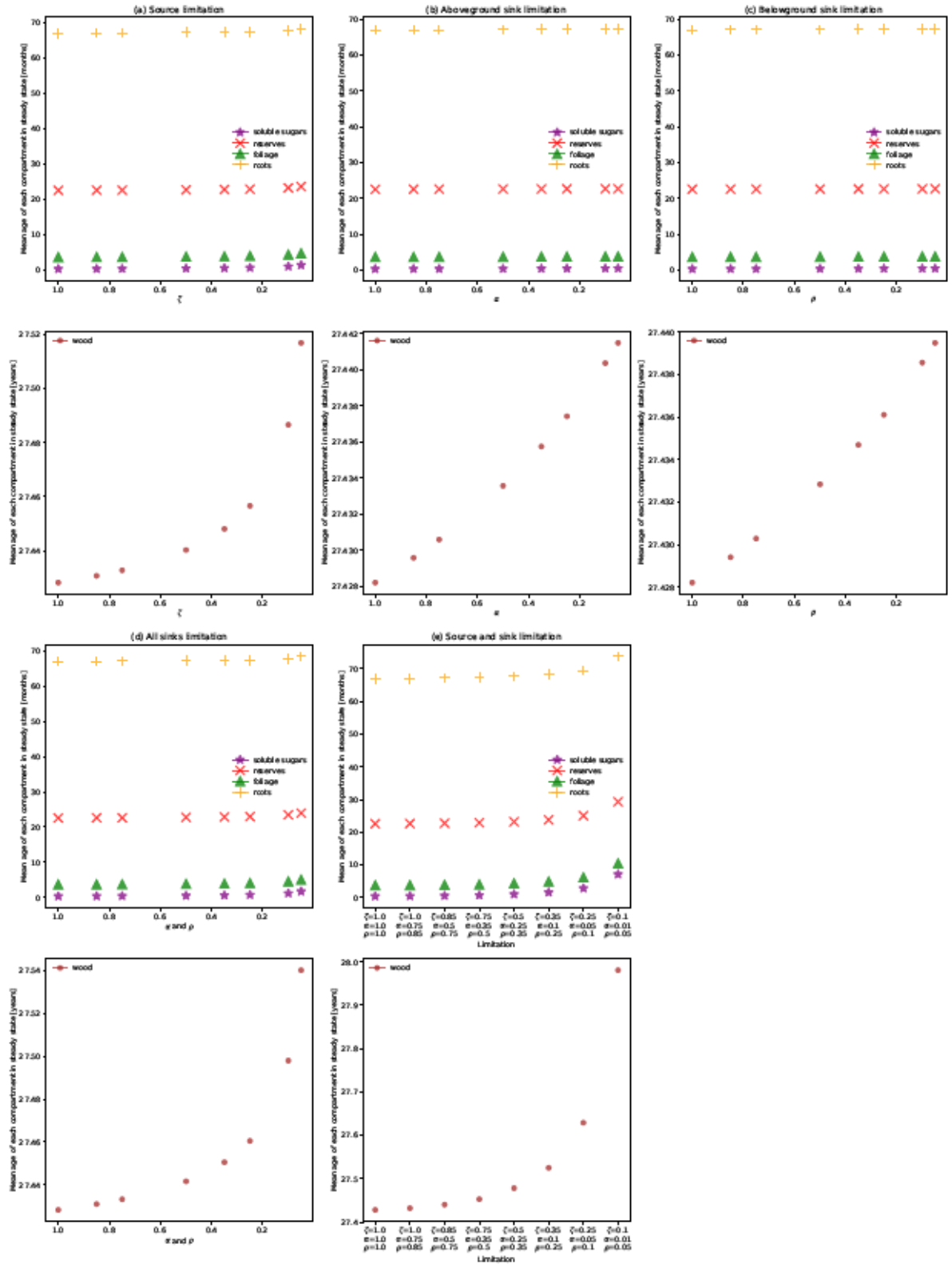


Figure 15: Mean ages predicted for the model with constant photosynthetic input, in steady state under different limitation conditions; (a) source limitation only $-\zeta$, (b) aboveground sinks limitation $-\alpha$, (c) belowground sinks limitation $-\rho$, (d) above and belowground limitation $-\alpha, \rho$, and (e) Source and sink limitation $-\zeta, \alpha, \rho$. The highest source or sink strength is achieved when the respective scalar is equal to 1.

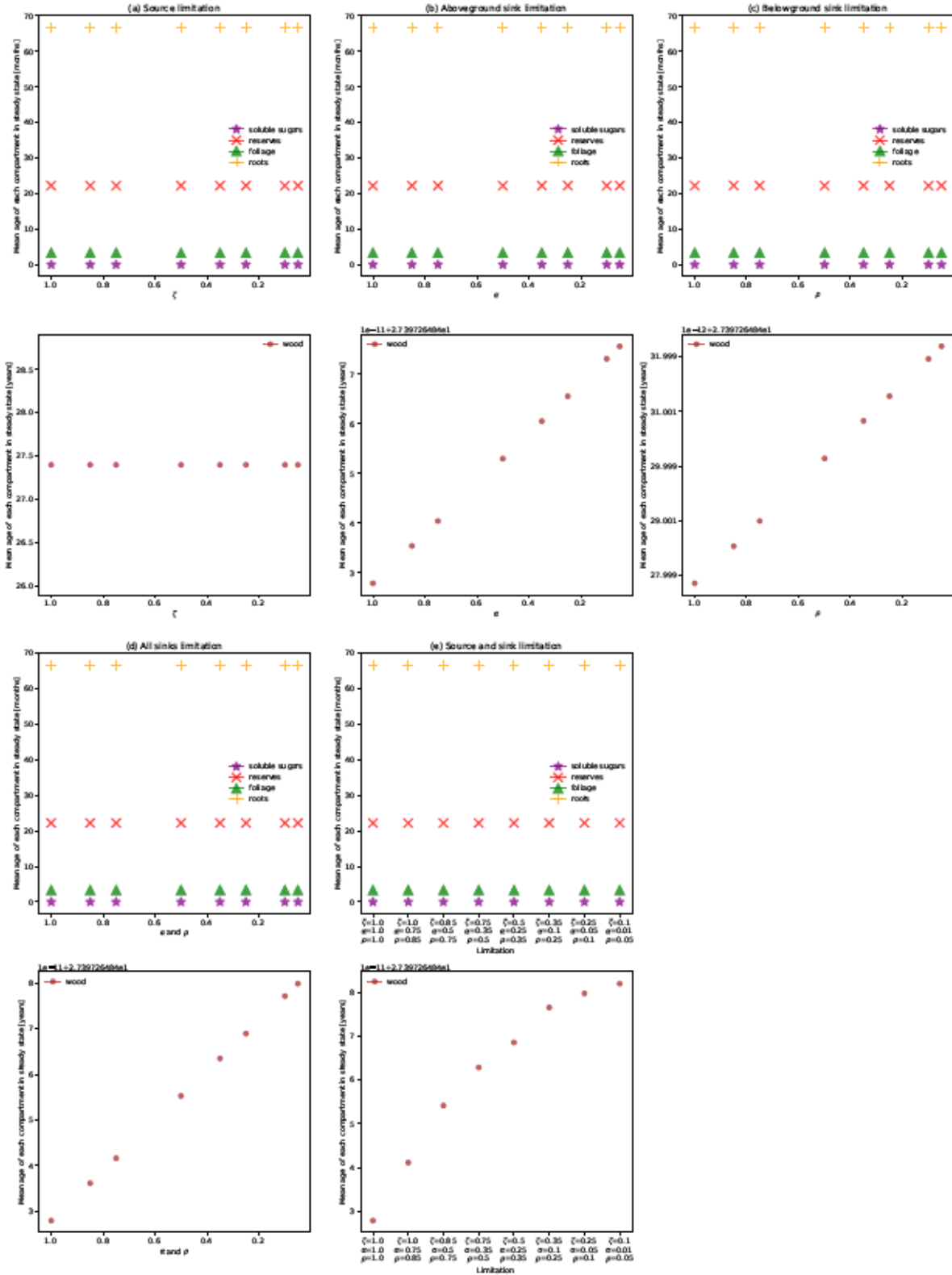


Figure 16: Mean ages predicted for the linear model with constant photosynthetic input, in steady state under different limitation conditions for a; (a) source limitation only $-\zeta$, (b) aboveground sinks limitation $-\alpha$, (c) belowground sinks limitation $-\rho$, (d) above and belowground limitation $-\zeta, \rho$, and (e) Source and sink limitation $-\zeta, \alpha, \rho$. The highest source or sink strength is achieved when the respective scalar is equal to 1.